THE EFFECTS OF PASSENGER LOADING AND VENTILATION AIR ON AIRFLOW PATTERNS WITHIN AN AIRCRAFT CABIN

by

MICHAEL LEVI MADDEN

B.S., Kansas State University, 2013

A THESIS

submitted in partial fulfillment of the requirements for the degree

MASTER OF SCIENCE

Department of Mechanical and Nuclear Engineering
College of Engineering

KANSAS STATE UNIVERSITY
Manhattan, Kansas

2015

Approved by:

Co-Major Professor
Dr. Mohammad H. Hosni

Approved by:

Co-Major Professor
Dr. Byron Jones

Copyright

Abstract

With the increasing number of passengers traveling on commercial aircraft, it is important to mitigate the possibility of diseases and contaminants spreading throughout aircraft cabins and becoming harmful to the health of passengers. The ventilation system on a Boeing 767 aircraft is designed to create lateral flow to isolate contaminants to a single row of the cabin and remove the harmful air quickly. There are many variables that can influence the airflow patterns inside the cabin. The thermal plumes created by occupants are one of the variables investigated in this experimentation. Another special case investigated is the transport of gases in the cabin when the ventilation air is eliminated.

Experimentation is performed in a mock-up Boeing 767 cabin. The mock-up enclosure consists of 11 rows and 7 columns of seats in each row. Ventilation apparatus, seating, and cabin dimensions used for testing are all representative of an actual aircraft. Thermal manikins are placed in the cabin seats to simulate the heat load from a seated person. A mixture of carbon dioxide (CO_2) and helium (He) is injected into the cabin as a tracer gas to simulate the release of contaminants. The CO_2 concentration is measured by analyzers placed at the cabin inlet, exhaust, and seat of interest. The tracer gas can be injected and sampled at any of the 77 seats.

In order to determine the effects of passenger density, testing is performed with maximum occupant load and repeated with half of the passenger load. Tracer gas is injected in three locations of the cabin and sampled in 32 seats for each injection seat. The testing revealed a significant effect of passenger load on airflow patterns. To determine the effects of removing the ventilation air, the cabin is supplied with 1400 cfm of outdoor air at 60 °F for three hours to bring the cabin to a steady state temperature. Then, the supply air is shut off, and tracer gas is injected into the cabin and the CO_2 concentration is sampled at 12 locations throughout the cabin. It was found that contaminants are still transported throughout the cabin without the ventilation air.

Table of Contents

List of Figures

List of Tables

Acknowledgements

I would like to thank my family and friends for their immeasurable support throughout the course of my education. I would also like to thank the professors on my supervisory committee. Dr. Hosni, Dr. Jones, and Dr. Eckels have all taught me a great amount throughout my time at Kansas State and helped significantly with my graduate research and this thesis. I would like to thank the FAA and the National Air Transportation Center of Excellence for Airliner Cabin Research under Cooperative Agreement 07-C-RITE-KSU for the organization and funding of this thesis. Finally, I would like to thank Boeing and the other corporate sponsors of the ACER program.

Chapter 1 - Introduction

Air quality standards in aircraft have an effect on a significant percentage of the world's population. The close proximity of passengers, low humidity levels inside the cabin, elevated cabin altitude, disease transmission, and supply air contaminants all pose potential health risks to aircraft passengers. In order to reduce the passengers' risk of infection, these contaminants need to be effectively removed by the ventilation system.

The Air Transportation Center of Excellence for Airliner Cabin Environment Research (ACER) team was created to address these concerns and to research transport phenomena in commercial aircraft cabins. The ACER project investigates many aspects of air quality in airliners: need and location of air quality sensors, prediction and sampling of combustion products in cabin air, delivery of decontaminating agents, prediction and sampling of ozone and pesticides, and prediction of transmission paths for respirable diseases (Air Transportation Center of Excellence (CoE) for Airliner Cabin Environment Research (ACER), 2007). The ACER team has used experimental data from mock-up airliner cabins and computational fluid dynamic (CFD) analysis as investigative methods. For the mock-up cabin used in this testing, experiments have already been completed examining dispersion of tracer gas and particulates (Lebbin, 2006), models for predicting transport (Jones, 2009), longitudinal particulate dispersion (Beneke, 2010), optimal particulate sensor locations (Shehadi, 2010), beverage cart wake effects (Trupka, 2011), and gasper effects (Anderson, 2012).

The testing completed for this document primarily focuses on two specific scenarios of commercial air travel. The first scenario is the effect of passenger density on the transport of contaminants throughout the aircraft cabin. A mixture of carbon dioxide (CO_2) and helium (He) is injected as a tracer gas at a seat location in the cabin, and the gas concentration is then sampled at various locations in the cabin. This testing is completed with thermal manikins occupying each of the 77 seats in the mock-up cabin and then repeated with only 38 of the seats (approximately half) occupied by thermal manikins. After both passenger loads are tested, the changes in tracer gas concentrations are examined. The second scenario is the transmission of contaminants throughout the aircraft cabin when the supply air is eliminated. This scenario is tested by bringing the mock-up cabin to normal operating conditions, then turning off the supply

air stream, injecting and sampling tracer gas throughout the cabin, and comparing the tracer concentrations sampled at different locations.

Chapter 2 - Background and Literature Review

More than 730 million people traveled on domestic commercial airliners in 2011 (BTS, 2012). This large number of passengers creates a major concern for the health effects caused by air quality inside the cabin. Possible contaminants can enter the cabin air by means of infected passengers, malicious intent, or unclean supply air. In order to ensure passenger safety, regulations are implemented to limit airborne contaminants.

2.1 Aircraft Air Quality Standards

The properties of the air in commercial aircraft cabins are regulated in the United States by the Federal Aviation Administration (FAA). The controlled air properties include pressure, temperature, supply air rate, and contaminant levels (Zhang & Sun, 2005). Although the relative humidity of cabin air can cause health issues and discomfort for passengers, it is not regulated by the FAA.

2.1.1 Pressure and Temperature Requirements

The outside environment at flying altitude can have temperatures as low as -67 °F (-55 °C) and one-fifth of atmospheric pressure at sea level (Zhang & Chen, 2007). According to section 25.841 of the Code of Federal Regulations written by the FAA, the pressure altitude of the aircraft cabin may not exceed 8000 ft (2440 m). The only exception is in the case of an emergency where the pressure altitude of the aircraft cabin is not allowed to exceed 15,000 ft (4570 m). The temperature of the cabin is required to be 67-73 °F (19.5-23 °C) during winter and 73-79 °F (23-26.1 °C) during summer (O'Donnell et al. 1991). Also, the temperature difference between various zones of the cabin cannot be greater than 5 °F (2.8 °C) in accordance with ASHRAE standard 55-2004.

2.1.2 Ventilation Requirements

Section 25.831 of the FAA standards requires a minimum ventilation rate of 0.55 lb/min (0.25 kg/min) of fresh air for each passenger, which is equivalent to 7.5 cfm (3.75 L/s) at sea level or 10 cfm (5 L/s) at 8000 ft altitude (ASHRAE, 2007). This regulation additionally limits CO_2

concentration in the cabin to 5000 ppm and carbon monoxide (CO) concentration to 50 ppm. Also, ozone concentration is not to exceed 0.25 ppm when the aircraft is above 32,000 ft (9750 m). All of the ventilation rates dictated by the FAA are for outside air. Most of today's aircraft possess air recirculation systems to reduce the amount of energy required to supply air. In addition to reducing energy consumption, this strategy also increases the relative humidity of the supply air, which alleviates some passenger discomfort caused by inhaling extremely dry air for extended periods of time. On the other hand, the recirculated air present a filtering problem, so HEPA filters are used to clean the air before recirculating it into the cabin (Lebbin, 2006). In general, most aircraft approximately double the ventilation rate to 20 cfm (10 L/s) per passenger, with approximately half of the mixture being outdoor air and the remaining half being recirculated air while still complying with FAA standards.

2.2 Air Flow Design

In the twin aisle aircraft addressed in this project, two linear slot diffusers run the entire length of the cabin and distribute supply air from the ceiling in the center of the cabin. Exhaust air is pulled from the cabin by vents that are located at the bottom of both sidewalls of the cabin along the entire length of the cabin except in the wing box area. These supply and exhaust locations that span the entire cabin length, are designed to enhance airflow in the lateral direction of the cabin and minimize airflow in the longitudinal direction. The advantage of a highly lateral flow is that any contaminants released in the cabin are confined to only several rows of the cabin, in theory, instead of being dispersed throughout the entirety of the cabin. It was discovered that, in actuality, large-scale eddies and non-uniform air distribution causes contaminants to spread along the length of the cabin (Wang et al. 2006). A cross section view of the designed airflow pattern for a twin aisle aircraft is shown in Figure 2.1.

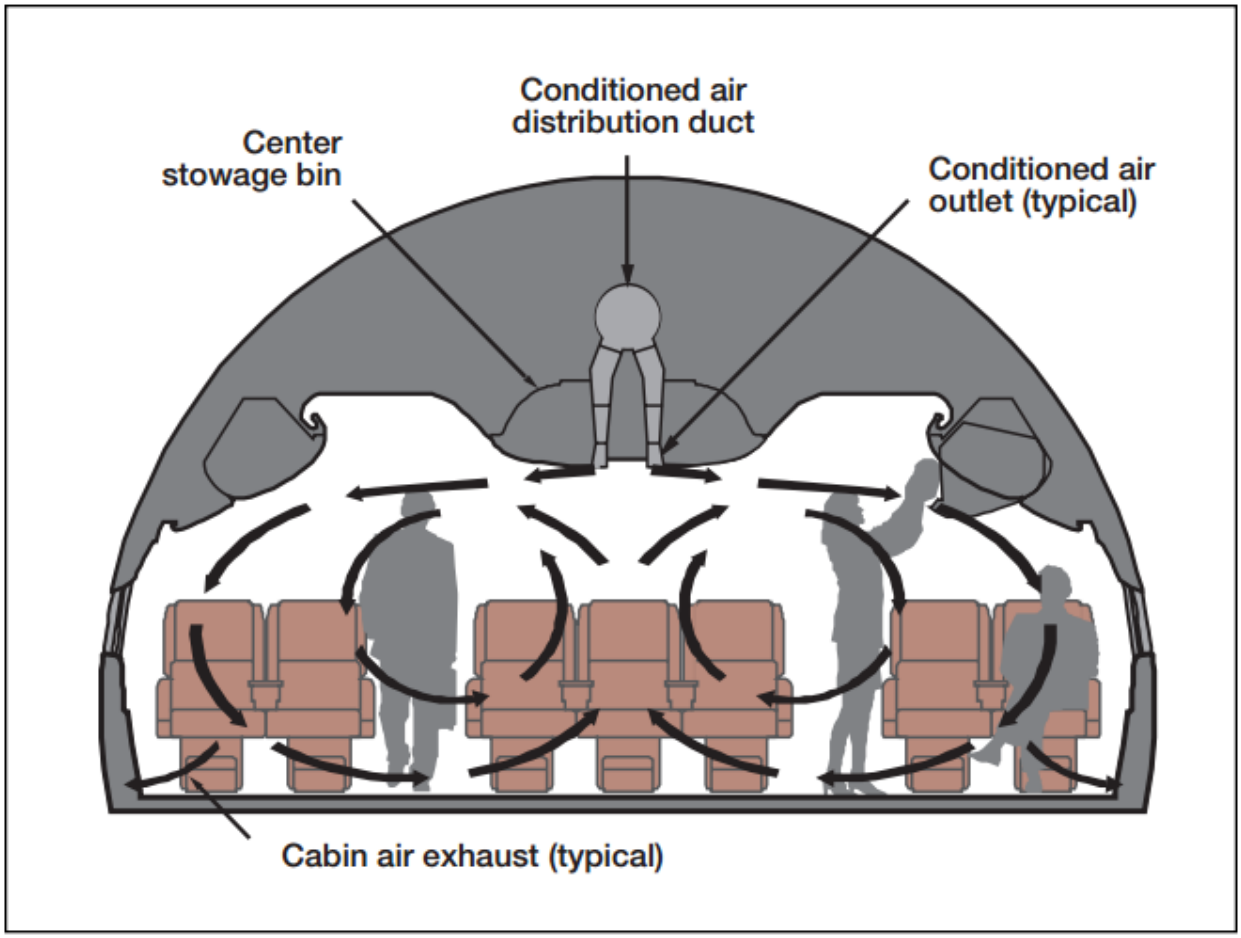

Figure 2.1: Cross Section Design Air Flow (Hunt & Space, 1994)

Chapter 3 - Experimental Setup

All of the testing takes place at the ACER (Aircraft Cabin Environmental Research) Lab at Kansas State University in Manhattan, KS. The laboratory contains a mock-up of an 11-row Boeing 767 cabin inside a wooden enclosure. The temperature, humidity, and flow rate of the inlet air to the cabin are controlled with a dehumidifier, chiller, hot water heater, electric heater, blower, and a series of sensors and controllers. The seats in the cabin are occupied by heated manikins to simulate the heat output of a resting adult, and there are gas injection and sampling devices in the enclosure for tracer gas testing. The wooden enclosure containing the mock-up cabin, as well as part of the air supply system, is shown in Figure 3.1.

There is a hallway running along each side of the cabin that houses tracer gas and data acquisition (DAQ) equipment and permits access to the outside wall of the cabin. There is also a ladder and access door in the west hallway, which allows access to the top of the enclosure where two of the CO2 analyzers and the vacuum pump are located. The two exhaust fans at the top of the south face of the enclosure pull exhaust air from the enclosure and cabin to increase circulation. All of these features are shown in Figure 3.1.

Figure 3.1: Mock-up Cabin Enclosure and Supply Air Inlet (Beneke, 2010)

3.1: Airliner Cabin Mock-up Facility

The mock-up aircraft cabin is contained inside of a wooden enclosure. The enclosure measures 7.4 x 9.8 x 4.9 m. There are two access hallways, one on the east side of the cabin and one on the west. The east hallway contains the mass flow controllers for CO_2 and He and data acquisition equipment. There is an entrance at both ends of both hallways. There are also two doors on the north end of the aisles of the cabin. A top view diagram of the cabin and enclosure is shown in Figure 3.2.

The columns of seats along the length of the cabin are labeled A to G from East to West. The rows of seats from front to back are numbered 1 to 11 in the South to North direction. These labels will be referenced repeatedly throughout this report to refer to specific seat locations. These labels are shown in Figure 3.2.

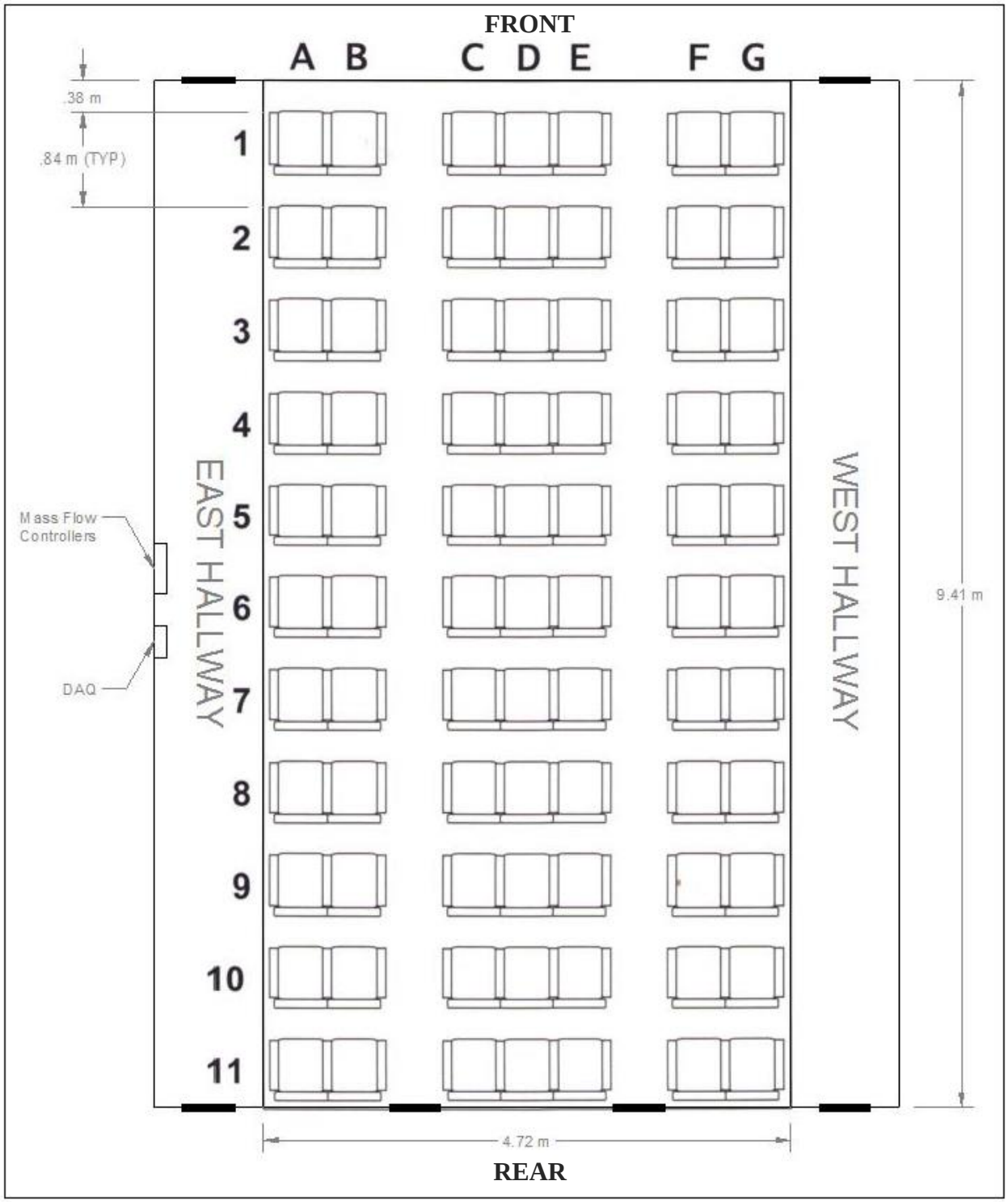

Figure 3.2: Top View of Airliner Cabin and Enclosure (Trupka, 2011)

There is a 1.2 m crawlspace underneath the floor of the cabin that allows access to the bottom of the cabin. The crawlspace holds the air compressor for the He mass flow controller and the piping for the water tubes that run along the outside walls of the cabin. These tubes permit the

control of the wall temperature of the cabin, but they were not used during any of this testing. The water tubes on the west wall of the cabin are shown in Figure 3.3.

Also shown in Figure 3.3, are the cabin supports and cabin air exhaust gaps. The air exhaust gaps run along both sides of the mock-up cabin for its entire length. After the air exits the cabin, it moves into the hallways of the enclosure until it is drawn out by the exterior exhaust fans. The cabin supports are connected to the floor and ceiling of the enclosure. The supports are the structure that holds up the walls and ceiling of the airliner cabin.

Figure 3.3: Cabin Supports and Exhaust Gaps (Trupka, 2011)

3.1.1: Cabin Dimensions

The mock-up cabin was designed to simulate a Boeing 767 aircraft as closely as possible. The inside surface of the cabin walls and ceiling is constructed of aluminum sheets. Figure 3.4 shows the dimensions of the designed cross-sectional view of the cabin. The equations for the dimensions of the cabin profile are derived in greater detail in (Lebbin, 2006).

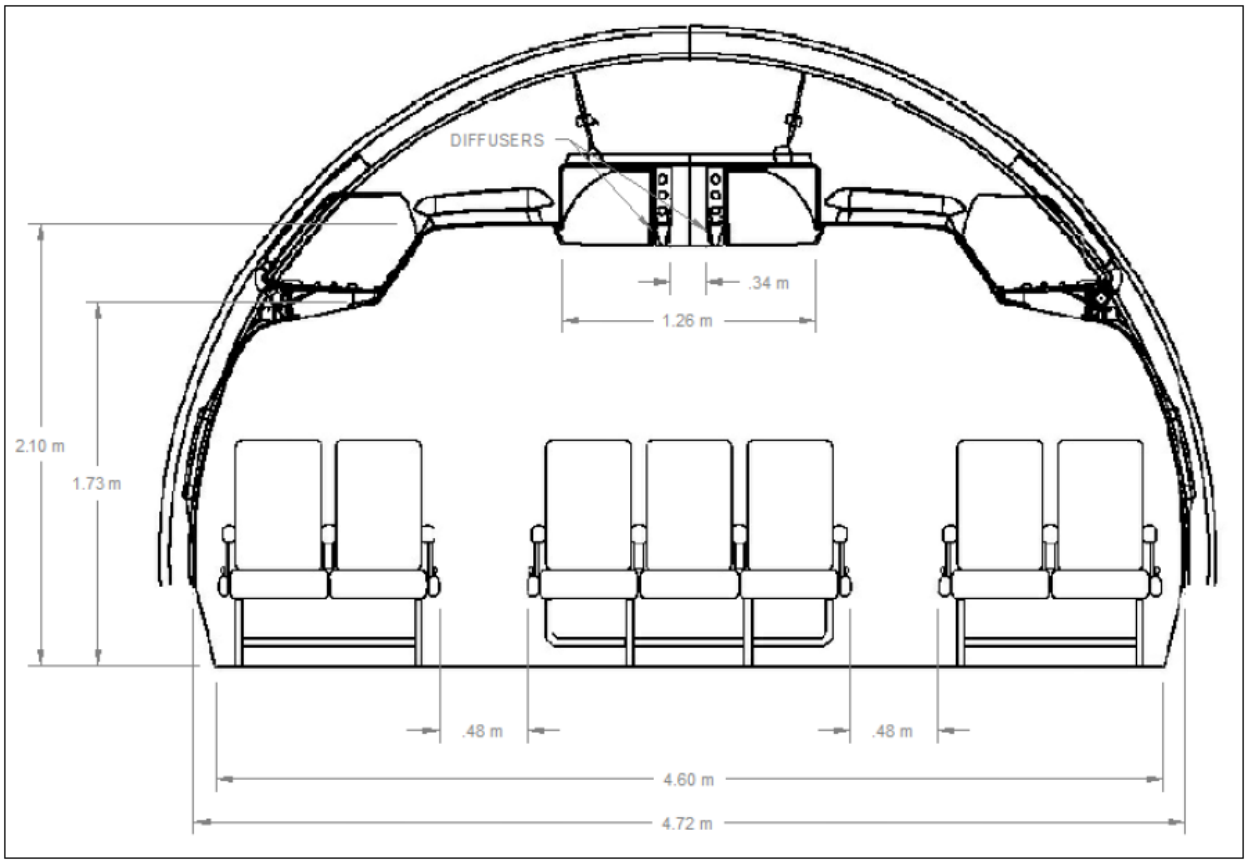

Figure 3.4: Cross-Sectional View of Airliner Cabin (Trupka 2011)

3.1.2: Seat Geometry

There are seven seats in each row of the cabin and 11 rows, which amounts to a total of 77 seats. The seats used in the cabin are seats from a salvaged Boeing 767 aircraft and are arranged in 2-3-2 pattern, similar to the commercial economy class. The width and height dimensions of the double and triple airliner seat combinations are shown in Figures 3.5 and 3.6, respectively. Figure 3.7 shows the depth and height dimensions of the airliner seats. All three of these figures are taken from (Trupka, 2011).

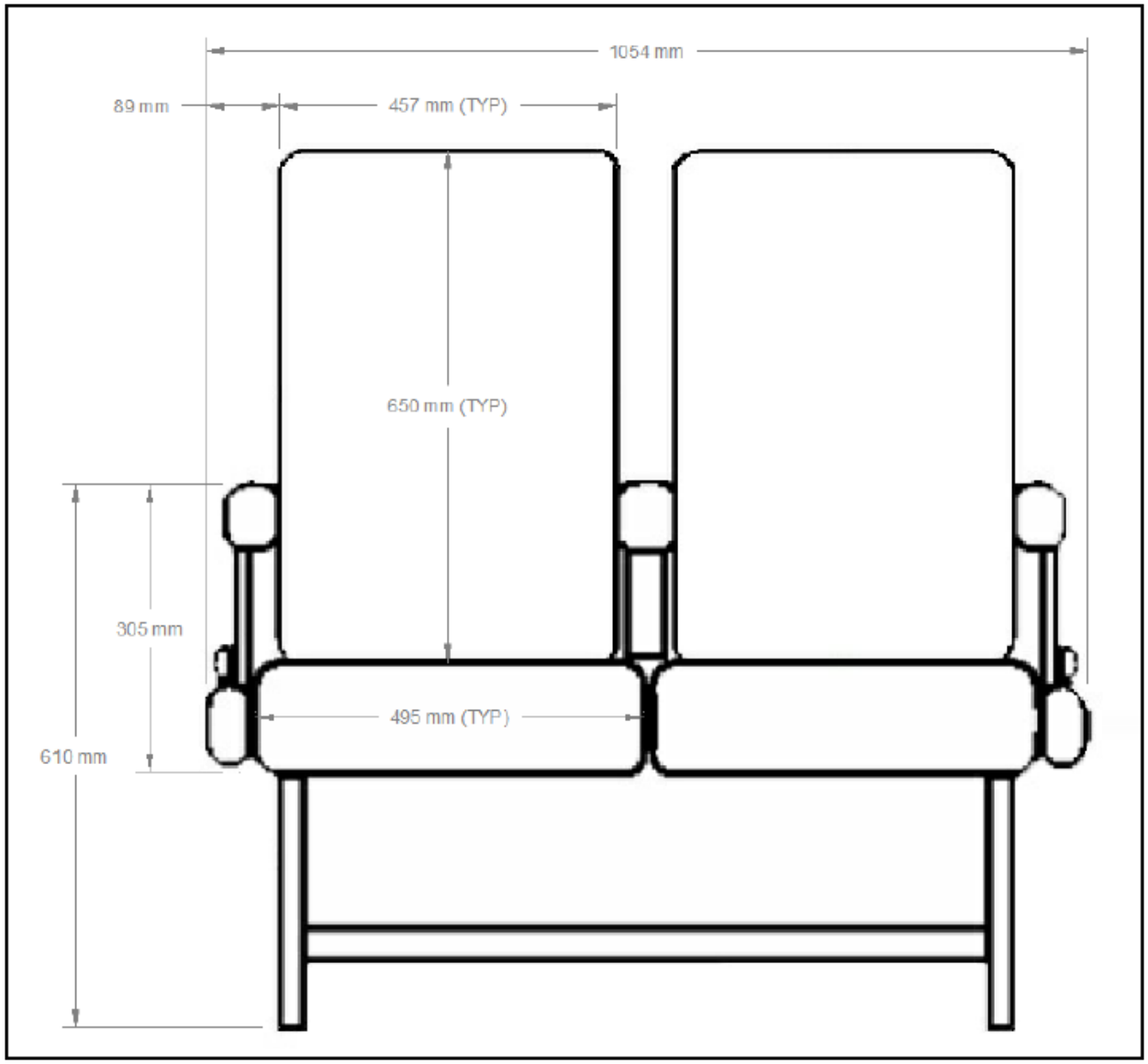

Figure 3.5: Double Seat Dimensions

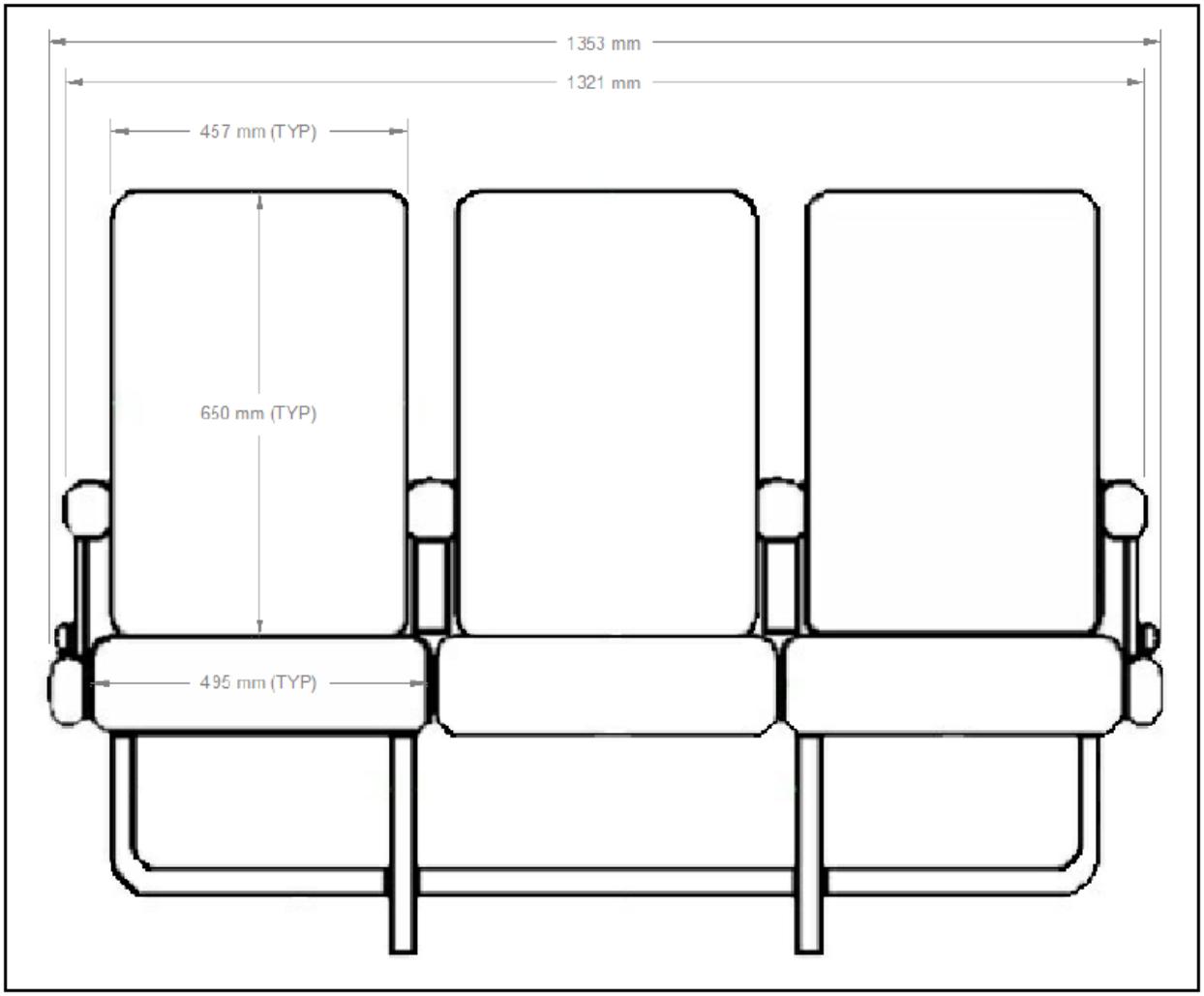

Figure 3.6: Triple Seat Dimensions

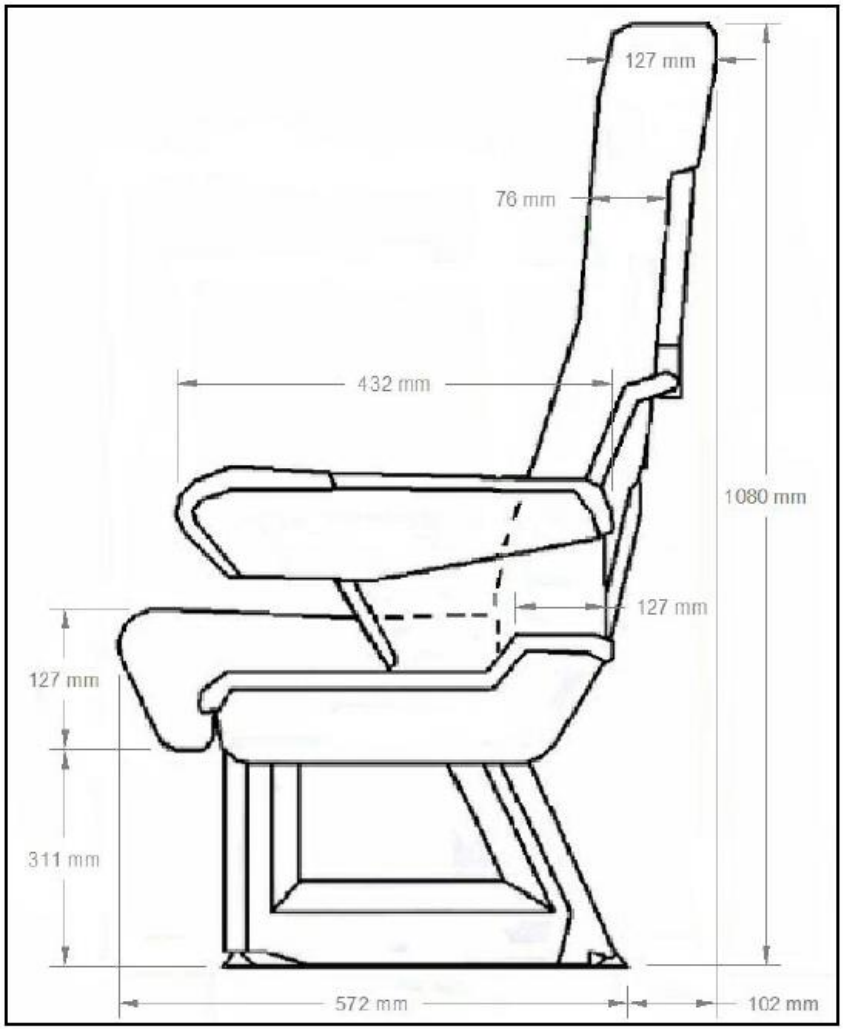

Figure 3.7: Seat Profile Dimensions

3.1.3: Thermal Manikins

Each seat of the cabin is occupied by a thermal manikin to simulate the heat load from a resting adult male passenger. The manikins are Rubie's Costume Company model 1724 inflatable male manikins. There is 25 m of Omega TFCY-015 thermocouple wire spread over the legs, arms, torso, and head of each manikin. The thermocouple wire is used as a distributed heating element in this case and not to measure temperature. The thermocouple wire is covered with duct tape for safety purposes. Each thermocouple wire is connected to a 115 V AC power outlet, which causes each manikin to generate approximately 102 W of heat. This power level accounts for approximately 70 W of sensible thermal output of a resting, seated adult (ASHRAE, 2005) plus it compensates for other heat loads, such as in-flight entertainment systems, in actual aircraft. Figure 3.8 shows one of the thermal manikins inside the cabin.

Figure 3.8: Thermal Manikin (Beneke, 2010)

There are several safety precautions taken in the cabin to prevent an electrical fire caused by the manikins. The first safety measure is a thermostat on the north wall of the cabin. The thermostat can be turned off to remove power to the manikins, or it can be set to any temperature between 60 and 100°F. If the air temperature in the cabin exceeds the maximum temperature, the manikins are turned off automatically, until the temperature returns below the maximum temperature. The second safety feature of the cabin is a pressure differential switch located in the air supply duct. If the flow rate of supply air is too low to overcome the switch, then the manikins will not turn on.

3.2: Air Supply System

The air supply system for the mock-up cabin is designed to supply the cabin with 1400 cfm of air at 60 °F. Outdoor air is drawn from the south end of the laboratory into the conditioning system. Once the air is conditioned, it is routed through the supply duct and into the airliner cabin.

3.2.1: Ductwork

The first section of duct work, which is connected to the outer wall of the building, is a rectangular duct 2.2 m long, 0.91 m wide, and 0.61 m tall. The duct then makes a 90° turn to the right, followed by a 90° turn downwards. There is a 2.7 m long vertical section ending in a 90° left turn connecting the duct to the dehumidification unit.

Leaving the air conditioning system, is a 3.8 m section of duct with a 0.41 m diameter that leads to a 90° bend to the right. After the bend, there is another 1.51 m section of 0.41 m diameter duct, which is connected to a series of 90° elbows. The first elbow is a turn to the right and is immediately followed by a turn in the upward direction. The upward elbow is connected to a 3.96 m section of duct with a 0.41 m diameter. The upward section ends at a 90° bend to the horizontal direction that is connected to the Boeing supply duct. The ductwork between the conditioning system and cabin enclosure is shown in Figure 3.9.

Figure 3.9: Air Supply Ductwork

The Boeing supply duct is 0.25 m in diameter and spans the entire length of the aircraft cabin. There are 34 flexible hoses connected to the supply duct, which mate the supply duct to the linear diffusers. Figure 3.10 shows the Boeing supply duct mounted in the enclosure and the flexible hoses connected to the duct. Figure 3.11 shows the other end of the flexible hoses that is connected to the linear diffusers on the ceiling of the airliner cabin. Both figures can also be found in (Trupka, 2011).

Figure 3.10: Boeing Supply Duct

Figure 3.11: Diffuser Connection

3.2.2: Air Conditioning System

The conditioning system for the supply air consists of a blower, dehumidifier, hot-water heater, water chiller, and an electric heater. The hot-water heater and chiller are only used if the outside air temperatures warrant the additional heating or cooling, and the electric heater brings the air to the desired temperature of 60 °F. Figure 3.12 shows a schematic diagram of the conditioning system, and Table 3.1 lists the description for each component.

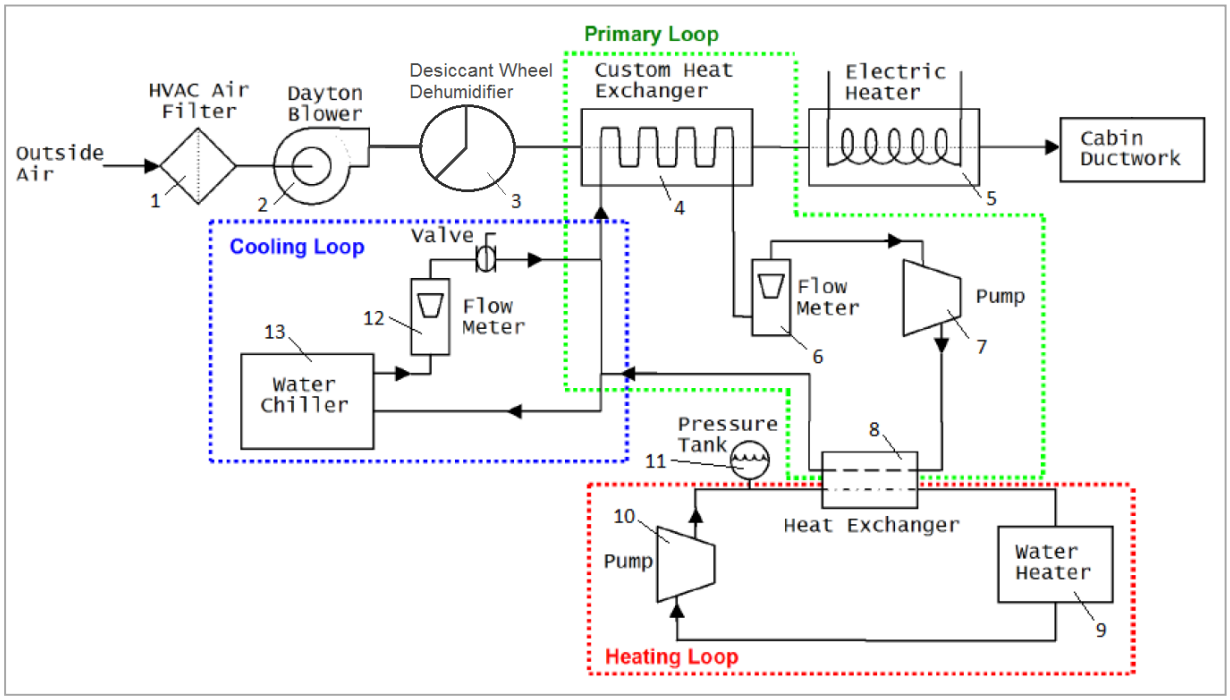

Figure 3.12: Conditioning System Schematic

Table 3.1: Air Conditioning System Components

No.	Item	Model	Details
1	HVAC Air Filters	Glass Floss ZL	2 parallel filters 24”x24”x2”
2	Blower	12.25” Dayton Blower at 3.0 hp	Yaskawa GPD315/V7 VFD
3	Dehumidifier	Munters ICA-0750-020	Desiccant type
4	Heat Exchanger	Custom-made	0.6 x 0.6 m
5	Electric Heater	AccuTherm DLG-9-3	240 V, 3ph., 9 kW
6	Flow Meter	Omega FL7204	
7	Pump	Marathon CQM 56C34D212OF P	120 V, 0.75 hp
8	Heat Exchanger	Alfa Laval CB27-18H T06	
9	Water Heater	Rheem GT-199PV-N-1	19,000-199,900 BTU
10	Pump	FHP C4T34DC35A	Yaskawa GPD205-1001 VFD
11	Pressure Tank	Dayton 4MY57	6.5 gal, 30 psi
12	Flow Meter	King 7205023133W	
13	Water Chiller	AccuChiller LQ2R15	PV-B311 condensing coils

The various components of the conditioning system can be lumped into three more generalized groups. The first group is the cooling loop. The cooling loop’s main component is the water chiller, and the loop is used to bring the air temperature down to 50 °F. The cooling loop is only used if the outdoor air temperature is above 50 °F. The second group is the heating loop. The heating loop’s main component is the natural gas water heater, and the loop is used to bring the temperature up to 50 °F. The heating loop is only used if the air temperature exiting the dehumidifier is below 50 °F. The final group is the primary loop. The primary loop’s main component is the electric heater, which is used at all times to raise the air temperature from 50 °F to the desired 60 °F. Figure 3.13 shows part of the dehumidifier and the three conditioning loops, except for the hot water heater, which is located by the north end of the enclosure.

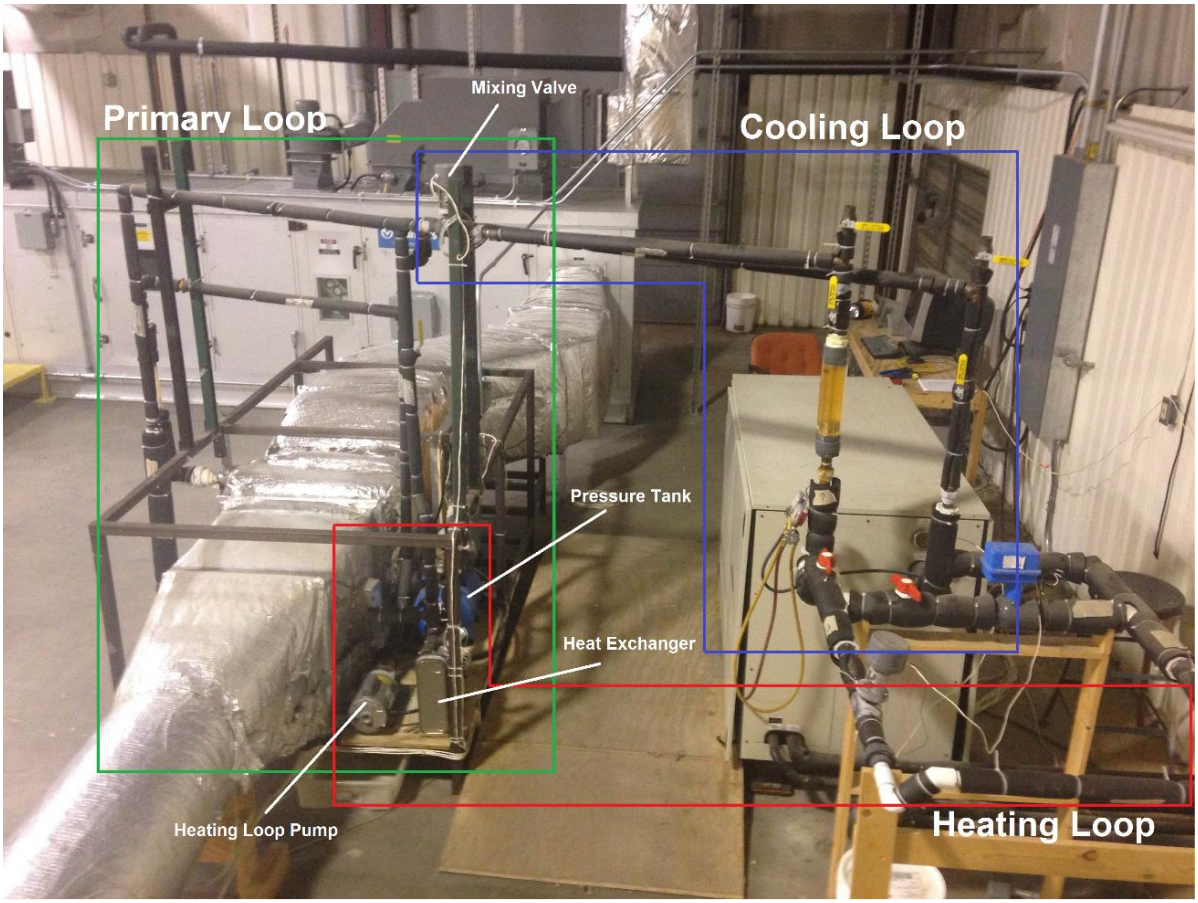

Figure 3.13: Air Conditioning System Loops

3.2.3: Control System

All of the supply air components are controlled by data acquisition and control units connected to a computer running National Instruments LabVIEW software. The computer acquires data through Agilent 34970A and National Instruments FP-1000 DAQ's and controls several output variables via the National Instruments FP-1000 with add-on modules PWM-520 and AO-210 for pulse width modulation and analog voltage output, respectively (Trupka 2011).

Air temperature is sampled at seven locations throughout the conditioning process. Relative humidity and flow rate of the supply air are sampled downstream of the conditioning system before the supply air enters the cabin. The LabVIEW system controls the final air supply temperature, by means of the electric heater output, and the air flow rate, by means of the blower speed. The only component of the conditioning system that is manually controlled is the set point of the chiller. This is an insignificant control, since the set point temperature remains constant throughout the entirety of a test. The details of the feedback and control of each of the

supply air properties are listed in Table 3.2. Also, Figure 3.14 shows a section of the front panel of the LabVIEW VI used to control the ventilation air system.

Table 3.2: Supply Air Conditioning System Control and Feedback Parameters

Feedback	Sensor Location	Control
Supply Air Temperature	Cabin Inlet Duct	Heater Temperatures
Electric Heater Temperature	Thermistor in Heater	Heating Loop Pump VFD
Hot Water Temperature	Water Heater Exit	Mixing Valves
Supply Flow Rate	Cabin Inlet Duct	Blower VFD
Glycol Supply Temperature	Chiller Exit Line	Duct Heater
Glycol Return Temperature	Chiller Inlet Line	Duct Heater
Supply Relative Humidity	Cabin Inlet Duct	None
Heat Exchanger Temperature	Primary Water Loop	None
Air Intake Temperature	Dehumidifier Inlet	None

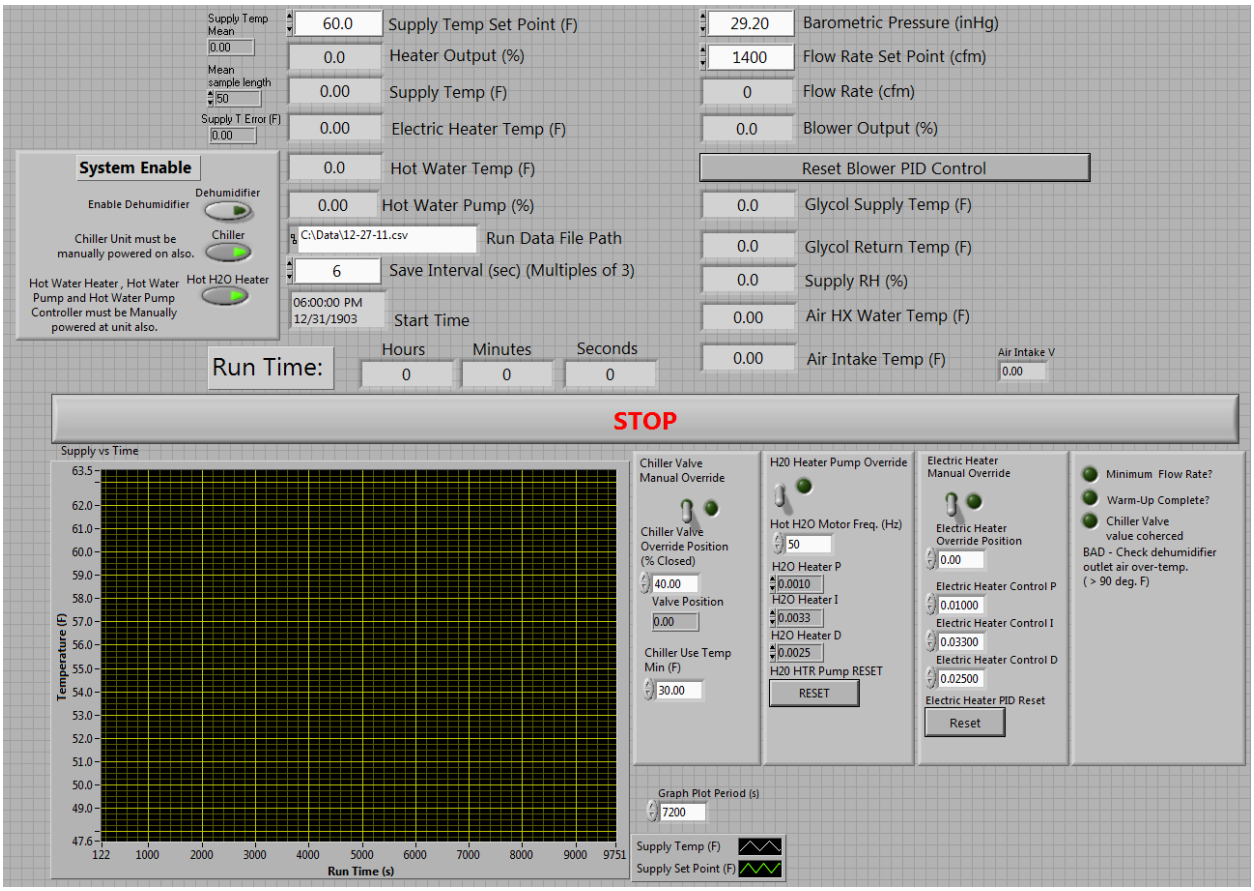

Figure 3.14: Supply Air LabVIEW VI

3.3: Tracer Gas Injection and Sampling

In order to map the movement of air throughout the cabin for this study, a tracer gas was injected and sampled at various locations in the cabin. Carbon dioxide was selected as an ideal tracer gas for its safety, low cost, availability, and the large variety of sensors available to sample its concentration. Since CO_2 is denser than air, it was blended with the proportional amount of helium to give the mixture neutral buoyancy in the cabin air. CO_2 concentrations of 7 to 10% by volume can cause unconsciousness within several minutes (United States Environmental Protection Agency, 2000), so a CellarSafe CS100 CO_2 detector/alarm was installed in the east hallway of the enclosure to ensure operator safety.

3.3.1: Tracer Gas Injection

Both species of gas are delivered to the lab by Matheson Tri-Gas. Industrial grade CO_2 in 50 lb cylinders and high purity helium in type T cylinders are used for this study. The gas cylinders are stored at the southwest corner of the enclosure, and supply lines are ran through the crawlspace of the enclosure to the mass flow controllers in the east hallway. The CO_2 and He arrive at gage pressures of 4 MPa and 16 MPa, respectively, so regulators are required on both tanks. The regulators reduce the gas pressures to 200 kPa to allow for low pressure, vinyl supply lines. The CO_2 and He cylinders, with regulators installed, are shown in Figure 3.15.

Figure 3.15: Gas Cylinders with Regulators

The vinyl supply lines connect the cylinders to the mass flow controllers. A mass controller is used for each of the two gases. For CO_2, an electric MKS 1559A-200L1-SV-S controller is used, while a pneumatic MKS 2179A00114CS controller is used for He (Trupka, 2011). Both mass controllers are controlled by a computer interface running LabVIEW. There is also a flow meter installed downstream of each mass flow controller to allow visual confirmation of the flow rate. The two mass flow controllers and the two flow meters are shown in Figure 3.16 and Figure 3.17, respectively.

Figure 3.16: Mass Flow Controllers

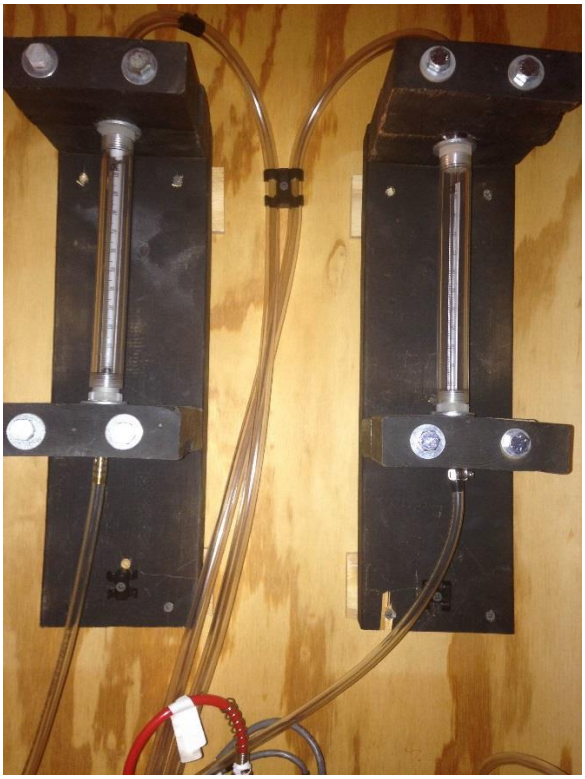

Figure 3.17: Flow Meters

After the CO_2 and He gases exit the two flow meters, the two gas streams mix together in a brass tee fitting. The tube inside diameter after the fitting increases to 25.4 mm to decrease the velocity of the tracer gas. The 5 m long injection tube is connected to a copper pipe mounted to the armrests of the seat at the injection location. The copper tube is mounted vertically, with its exit located 120 cm above the cabin floor. The standard injection rate for testing is 7.0 liters per minute (LPM) of CO_2 and 4.21 LPM of He, which results in an overall injection rate of 11.2 LPM. The tracer gas mixture exits the injection tube at 0.37 m/s at this injection rate. The injection tube and its mounting system are shown in Figure 3.18 for one test, but the injection location is varied over the duration of testing.

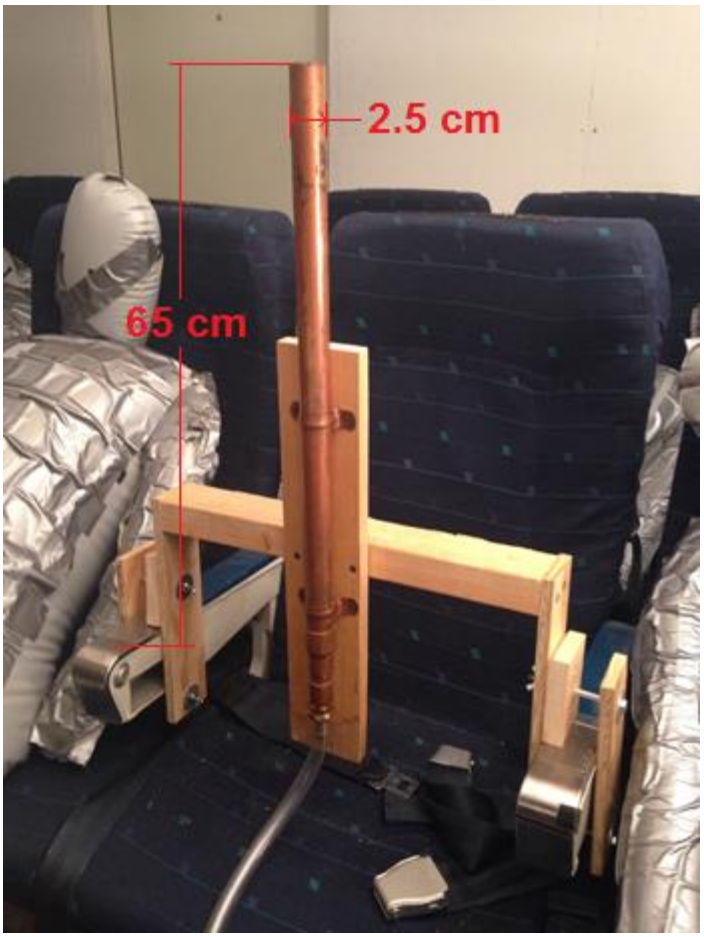

Figure 3.18: Tracer Gas Injection Tube and Mounting

3.3.2: Tracer Gas Sampling

The tracer gas is sampled by the use of infrared CO_2 analyzers at three locations inside the lab. The first sensor is located on the roof of the enclosure and samples the supply air at the inlet of the enclosure. This sensor was custom made using an Edinburgh Instrument gas sampling card and a 24V power supply with 60 Hz noise filter (Trupka 2011). The second analyzer is also located on the roof of the enclosure and samples the exit air at the enclosure exhaust fans. This sensor is a WMA-4 model analyzer from PP System instruments. Both of these analyzers were placed on the roof to allow for short sampling lines. The inlet and exhaust analyzers are shown in Figure 3.19 and Figure 3.20, respectively.

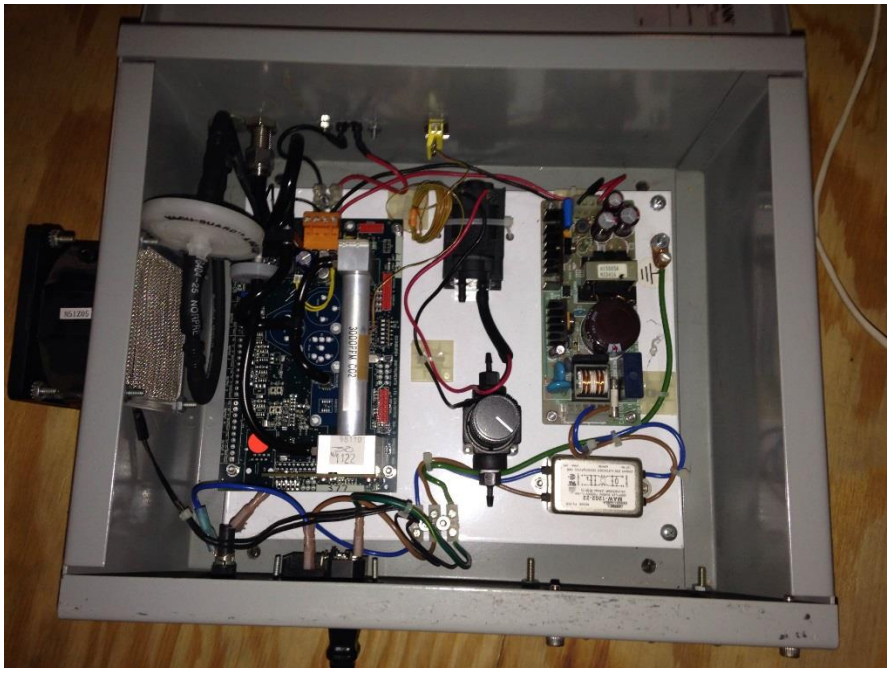

Figure 3.19: Inlet CO_2 Analyzer

Figure 3.20: Exhaust CO_2 Analyzer

The third analyzer is located inside the mock-up cabin and is a PP Systems WMA-4 model CO_2 analyzer, exactly like the exhaust analyzer. The cabin analyzer is sitting on seat 4B of the cabin, and its sampling line is connected to the sampling tree. The cabin analyzer can be seen in Figure 3.21, and the operable ranges for the three analyzers are listed in Table 3.3.

Figure 3.21: Cabin CO_2 Analyzer

Table 3.3: CO_2 Analyzer Details

Sensor Location	Sensor Model	CO_2 Concentration Range	Voltage Range
Inlet	Edinburgh Gascard NG	0 – 3000 ppm	0 – 5 Volts
Exhaust	PP Systems WMA-4	0 – 2000 ppm	0 – 5 Volts
Cabin	PP Systems WMA-4	0 – 2000 ppm	0 – 5 Volts

All of these analyzers require a pump to draw sampling air into the instrument. In order to increase simplicity, only one vacuum pump was installed downstream to provide air for all three of the analyzers. The vacuum pump is shown in Figure 3.22.

Figure 3.22: Sampling Vacuum Pump

The analyzers are at various heights and various distances from the pump, and therefore, have different pressure drops. A balancing system was installed upstream from the pump to ensure that all three analyzers have the desired sample rate of 1 LPM. The balancing system consists of a 4 m long 10 mm inside diameter vinyl tube running from the vacuum pump on the roof of the enclosure, to a Wiegmann utility box in the east hallway of the enclosure. The single line is connected to a fitting that splits the line into three tubes. Each of these tubes is connected to an Omega FL-2012 flow meter. Each flow meter is then attached to a 10 mm inside diameter vinyl tube that runs to one of the CO_2 analyzers. The flow meters and Weigmann utility box are shown in Figure 3.23.

Figure 3.23: Flow Balancing System

The sampling tree is a device installed in the mock-up cabin that allows for more efficient testing by allowing four consecutive seat locations in the same column to be sampled during a single experiment. The sampling tree has an overall length of 3.1 m with four sampling tubes of varying lengths. The distance between each sampling tube port is 0.84 m. The port of each tube is located 0.24 m in front of and 0.14 m above the headrest of the sampling seat location, which is meant to align with the breathing zone of a passenger in the seat. The sampling tree is shown in Figure 3.24.

Figure 3.24: Cabin Sampling Tree (Trupka, 2011)

All four sampling tubes are 5 mm inside diameter 304 stainless steel. Each sampling tube is connected to an SMC Pneumatics NVKF334V-3G two-way solenoid valve. The four solenoid valves are all connected to a single outlet port. The outlet port on the manifold block is attached to a vinyl tube, which leads to the sampling port of the cabin CO_2 analyzer. There is a fifth solenoid valve on the tree that is open to the atmosphere, and it allows the cabin analyzer to continuously draw a sample if the other four ports are closed.

3.3.3: Control System

All of the CO_2 sampling and injection equipment and sensors are controlled by a computer running a LabVIEW data acquisition program. A screenshot of the tracer gas LabVIEW program is shown in Figure 3.25, and it is the same program used by (Trupka 2011).

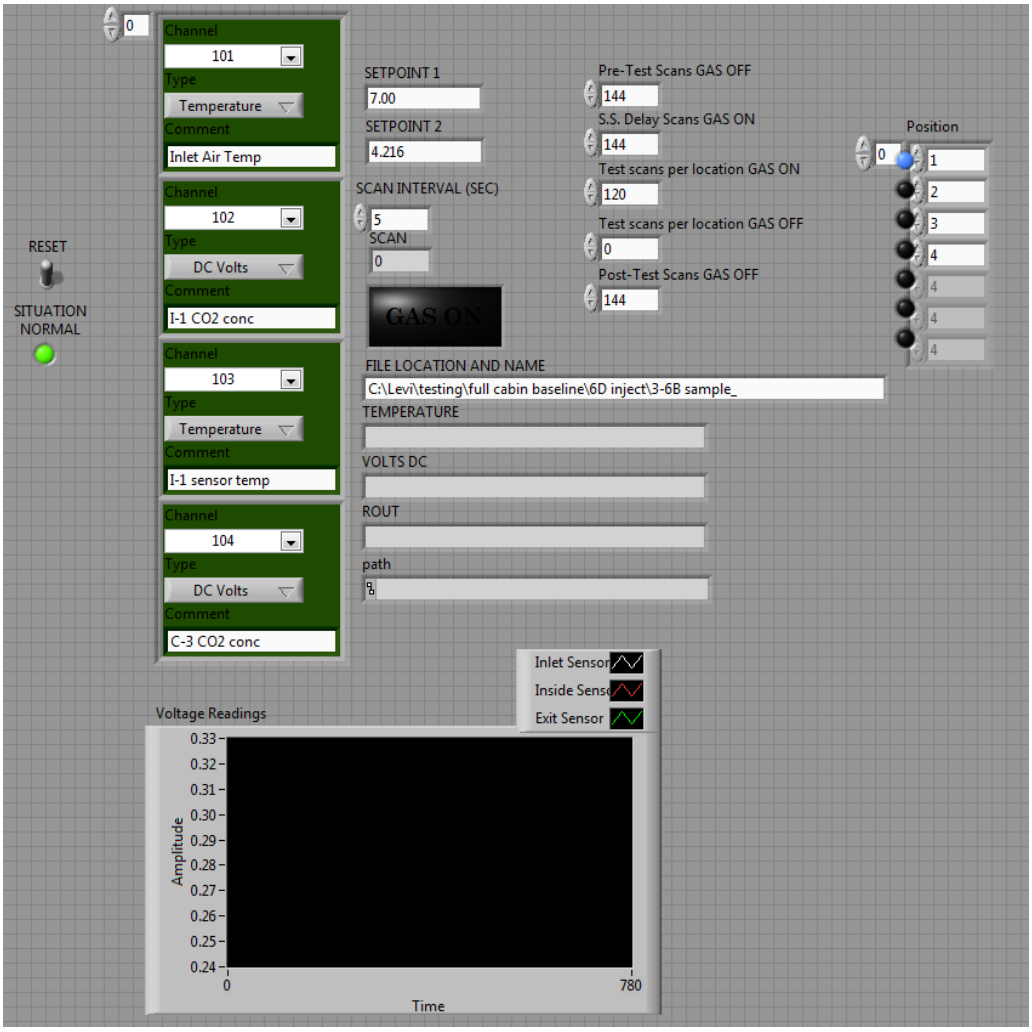

Figure 3.25: Cabin Sampling and Control Program

The computer saves the sensor data into a comma-separated values (.csv) file that the user can open with Excel. The LabVIEW program allows the user to select CO_2 injection rate, He injection rate, sampling rate, and the file name by changing the input values shown in the second column of Figure 3.25. The number of scans at the different ports on the sampling tree can also be changed to permit a greater variety of tests by changing the values shown in the third and fourth columns of Figure 3.25.

The computer is connected to an Agilent 34970A DAQ, which collects data from the three CO_2 analyzers, 12 thermistors on the east wall of the cabin, 12 thermistors on the west wall of the cabin, and 14 thermistors on the temperature tree in the center of the cabin. The Agilent unit is equipped with a 34903A SPDT module that allows the DAQ to control the solenoid valves on the sampling tree. The tracer gas mass flow controllers are controlled by an MKS PR4000

power supply paired with an RS-232 interface unit. The power supply, stacked on top of the Agilent DAQ, is shown in Figure 3.26.

Figure 3.26: Power Supply and DAQ

Chapter 4 - Testing Procedures

There were two different types of experiments completed in the mock-up aircraft cabin. The objective of the first series was to determine the effect of a reduced passenger load on the transport of contaminants in the cabin. The second series was completed to find contaminant movement when the supply air is turned off. Both tests utilized the same air supply system and tracer gas system that were described in Chapter 3. The details of each experiment are described in the following sections.

4.1 Reduced Passenger Load Testing

The first series focuses on how the number of passengers in the aircraft cabin affects the airflow characteristics. This effect is determined by comparing the transport of tracer gases throughout the cabin at two different passenger densities. To begin the test, tracer gas is injected into the cabin until the concentration reaches a steady state condition. This steady state concentration is measured at 32 seat locations for each of the three injection locations. The previous testing procedure is completed when all of the cabin seats are occupied by heated manikins, as a baseline test, and again when half of the cabin seats are occupied, for comparison.

Before actual testing began, detailed procedures for each of the tests were established. The injection and sampling locations that would best depict the airflow characteristics in the cabin, but still allow for a realistic number of tests, were determined, and three tracer gas injection locations were selected. The first injection seat was 4B, which is in the front-left section of the cabin. The second injection seat was 6D, which is in the center section of the cabin. The final injection seat was 8F, which is in the rear-right section of the cabin. These three tracer gas injection locations are shown in Figure 4.1, and the same injection locations are used for both the full load cabin testing and the half-full load cabin testing.

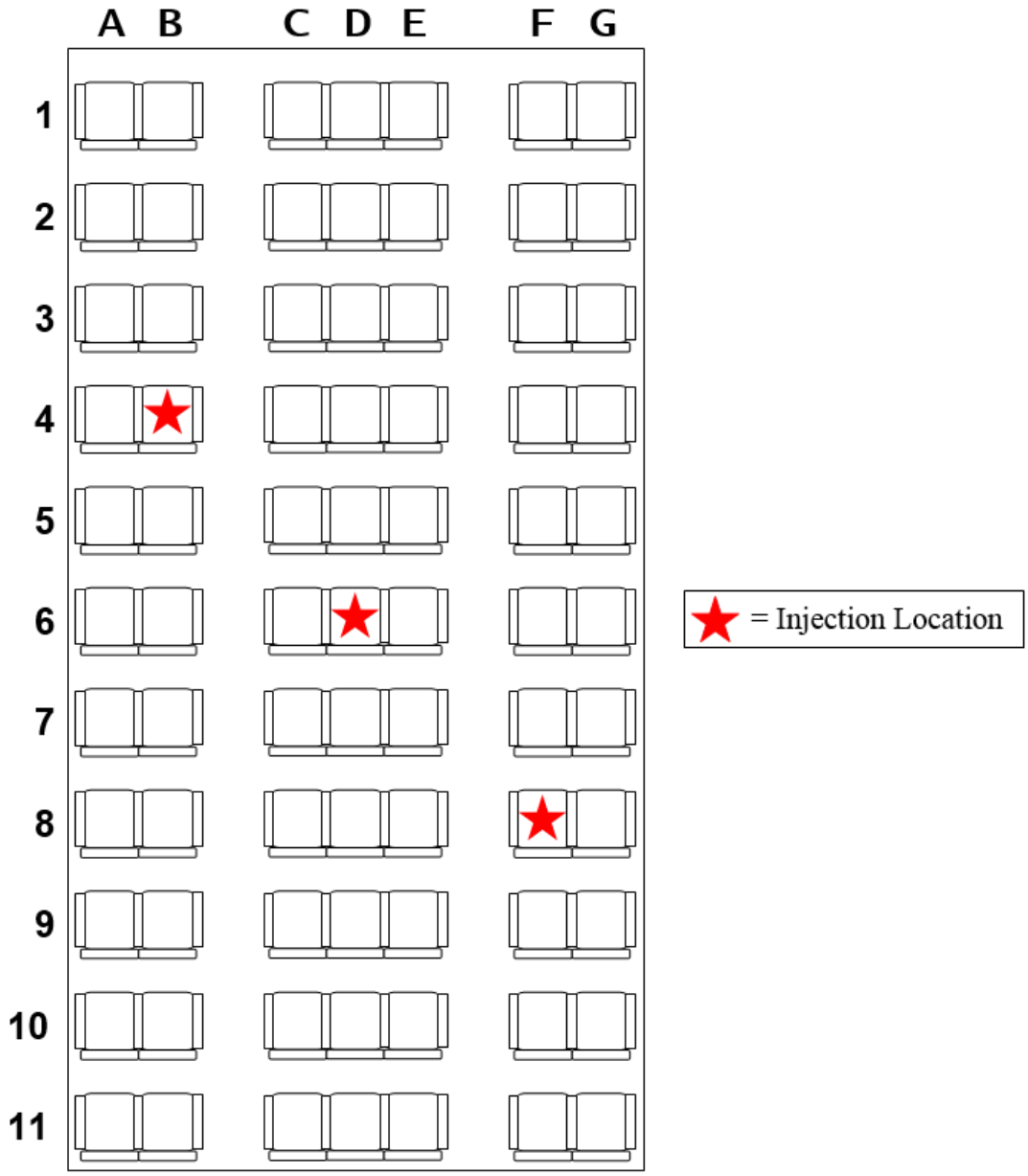

Figure 4.1: Passenger Load Test Injection Locations

The tracer gas sampling locations also needed to be selected for each of the injection locations. In order to reduce the number of tests required, it was decided to only place the sampling tree in 4 of the 7 columns of the aircraft cabin. Columns B, C, E, and F were chosen for all of the testing. Since the sampling tree has the ability to sample 4 consecutive seats in a single column of the cabin, it was decided that 8 rows of seats would be sampled for each tracer gas injection location. These locations amount to a total number of 32 seat locations sampled for each of the three injection locations. The sampling locations for each of the three injection locations are listed in Table 4.1.

Table 4.1: Passenger Load Test Sampling Locations

Injection Location	Sampling Rows	Sampling Columns
4B	1, 2, 3, 4, 5, 6, 7, and 8	B, C, E, and F
6D	3, 4, 5, 6, 7, 8, 9, and 10	B, C, E, and F
8F	4, 5, 6, 7, 8, 9, 10, and 11	B, C, E, and F

Once the tracer gas injection and sampling locations were chosen for testing, the next step was to determine the tracer gas injection rate and sampling test length for each seat. The flow meter for CO_2 has a maximum flow rate of 10 LPM, but the injection rate must be large enough that the cabin analyzer can accurately measure the concentration across the cabin. Seven LPM of CO_2 was determined to be an ideal injection rate for the passenger load testing.

The next step was to determine the amount of time it takes the CO_2 concentration in the aircraft cabin to reach a steady state. The greatest seat distance between the injection and sampling locations during testing is approximately 6 seats, therefore this was chosen as the distance for the steady state baseline testing. Tracer gas was injected from seat 2D, the sampling port was placed in seat 8D, and was sampled for 30 minutes. The injection was then stopped, and the concentration was sampled for 30 minutes. The sampling tree and injection apparatus are shown in Figure 4.2, and the results from the steady state baseline testing is shown in Figure 4.3. The results in Figure 4.3 show that 12 minutes is an adequate time lapse to allow the cabin to rise to steady state CO_2 concentration, and 10 minutes is enough time for the cabin to return to atmospheric levels.

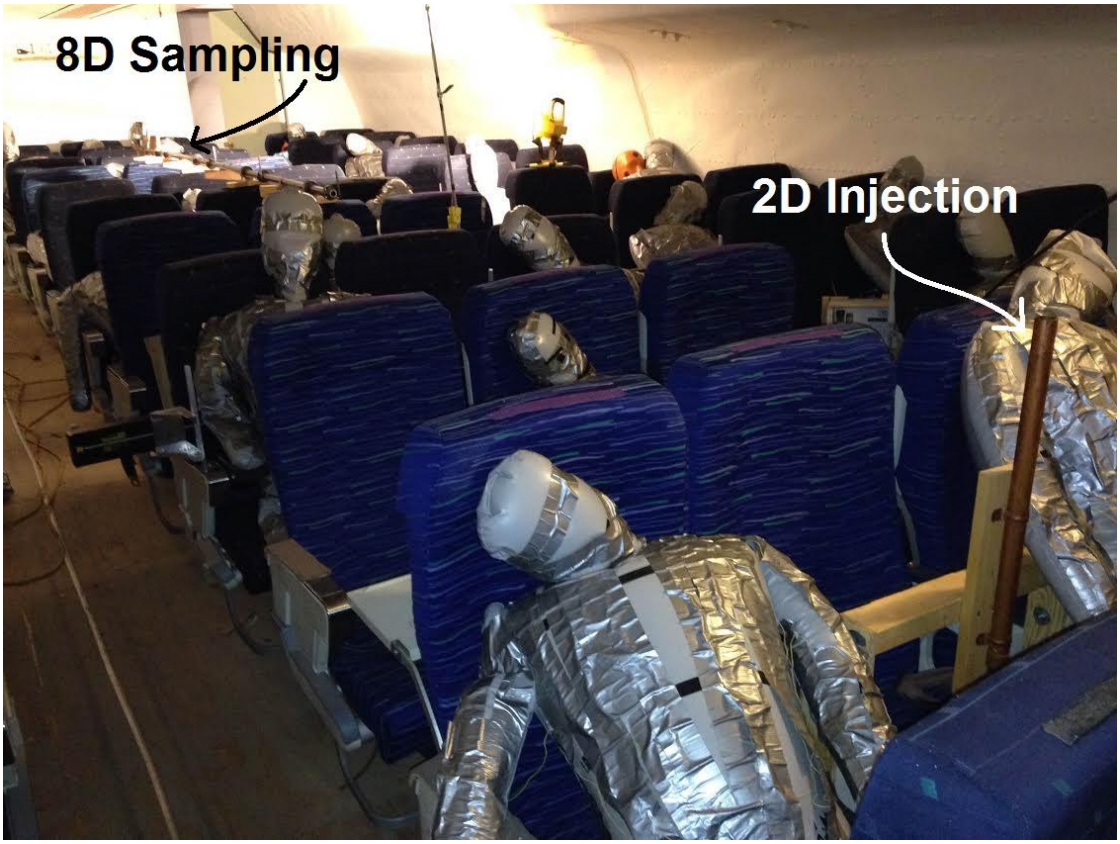

Figure 4.2: Passenger Load Test Steady State Test Location

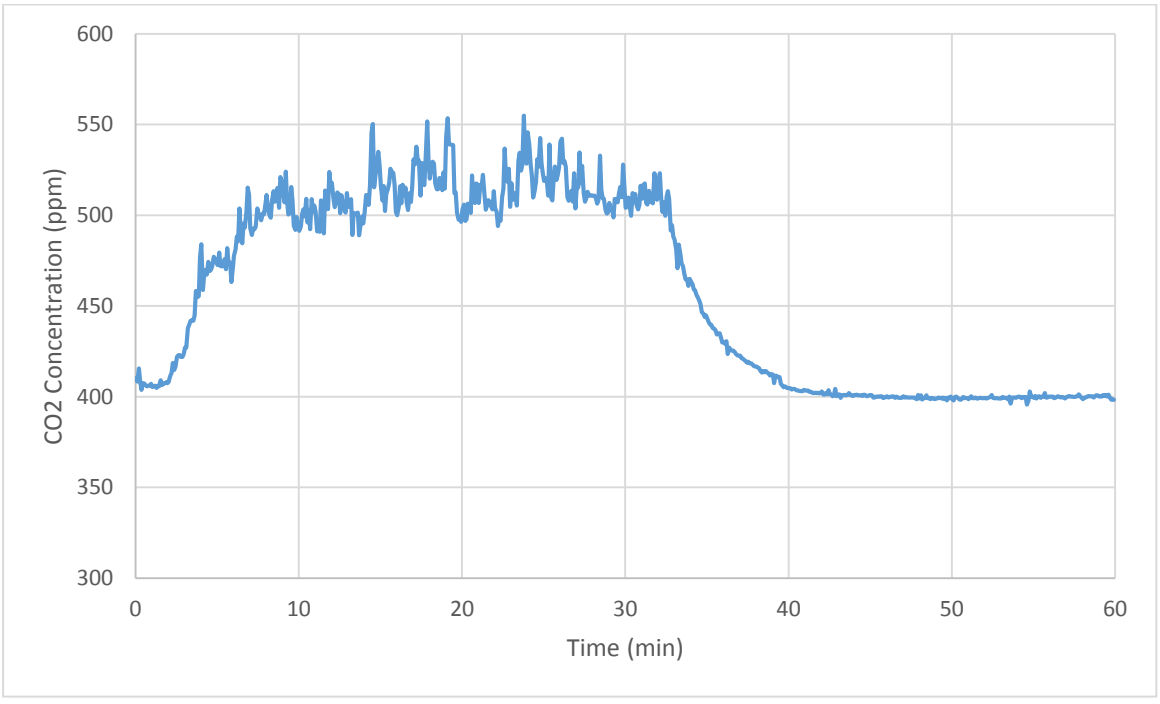

Figure 4.3: Tracer Gas Steady State Results

After the initial and final steady state times were determined, the next step was to find the optimal sampling duration for each sampling seat location. Three sampling durations of 5, 10, and 20 minutes were tested. It was found that the 10 minute sampling period was ideal to give an adequate CO_2 concentration for each seat location, without grossly increasing the experiment duration. The steady state and sampling time periods found from initial testing established the final testing procedure for the passenger load testing that are listed in Table 4.2.

Table 4.2: Passenger Load Testing Procedure

Stage	Process	Injection	Length (min)	Details
1	Steady state delay	On	12	Allows chamber to reach steady CO_2 concentration
2	Test sampling	On	10	Samples first seat
3	Test sampling	On	10	Samples second seat
4	Test sampling	On	10	Samples third seat
5	Test sampling	On	10	Samples fourth seat
6	After test delay	Off	10	Allows chamber to reach ambient CO_2 concentration

4.1.1 Full Cabin Baseline Test

The testing procedures listed in Table 4.2 were completed with the mock-up aircraft cabin completely occupied by thermal manikins in order to provide a baseline comparison for the half-full load cabin testing. Tests were repeated three times at all of the 32 sampling locations for each of the three injection locations to improve the repeatability of the results. For the full cabin testing, all 77 seats of the aircraft cabin were occupied by heated manikins as shown in Figure 4.4

Figure 4.4: Full Cabin Manikin Configuration

4.1.2 Half-Full Cabin Test

For the half-full cabin testing, only 38 of the seats in the aircraft cabin were occupied by heated manikins. There were three manikins in the odd numbered rows of the cabin, and the manikins were seated in columns B, D, and F. There were four manikins in the even numbered rows of the cabin, and the manikins were seated in columns A, C, E, and G. The manikin arrangement for the half-full testing is shown in Figure 4.5.

Figure 4.5: Half-Full Cabin Manikin Configuration

4.2 Contaminant Transport without Ventilation Test

The objective of the second round of testing was to determine the airflow characteristics inside the cabin after the ventilation air supply was turned off. Before testing began, the first step was to find the amount of time it took the cabin to achieve a steady state temperature. The supply air was maintained at the previously mentioned standard of 1400 cfm and 60°F, and the thermistors on the walls of the aircraft cabin were used to measure the temperature. Figure 4.6 shows the average temperature of the west and east cabin walls throughout the duration of the six hour steady state test. It can be seen that the cabin is brought to steady state temperature for the first four hours of the test. After four hours, the supply air was turned off and the manikins heated the cabin for the next 80 minutes until the maximum cabin temperature was reached. At this point, the safety switch was activated and the manikins turned off until the temperature of the cabin decreased to a safe level. From the data shown in Figure 4.6, it was determined that three hours was a sufficient amount of time to allow the cabin to reach a steady state temperature, and thirty minutes without any supply air would allow the CO_2 concentration and cabin temperature to increase to the desired levels.

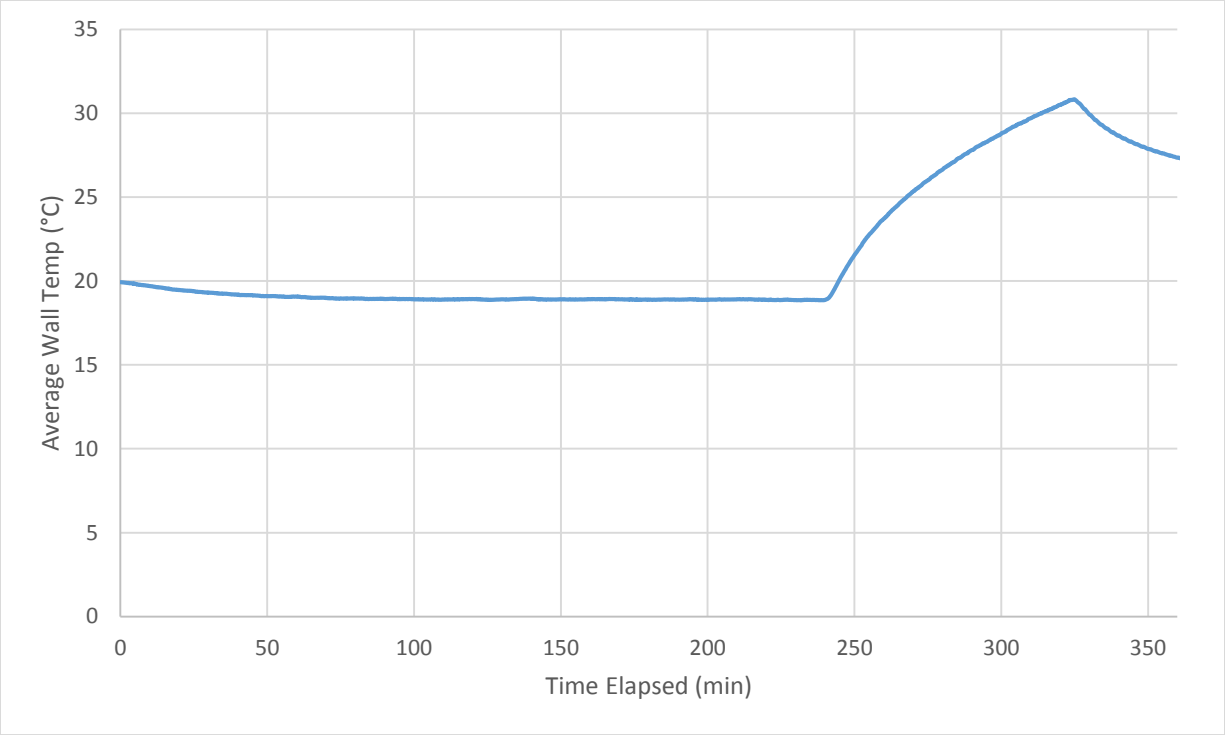

Figure 4.6: Steady State Temperature Results

Without the supply air being introduced to the cabin, the tracer gas concentrations increased much more rapidly. The cabin CO_2 analyzer can only measure a maximum concentration of 2000 ppm, so the tracer gas injection rate was decreased as the distance between the sampling and injection locations decreased. For the minimum spacing of one seat in the cabin, it was discovered that 2 LPM was the ideal injection rate of CO_2. Figure 4.7 shows the measured CO_2 concentration when the injection apparatus is releasing 2 LPM of CO_2 and is placed in seat 2D and the sampling tree is collecting in seat 3D.

Figure 4.7: Minimum CO_2 Injection Testing

The other limitation of the CO_2 analyzer is that it is difficult to achieve an accurate measurement if the CO_2 normalized concentration in the aircraft cabin is close to the atmospheric level (roughly 400 ppm). Further testing showed that the 2 LPM injection rate was insufficient if the injection and sampling apparatuses were further than 3 seats apart. It was found that three different injection rates must be utilized in order to allow accurate testing throughout the entirety of the cabin. Table 4.3 shows the various injection rates and their effective ranges.

Table 4.3: CO_2 Injection Rates and Ranges

CO_2 Injection Rate (LPM)	He Injection Rate (LPM)	Usable Range (seats)
2.00	1.20	1-3
4.00	2.41	4-6
7.00	4.21	7-9

After the CO_2 injection parameters were determined, the next step was to select the injection and sampling locations required to effectively understand the air movement inside the test cabin. It

was decided that the testing could be completed by injecting the tracer gas from a single seat in the cabin. Seat 2D was selected as the ideal injection location, because it is in the center column of the cabin, allowed for testing a long span of seats behind the injection location, allowed for sampling in front of the injection location, and allowed for the 6 other seats in row 2 to be sampled. Figure 4.8 shows the selected injection and sampling locations, and symbol description is provided in the legend.

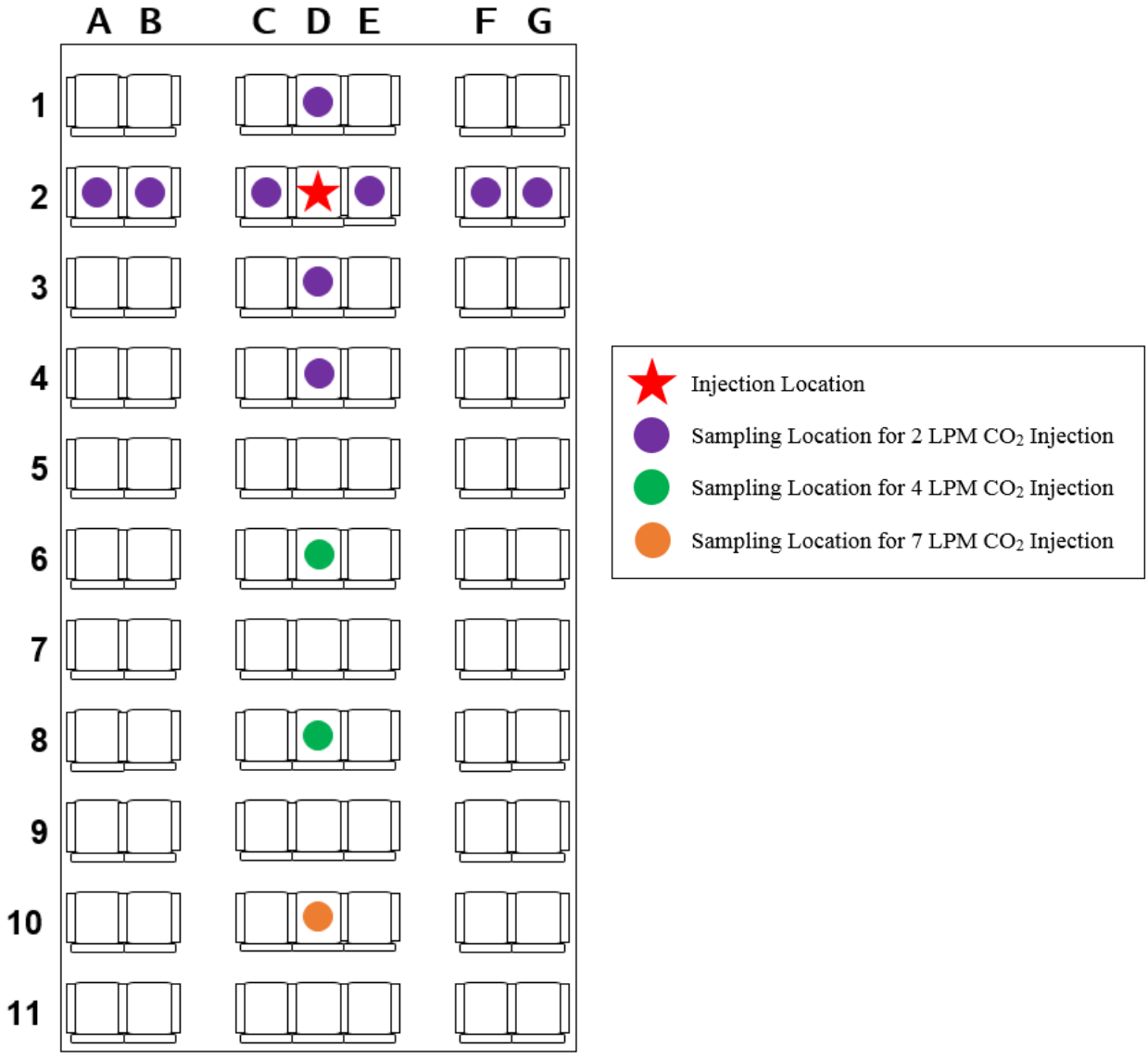

Figure 4.8: No Air Supply Sampling and Injection Locations

The test procedure listed in Table 4.4 was executed for each of the 12 sampling locations three times to improve repeatability. Each test began with the three hour steady state temperature

period. The tracer gas injection then begins for 30 minutes until the cabin reaches a steady CO_2 concentration. After steady tracer gas concentration and temperature were achieved, the cabin supply air was turned off and the transient CO_2 concentration was sampled for an additional 30 minutes. There was no post-test steady state period, since the lingering tracer gas was flushed from the enclosure during the first three hours of the following test.

Table 4.4: No Air Flow Testing Procedures

Stage	Process	Injection	Supply Air	Length (min)
1	Bring cabin to steady temperature	Off	On	180
2	Bring cabin to steady CO_2 concentration	On	On	30
3	Test sampling	On	Off	30

Chapter 5 - Results and Data Analysis

This chapter presents the results of testing and the analysis of test results. The results from each individual test completed for this thesis is not presented in this chapter, but each test result is archived in the electronic appendix that is included with this document. The results shown in this chapter are from three tests averaged together to provide more accurate results. The instructions for the electronic appendix are in Appendix B.

5.1 Data Analysis

When a test is executed in the mock-up aircraft cabin, the LabVIEW software collects all the sensor data and compiles them into a comma separated value (.csv) file. This file can be opened by Excel spreadsheet software and shows the tracer gas injection status, time elapsed, the voltage output of all 3 CO_2 analyzers, and the temperature measured by all 34 thermistors in the cabin. This raw collected data must be analyzed in order to provide useful information. The time elapsed is already in milliseconds and the thermistor values are already in degrees Celsius, so these results require no further modification. On the other hand, the voltage output of the CO_2 analyzers must be converted into parts per million (ppm) of CO_2 in air.

The analyzers' voltage readings are converted to ppm of CO_2 by calibrating the analyzers. All of the analyzers are calibrated every other week throughout the testing duration. Calibration is performed by connecting the analyzers to 50 lb cylinders containing CO_2 mixed with air. Three concentrations of CO_2 and air are used for calibration: 500, 1000, and 2000 ppm of CO_2 in air. The 50 lb cylinders are connected to a pressure regulator to allow for only a small amount of mixture to be bled out to the analyzers, but a balancing system was also installed downstream to further protect the analyzers. This balancing system is shown in Figure 5.1. It ensures that any of the mixture not sampled through the analyzer is exhausted to the atmosphere, without allowing any atmospheric air to contaminate the calibration process.

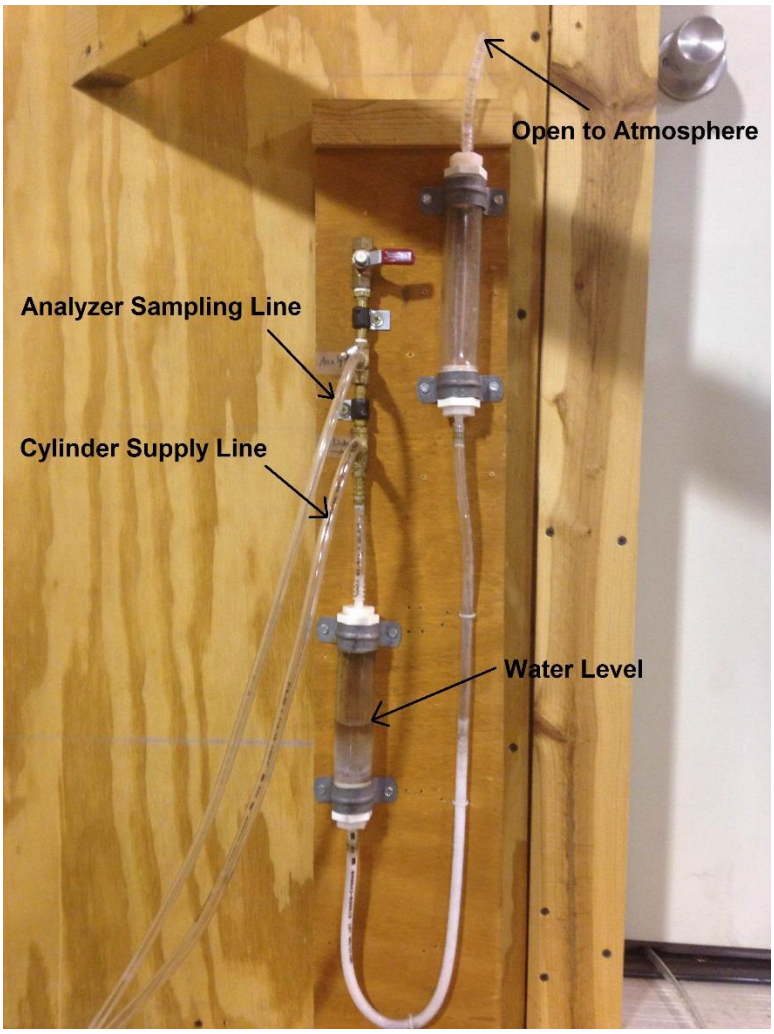

Figure 5.1: Calibration Balancing System

Each of the mixtures is sampled by all three of the analyzers for 10 minutes, and the average of each analyzer's output voltage is recorded. Using these three points, a line of best fit is created to convert from output voltage to CO_2 concentration for all of the analyzers. An example of this conversion equation is shown in Figure 5.2 from a calibration performed on the cabin analyzer on 8/21/14.

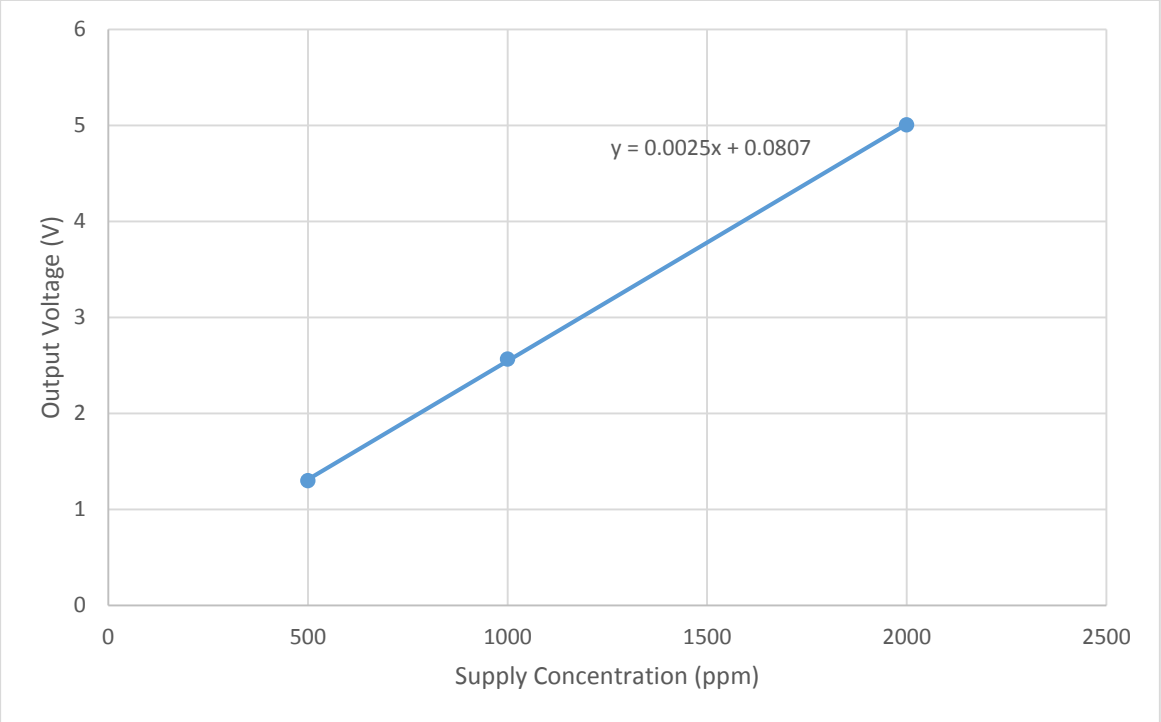

Figure 5.2: Voltage to PPM Line of Best Fit

5.1.1 Normalization for Reduced Passenger Load Testing

After the sensor data is manipulated to the proper units, the results must be normalized to account for variations in atmospheric CO_2 levels, different tracer gas injection rates, and different ventilation air rates. This is accomplished by using Equation (5.1), where N is the normalized CO_2 count, C is the measured CO_2 concentration, and V is the volumetric flow rate.

$$N = \frac{C_{cabin} - C_{inlet}}{\dot{V}_{CO_2} \Big/ \dot{V}_{supply}} \tag{5.1}$$

It was found by (Trupka, 2011), that the normalization process could be further improved by utilizing a transient average of the inlet CO_2 concentration. The transient average is calculated by averaging current inlet CO_2 concentration with the 29 concentrations preceding it. These 30 samples span a time of 2.5 minutes. The inlet CO_2 concentration for a test in the cabin is shown in Figure 5.3, and the same test data are shown in Figure 5.4 using the transient average previously described. It is obvious from the two figures that transient average effectively smoothed the test data, but the first 2.5 minutes of test data are neglected to create the average.

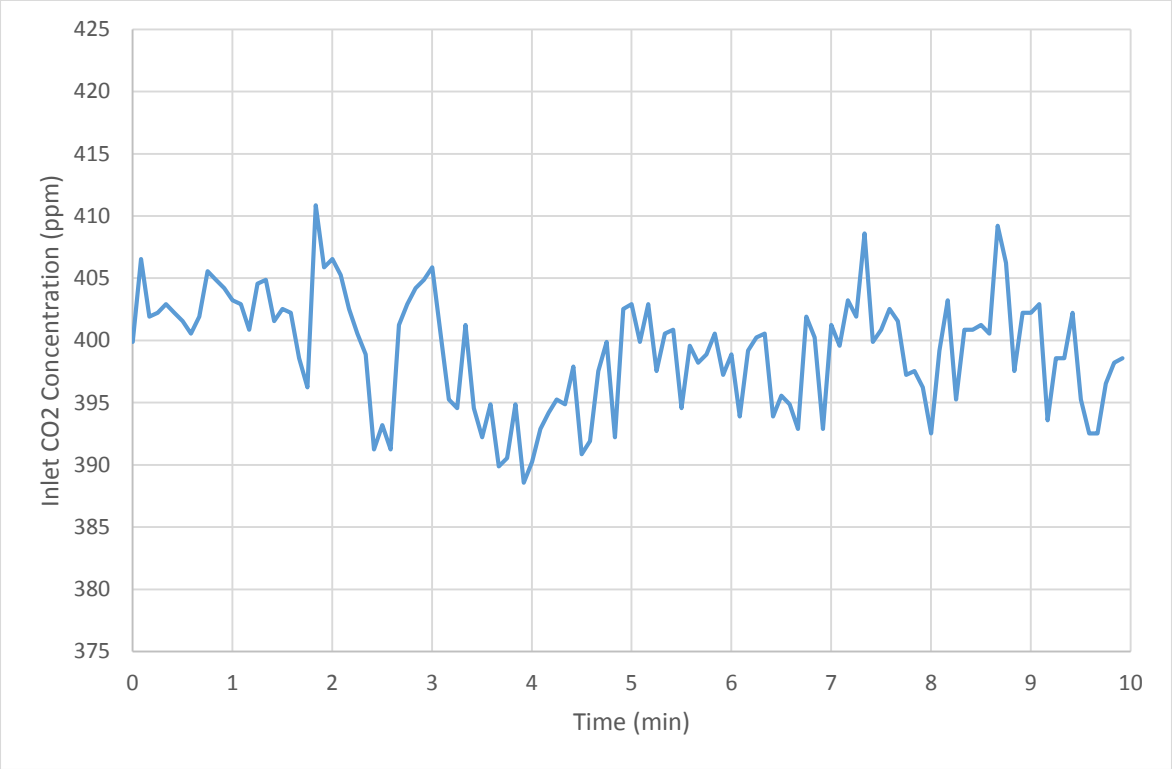

Figure 5.3: Raw Inlet CO_2 Concentration

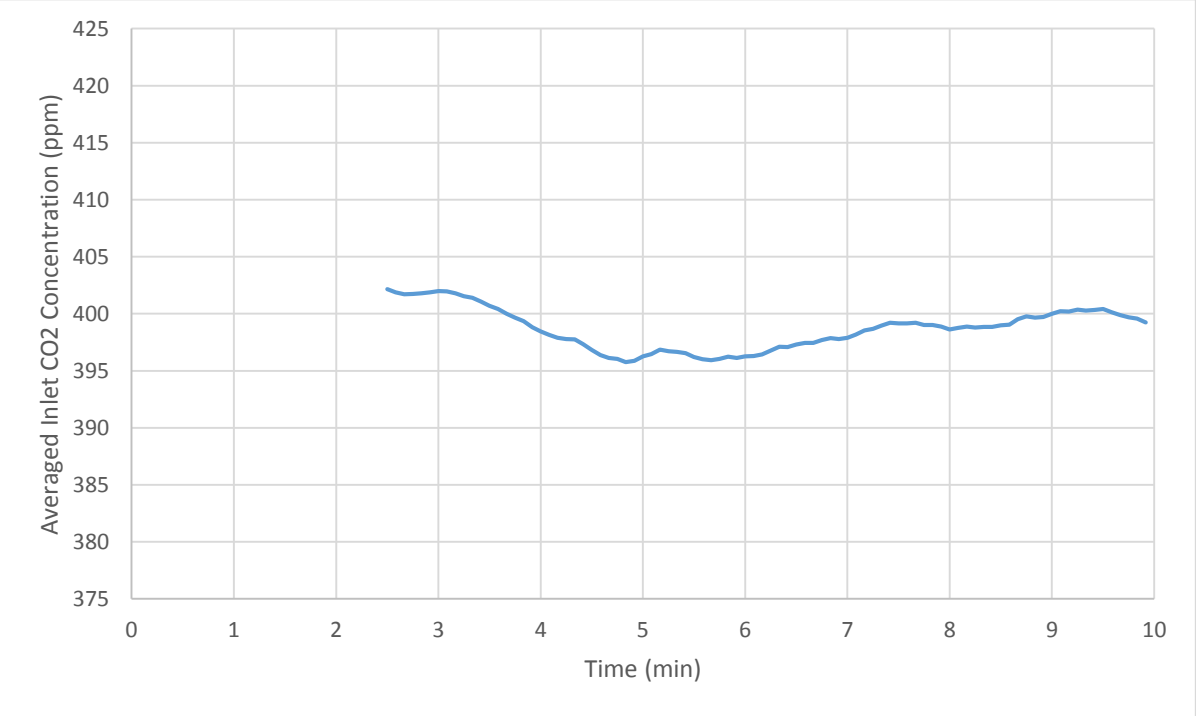

Figure 5.4: Transient Average Inlet CO_2 Concentration

5.1.2 Normalization for no Ventilation Air Testing

The normalization method used in the reduced passenger load testing must be slightly modified for the testing without ventilation air. Since the CO_2 injected into the cabin is no longer being removed by the supply air, the normalization equation must also be a function of time. The normalizing equation used is shown in Equation (5.2), where N is the normalized CO_2 count, C_{sample} is the sampled cabin CO_2 concentration, C_{start} is the cabin CO_2 concentration when the supply air is eliminated, T is the time elapsed since the supply air is eliminated, and V_{CO2} is the volumetric flow rate of CO_2 injected into the cabin, and V_{cabin} is the volume of air inside the mock-up cabin. The cabin's volume term is included so the normalized results will be repeatable in any testing scenario.

$$N = \frac{C_{sample} - C_{start}}{\dot{V}_{CO_2} \times T \Big/ V_{cabin}} \tag{5.2}$$

5.2 Reduced Passenger Load Results

In the following sections, the results of the reduced passenger load testing are discussed. Due to the length constraints, the results for each individual test are not presented in this document, but are attached in the electronic appendix. Testing begins by completing the tests with a fully loaded aircraft cabin to be used as a baseline comparison. The same tests are then repeated with a half-fully loaded aircraft cabin, and the results are compared to determine the passenger loading effects.

5.2.1 Full Cabin Results

Tracer gas is injected at seat locations 4B, 6D, and 8F in order to identify the passenger loading effects throughout the entirety of the aircraft cabin. Since the amount of the data that can be presented in this report is limited, only the full cabin test results for the 4B seat injection location are shown. The full cabin results for the 6D and 8F injection locations are attached in the electronic appendix. The seats in rows 1 through 8 and columns B, C, E, and F are sampled for the 4B injection location, which totals to 32 sampling seats. Each sampling test is performed three times using the procedures outlined in Table 4-2. The results from the three averaged test

runs for the first injection location are shown in Figure 5.5 through Figure 5.12. Each figure shows the sampled CO_2 concentrations for the four seats the sampling tree evaluated.

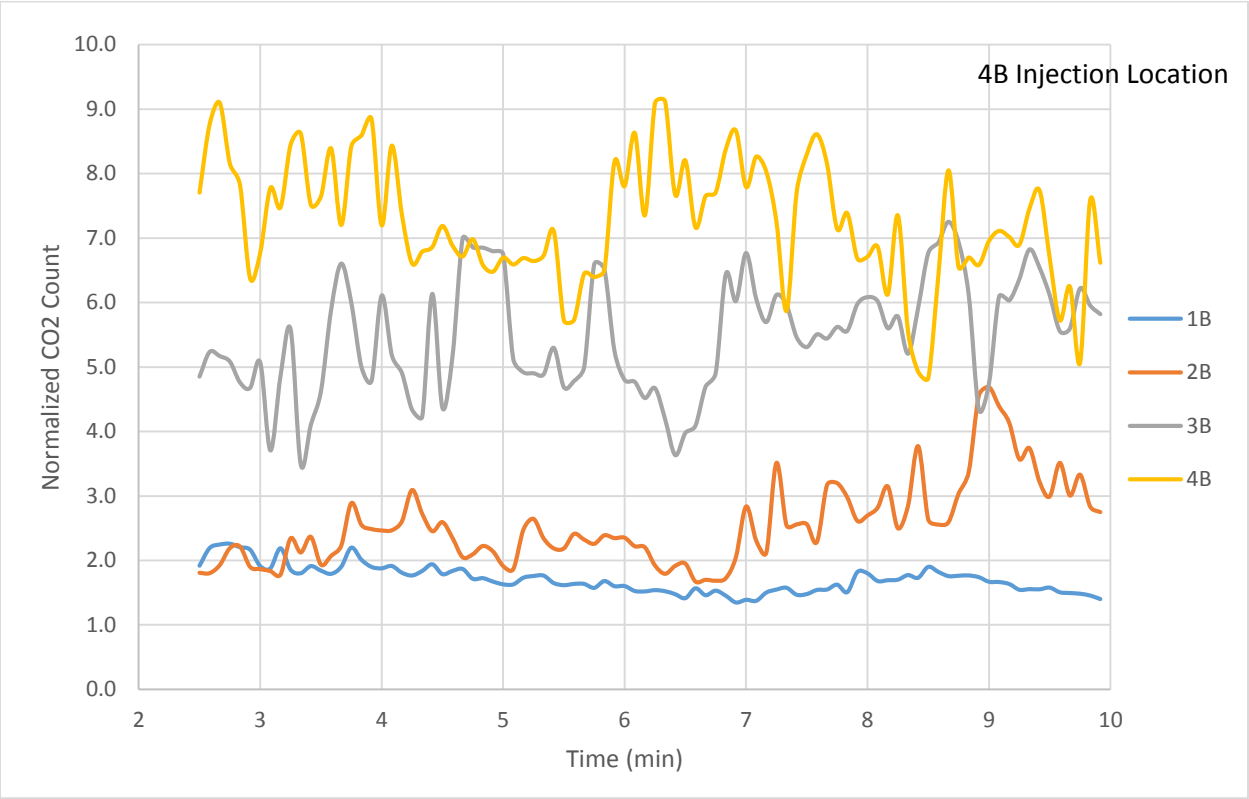

Figure 5.5: Seats 1-4B Full Load (3 Run Average)

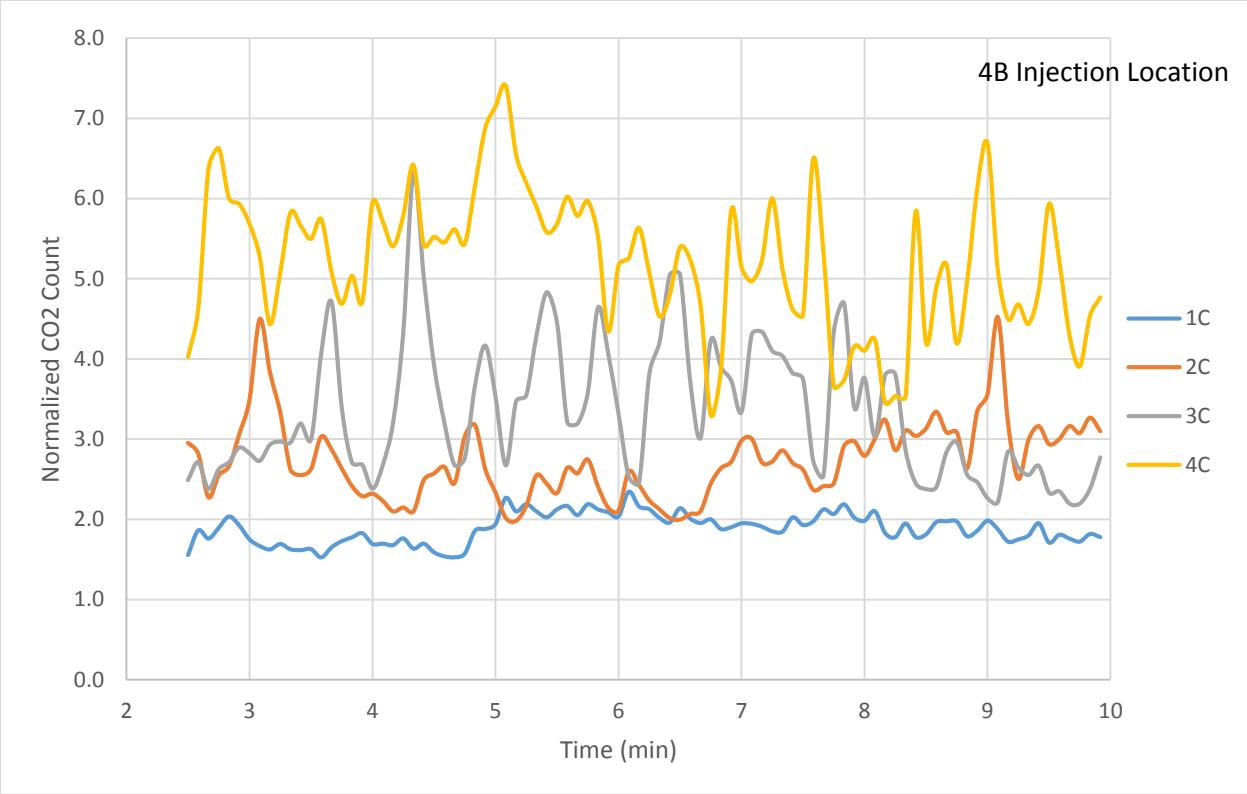

Figure 5.6: Seats 1-4C Full Load (3 Run Average)

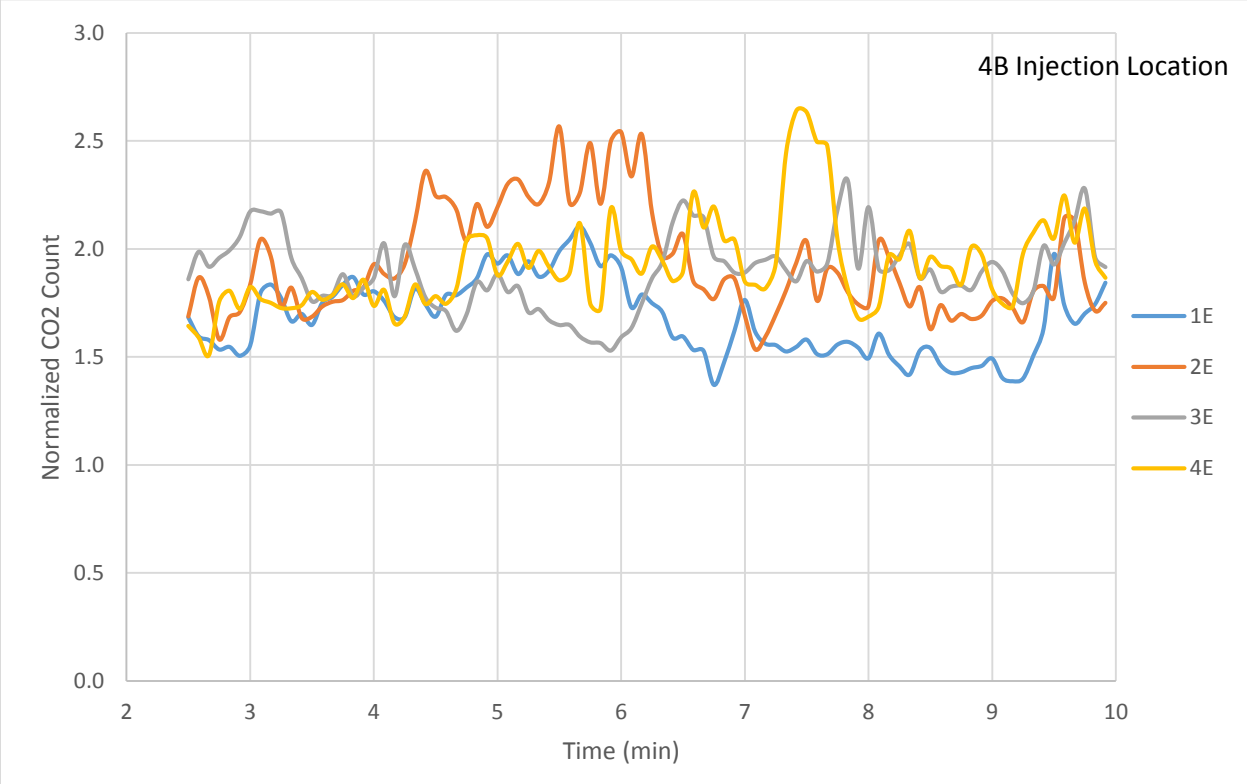

Figure 5.7: Seats 1-4E Full Load (3 Run Average)

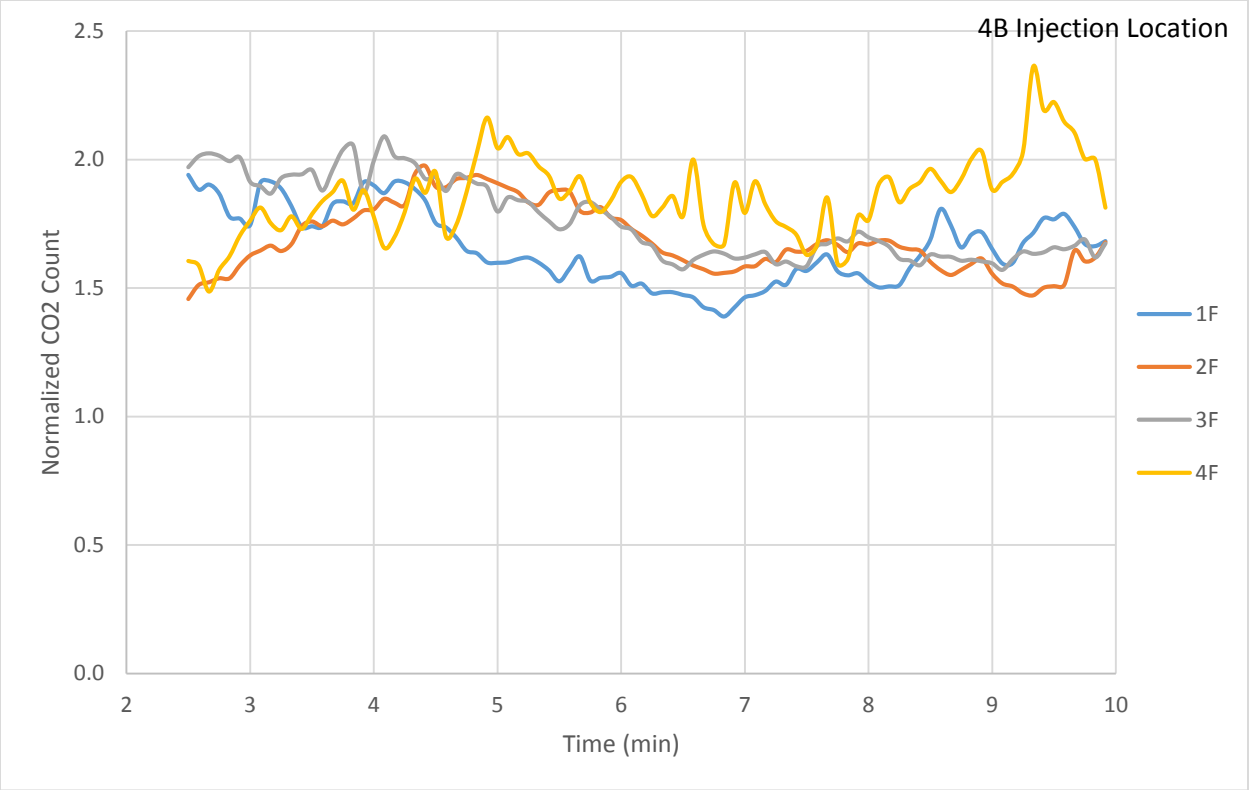

Figure 5.8: Seats 1-4F Full Load (3 Run Average)

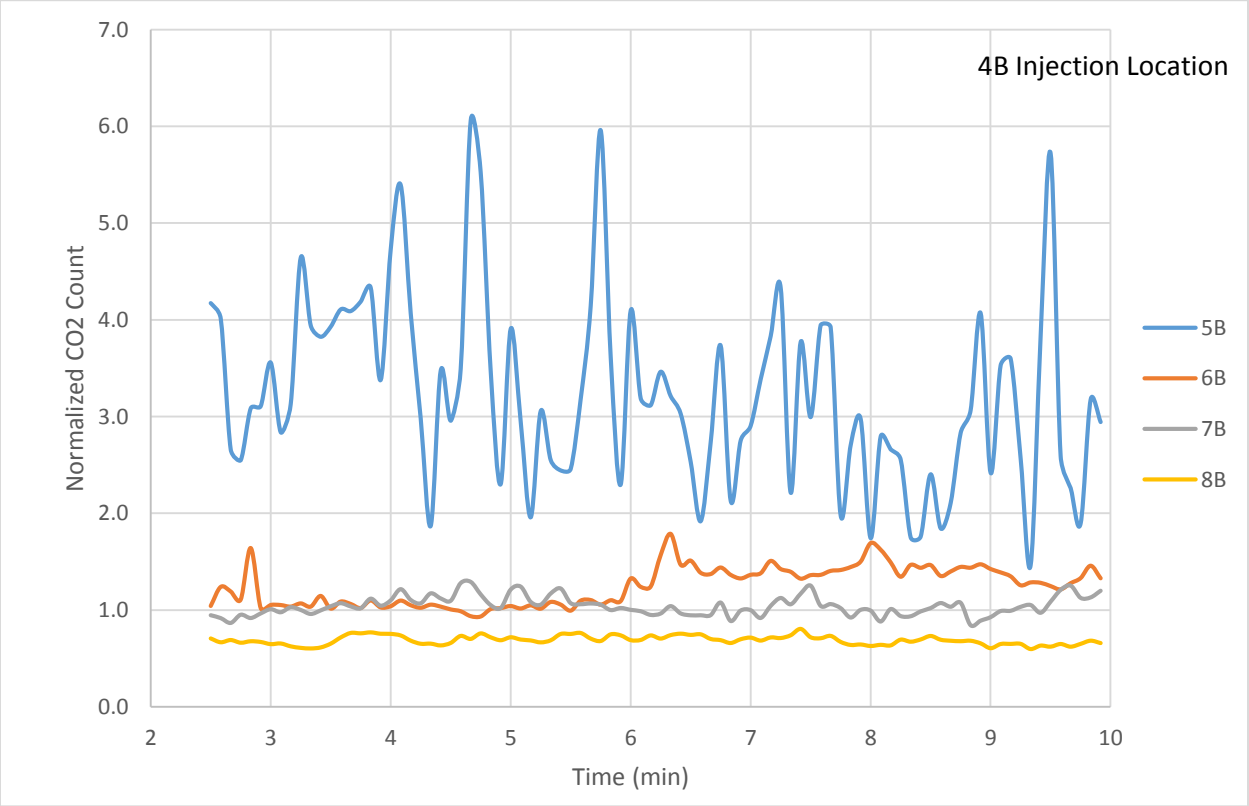

Figure 5.9: Seats 5-8B Full Load (3 Run Average)

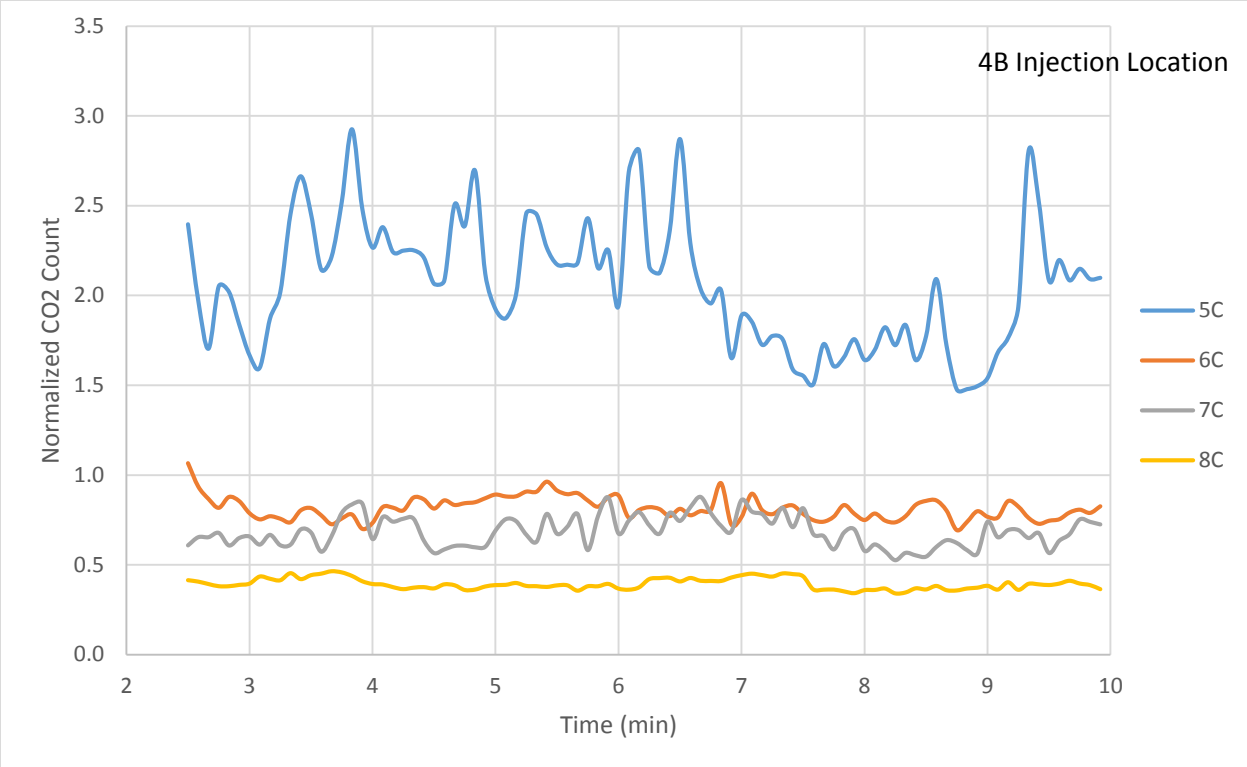

Figure 5.10: Seats 5-8C Full Load (3 Run Average)

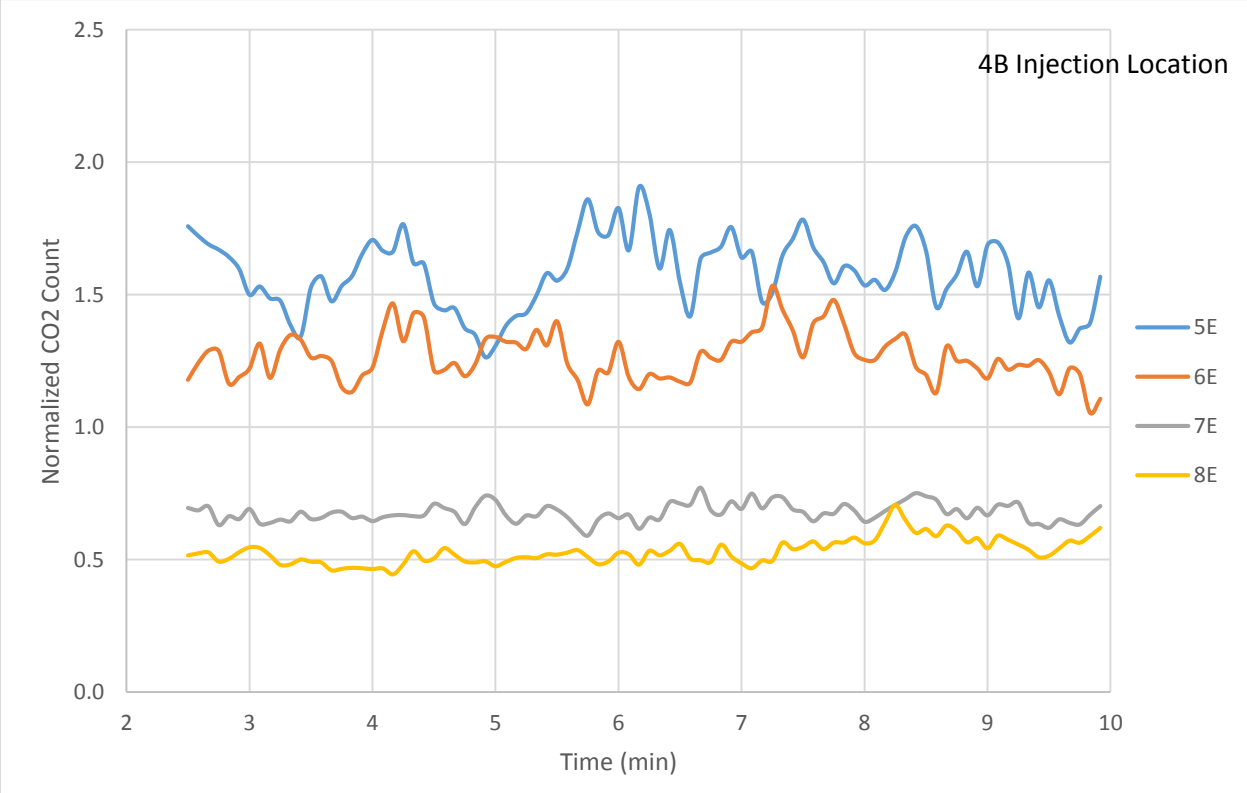

Figure 5.11: Seats 5-8E Full Load (3 Run Average)

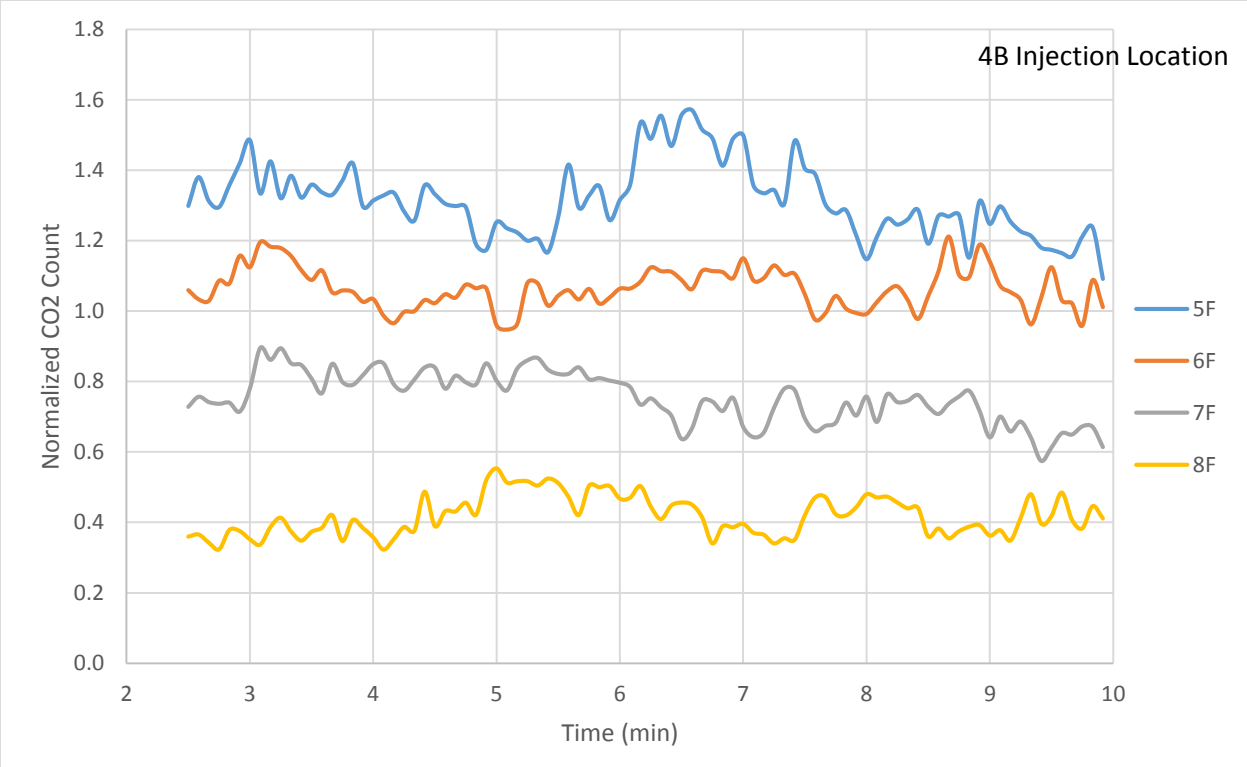

Figure 5.12: Seats 5-8F Full Load (3 Run Average)

After the three test runs for each sampling seat location are completed, the average normalized CO_2 concentration is calculated. This procedure is performed for all 32 sampling seat locations for each injection seat location. The average normalized CO_2 concentrations for the 4B injection location are shown in Figure 5.13 and listed in Table 5.1. Again, the results for the 6D and 8F injection locations can be found in the electronic appendix.

Table 5.1: Full Load Average Normalized CO_2 Concentrations

	A	B	C	D	E	F	G
1		1.71	1.88		1.68	1.66	
2		2.55	2.73		1.94	1.69	
3		5.48	3.32		1.89	1.77	
4		7.26	5.21		1.92	1.86	
5		3.23	2.06		1.58	1.32	
6		1.25	0.81		1.27	1.06	
7		1.04	0.68		0.68	0.75	
8		0.69	0.39		0.53	0.42	

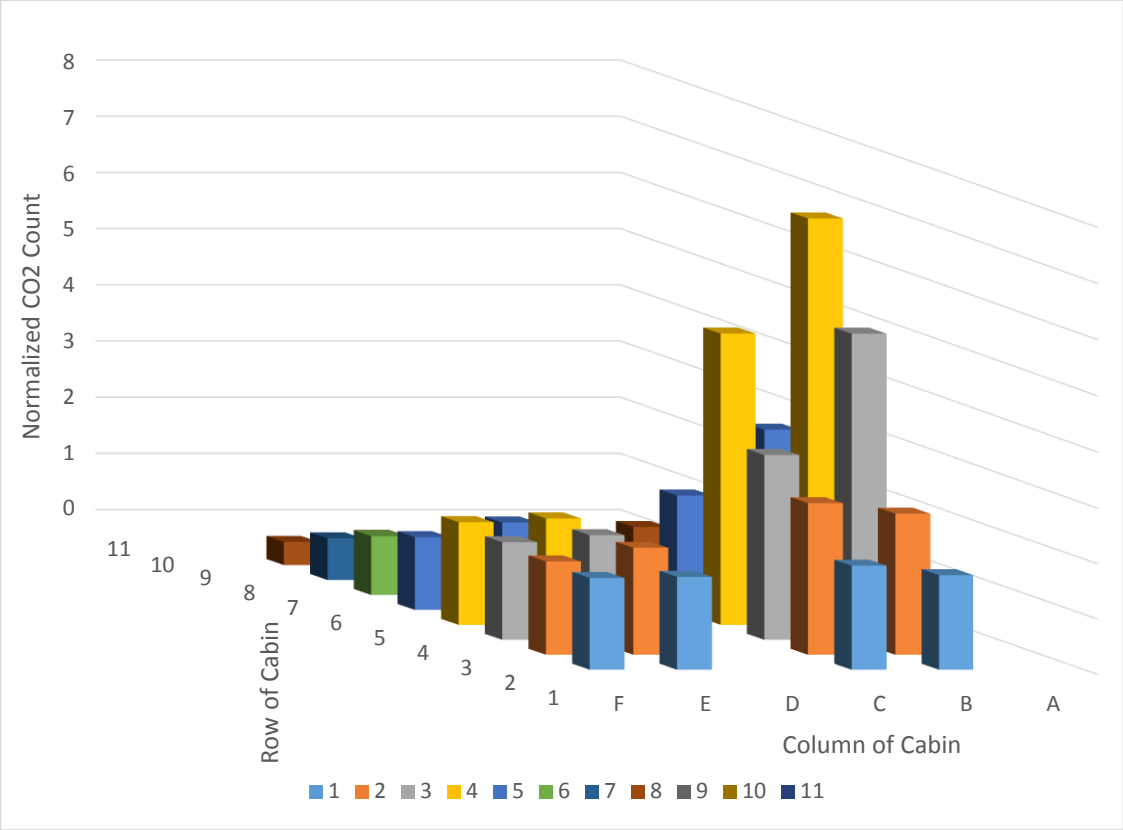

Figure 5.13: Full Load Average Normalized CO_2 Concentrations

5.2.2 Half-Full Cabin Results

Once the full load baseline test is completed, the half-full load testing begins. The same tracer gas injection locations are repeated for both testing scenarios (4B, 6D, and 8F). The same tracer gas sampling locations are also repeated (rows 1 through 8 and columns B, C, E, and F for the 4B injection location). The half-full test data for the 6D and 8F injection locations can be found in the electronic appendix. Each seat location is sampled for three independent tests, and the results from the three averaged test runs for the half-full load testing for the 4B injection location are shown in Figure 5.14 through Figure 5.31. Each figure shows the normalized CO_2 concentration measured by the sampling tree for the four seat locations mentioned in the legend and figure title.

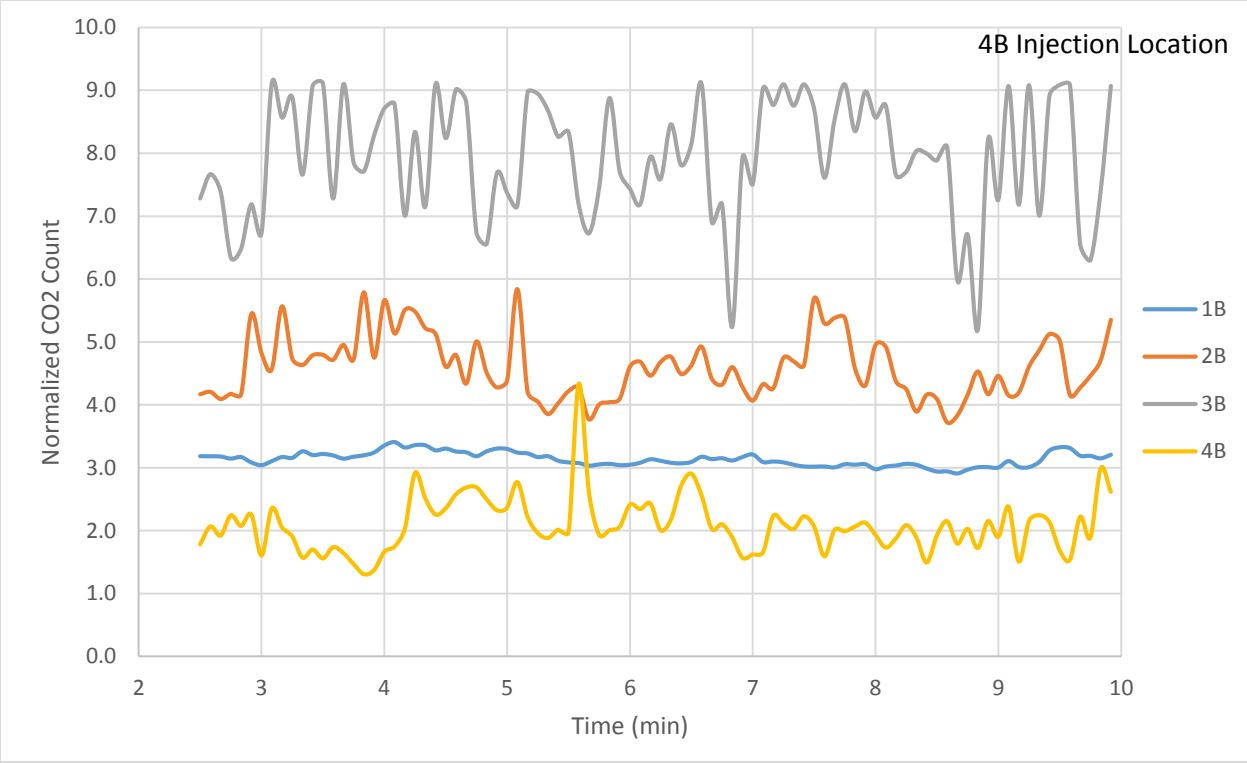

Figure 5.14: Seats 1-4B Half-Full Load (3 Run Average)

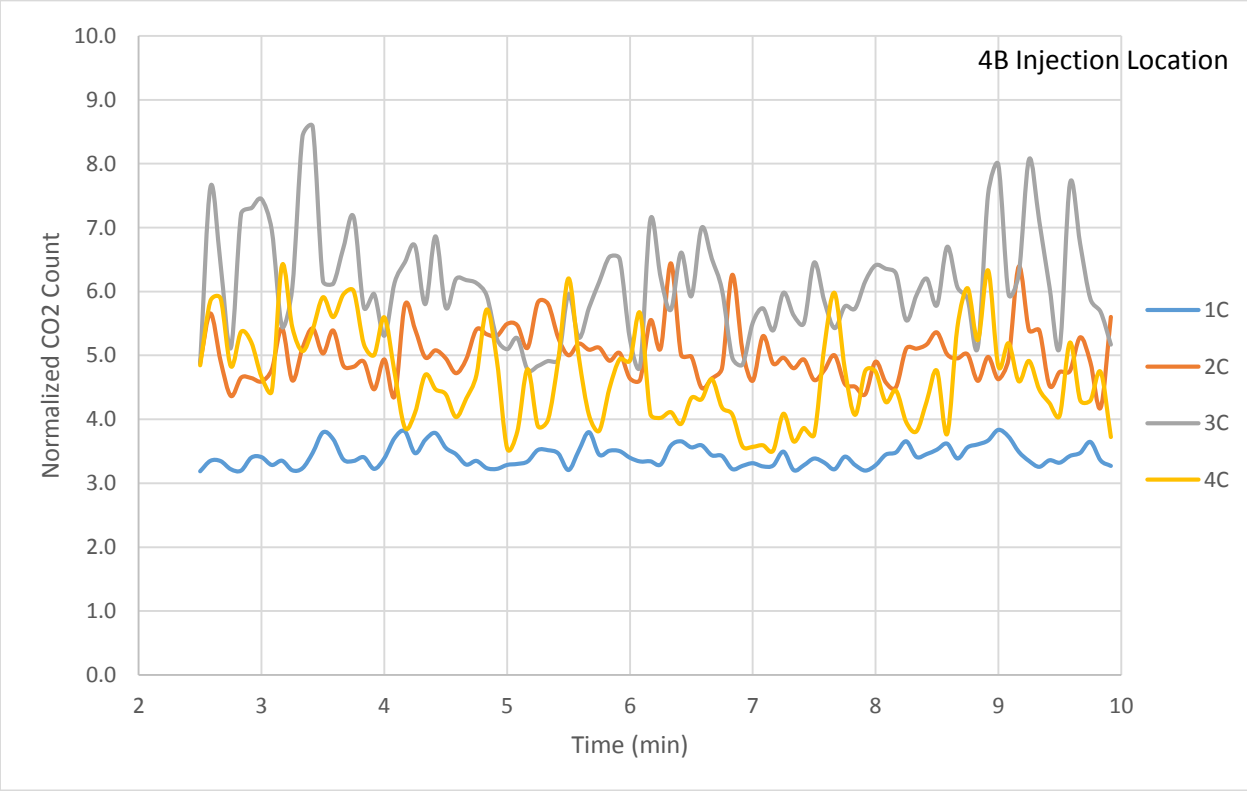

Figure 5.15: Seats 1-4C Half-Full Load (3 Run Average)

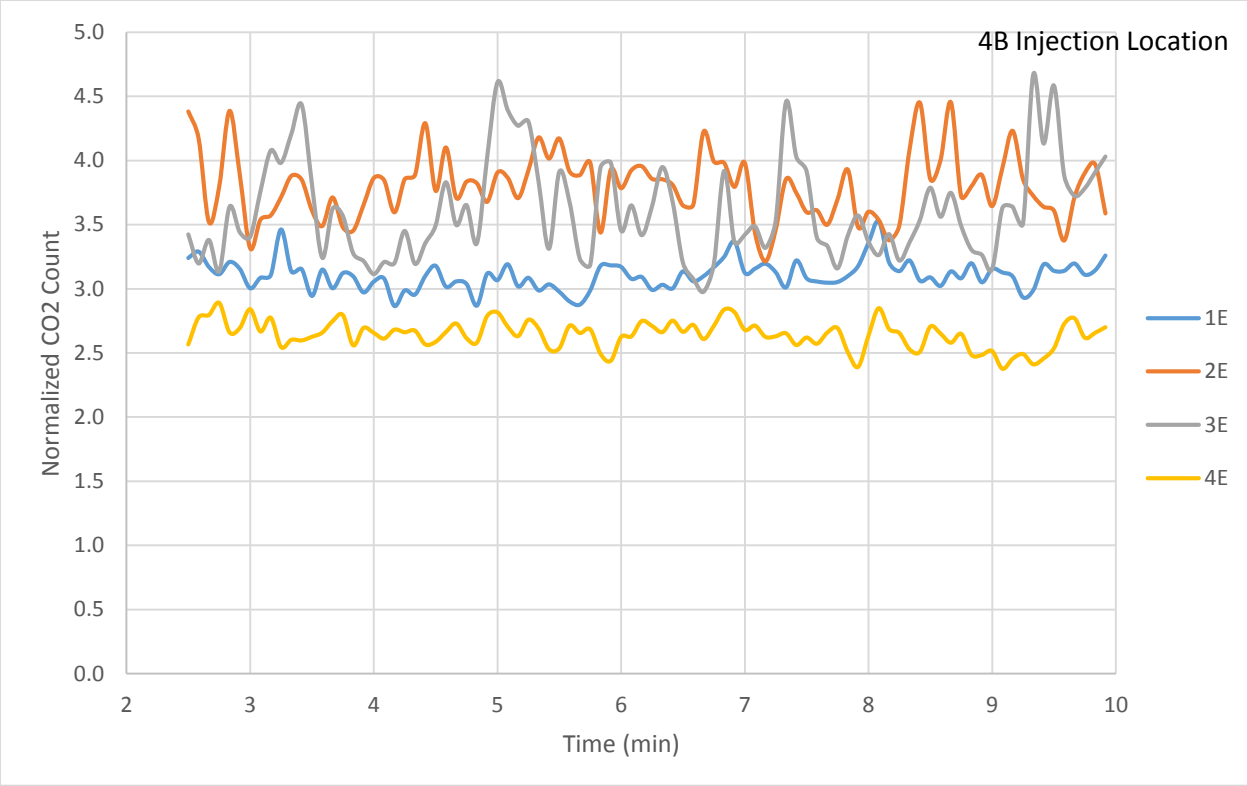

Figure 5.16: Seats 1-4E Half-Full Load (3 Run Average)

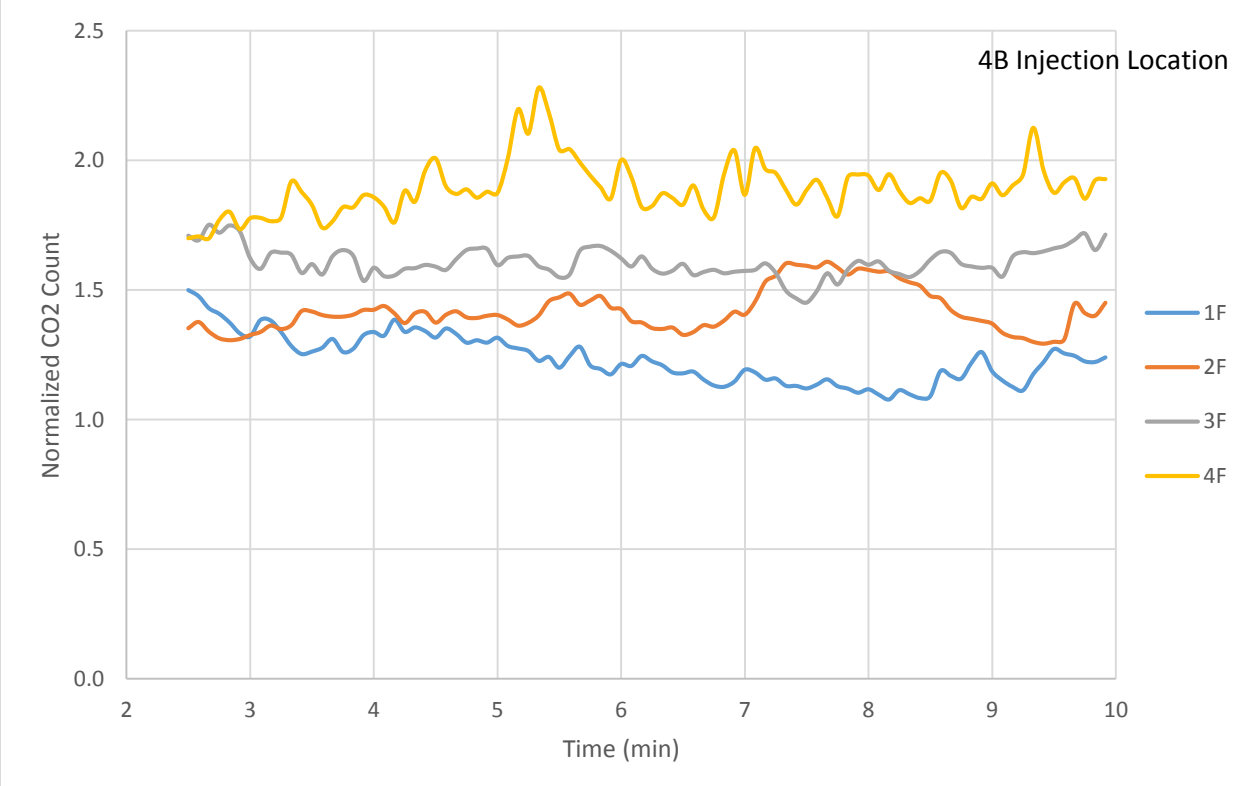

Figure 5.17: Seats 1-4F Half-Full Load (3 Run Average)

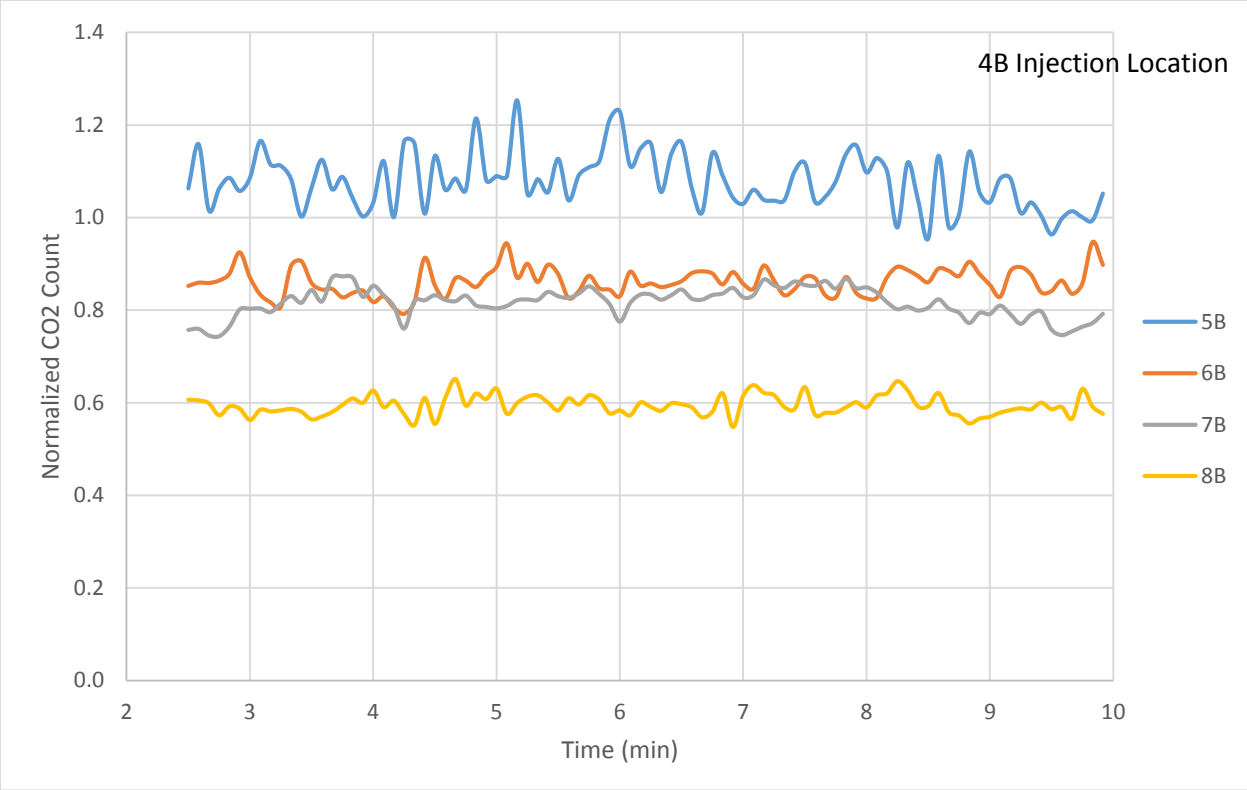

Figure 5.18: Seats 5-8B Half-Full Load (3 Run Average)

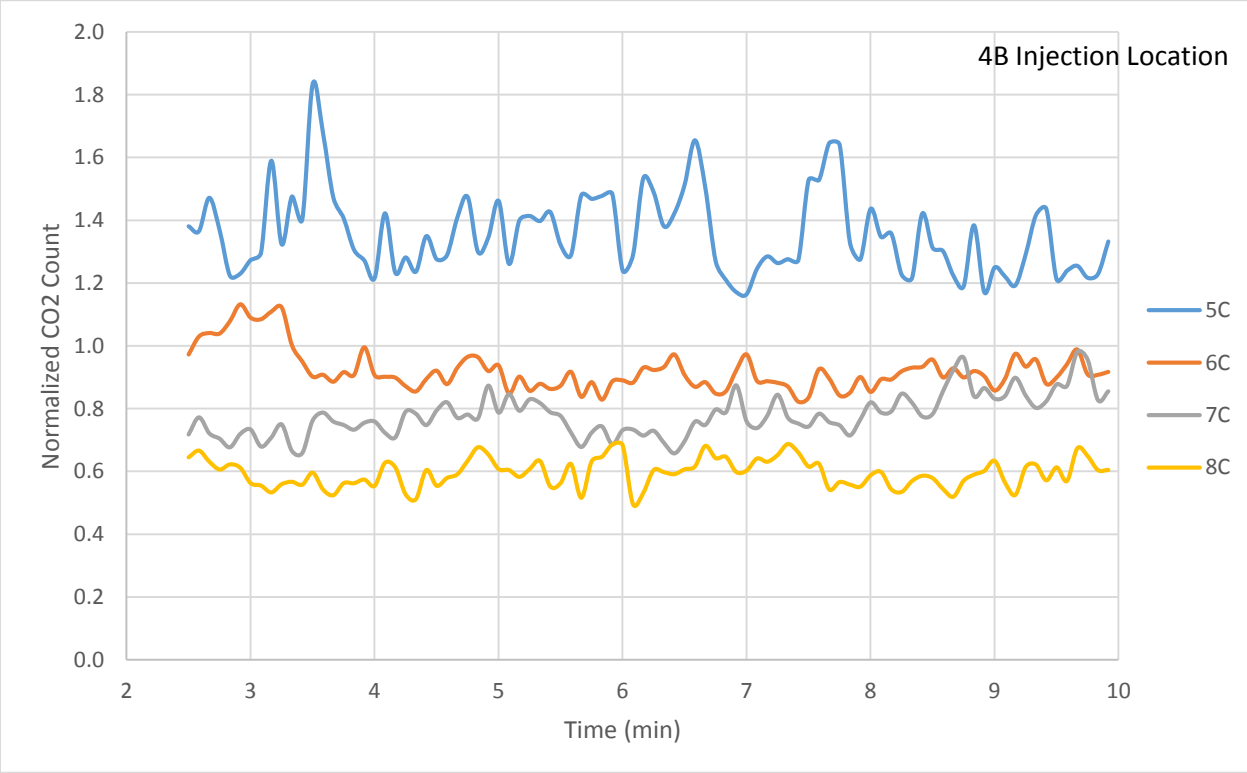

Figure 5.19: Seats 5-8C Half-Full Load (3 Run Average)

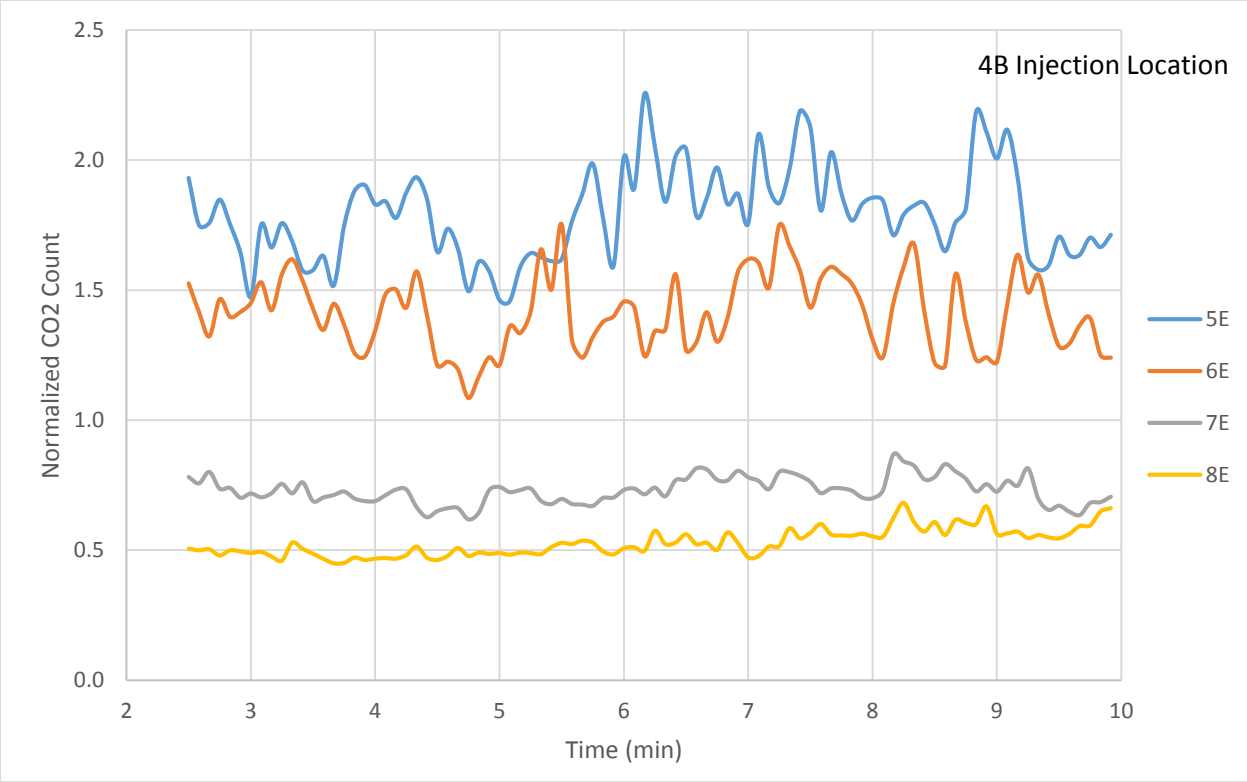

Figure 5.20: Seats 5-8E Half-Full Load (3 Run Average)

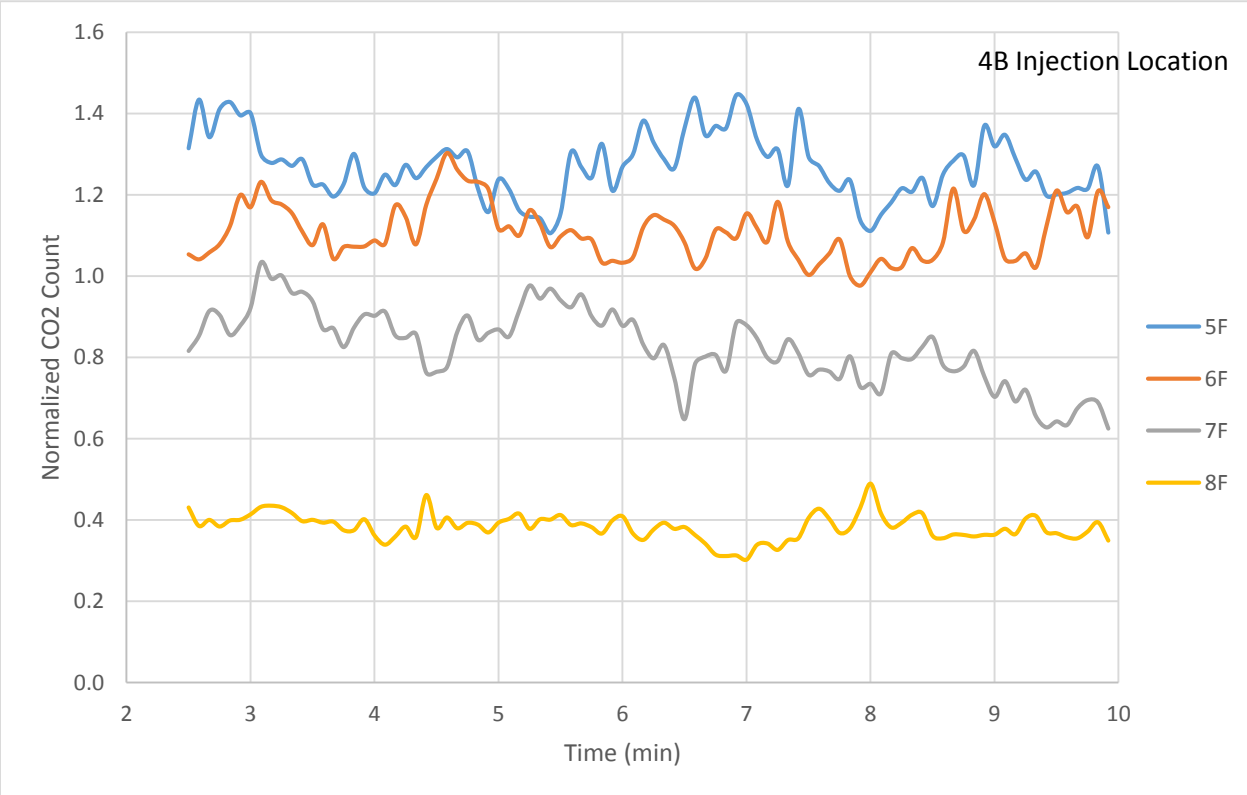

Figure 5.21: Seats 5-8F Half-Full Load (3 Run Average)

Similarly to the fully loaded cabin baseline test, the average normalized CO_2 concentration is calculated from the three tests at each sampling location for the half-full passenger load. The average concentrations for the 4B injection location are shown in Figure 5.22 and listed in Table 5.2. Again, the average concentrations for the two additional injection locations are shown in the electronic appendix.

Table 5.2: Half-Full Load Average Normalized CO_2 Concentrations

	A	B	C	D	E	F	G
1		3.14	3.43		3.11	1.23	
2		4.60	5.02		3.80	1.42	
3		7.94	6.11		3.62	1.61	
4		2.09	4.67		2.64	1.89	
5		1.08	1.36		1.79	1.27	
6		0.86	0.92		1.41	1.11	
7		0.82	0.78		0.73	0.83	
8		0.59	0.60		0.53	0.38	

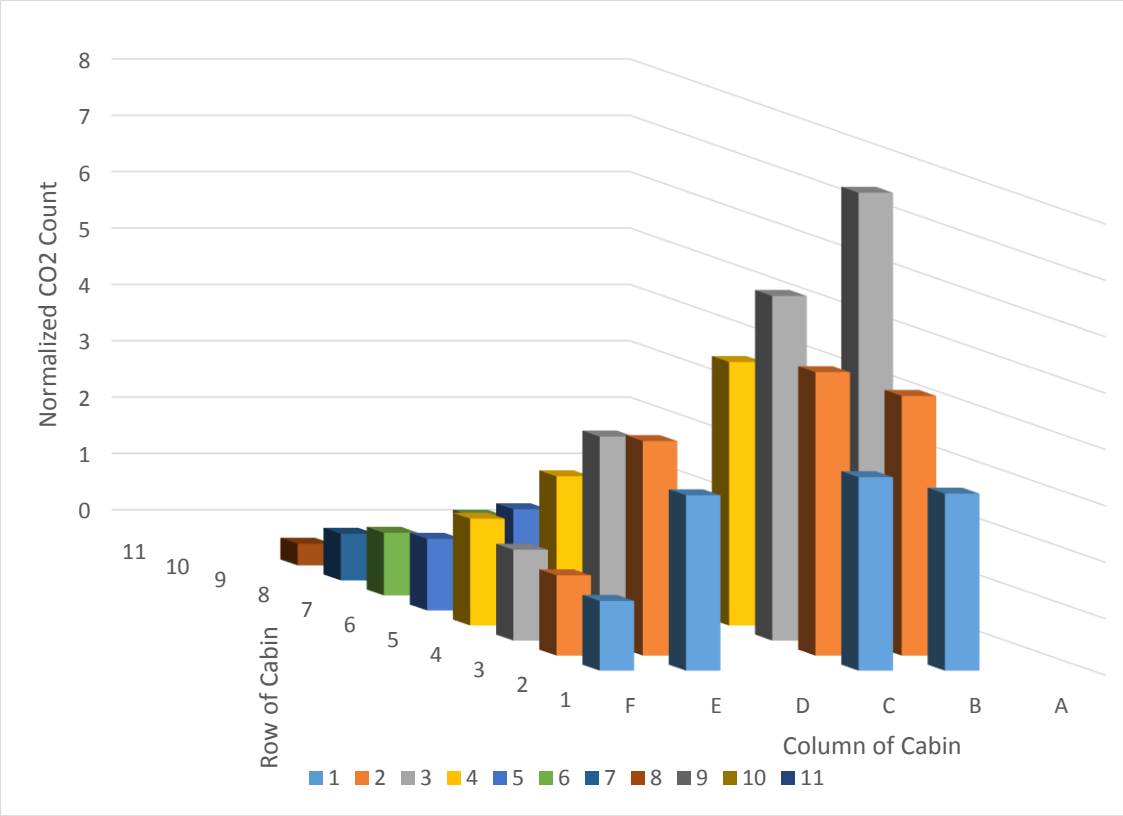

Figure 5.22: Half-Full Load Average Normalized CO_2 Concentrations

5.2.3 Cabin Load Comparison Results

The two types of tests are compared in order for useful conclusions to be drawn. The differences between the average normalized CO_2 concentrations for each seat location for the two tests are calculated by subtracting the half-full load average concentration from the full load average concentration. This difference is calculated for the all of the 32 sampling locations in each of the three injection locations. The data for the 4B injection comparison are shown in Table 5.3 and Figure 5.23. The data for the 6D injection comparison are shown in Table 5.4 and Figure 5.24. The data for the 8F injection comparison are shown in Table 5.5 and Figure 5.25.

Table 5.3: Normalized Change from Full to Half Load Test 4B Injection

	A	B	C	D	E	F	G
1		-1.42	-1.55		-1.43	0.43	
2		-2.05	-2.29		-1.87	0.27	
3		-2.46	-2.79		-1.72	0.16	
4		5.17	0.54		-0.72	-0.04	
5		2.15	0.70		-0.21	-0.11	
6		0.39	-0.11		-0.15	-0.16	
7		0.22	-0.09		-0.05	-0.24	
8		0.09	-0.20		0.00	-0.14	

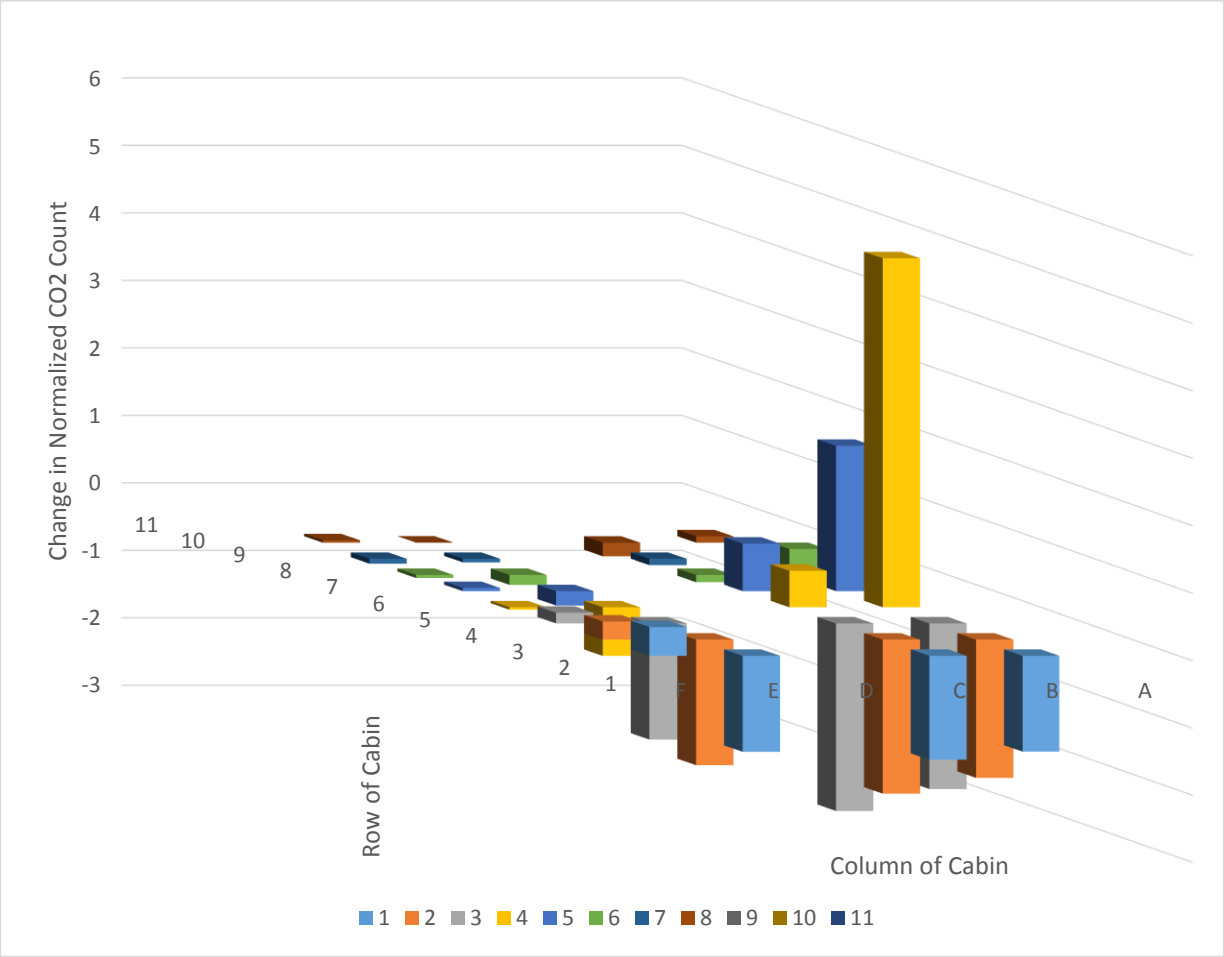

Figure 5.23: Normalized Change from Full to Half Load Test 4B Injection

Table 5.4: Normalized Change from Full to Half Load Test 6D Injection

	A	B	C	D	E	F	G
3		-0.40	-0.09		0.12	0.58	
4		-0.55	-0.11		1.15	0.69	
5		-1.27	-1.34		1.24	0.65	
6		-0.08	1.32		0.39	-0.47	
7		0.19	0.69		-0.48	0.04	
8		0.02	0.36		-0.28	-0.28	
9		0.20	0.23		-0.25	0.04	
10		0.14	0.10		-0.01	0.06	

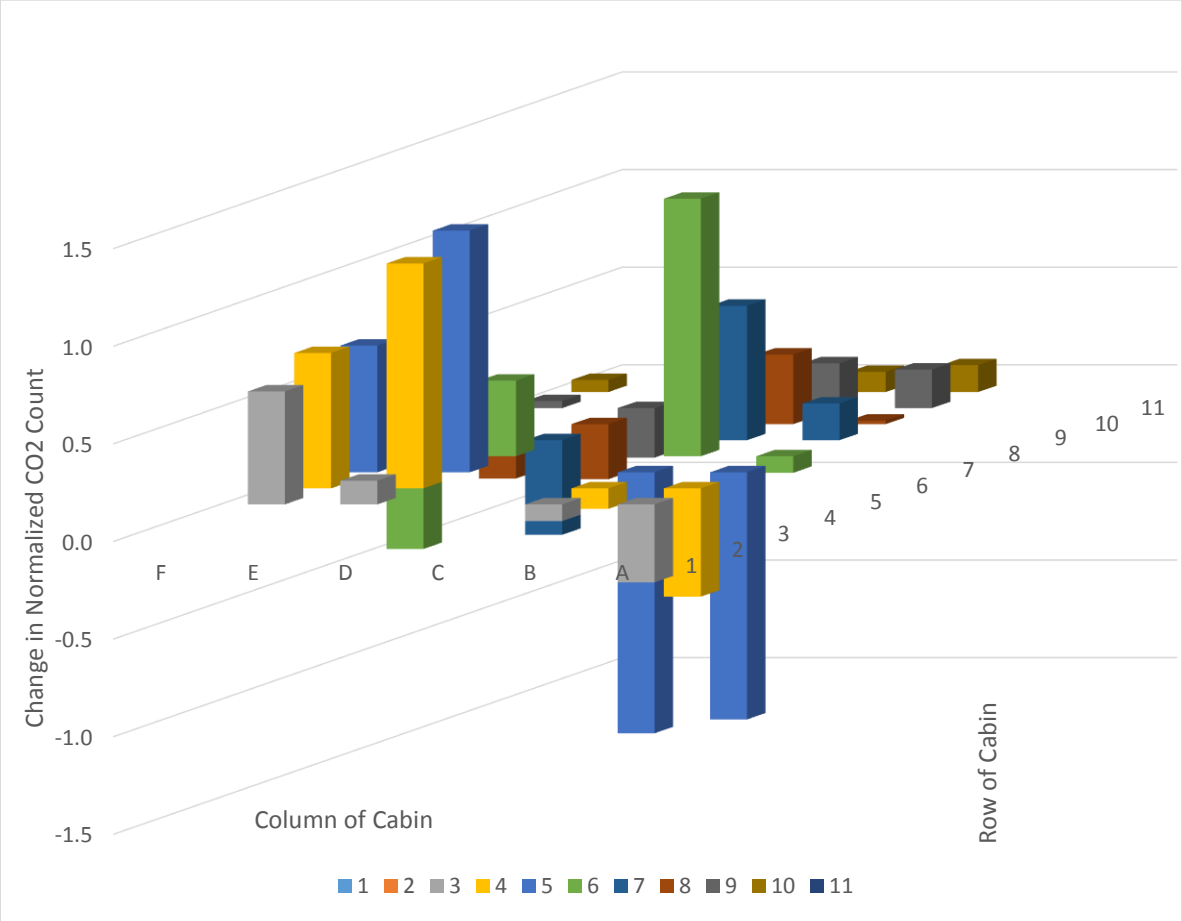

Figure 5.24: Normalized Change from Full to Half Load Test 6D Injection

Table 5.5: Normalized Change from Full to Half Load Test 8F Injection

	A	B	C	D	E	F	G
4		-0.02	-0.06		0.21	-0.05	
5		0.16	-0.19		0.46	0.28	
6		0.71	0.40		0.49	0.39	
7		0.80	1.17		1.37	0.98	
8		0.61	1.12		1.12	1.01	
9		0.51	0.98		-1.24	-0.68	
10		0.40	0.37		-0.51	-0.22	
11		0.32	0.04		0.18	0.07	

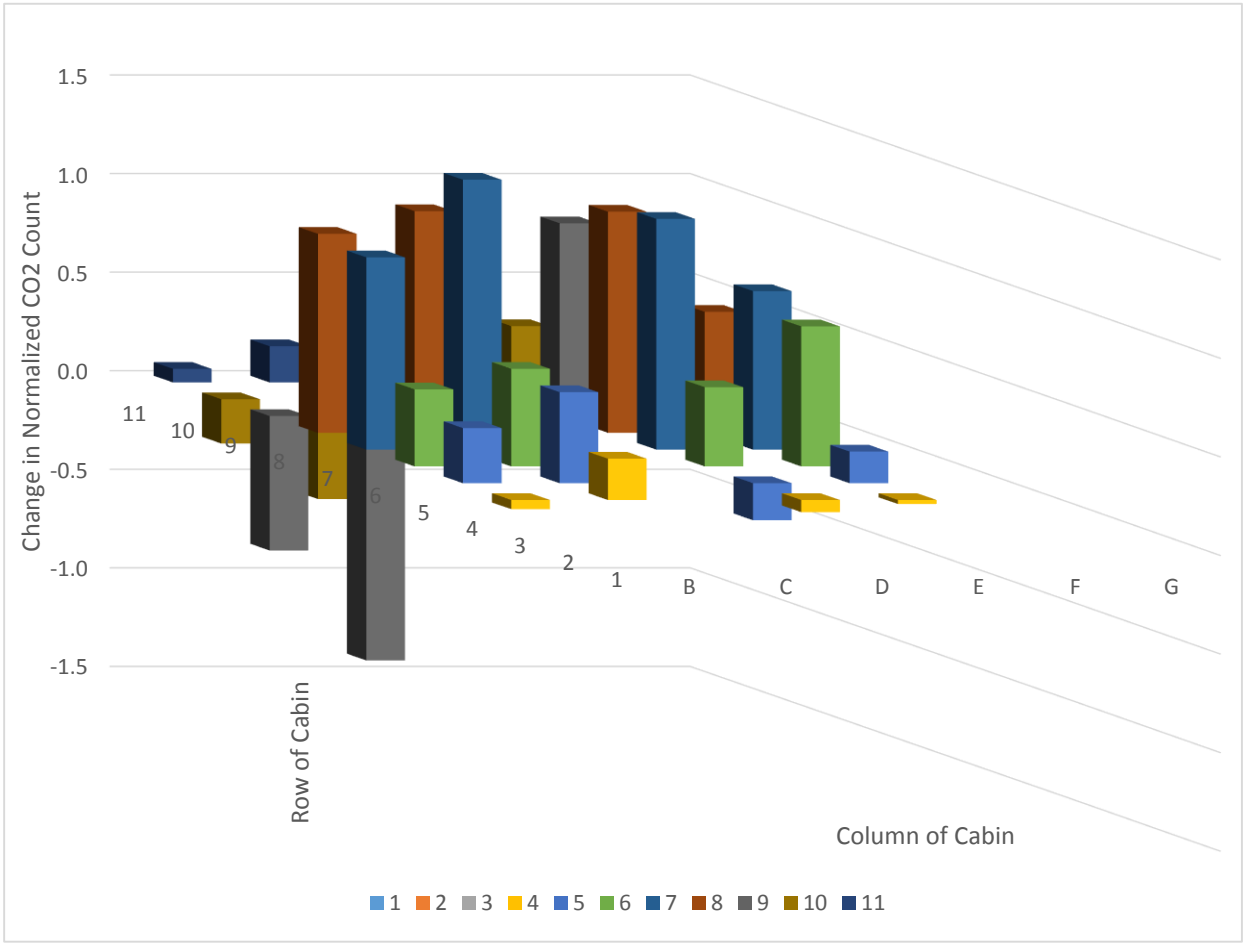

Figure 5.25: Normalized Change from Full to Half Load Test 8F Injection

For a relative comparison, the change in normalized CO_2 concentration from the full load test to the half-full load test is also calculated as a percent change. This calculation is shown in Equation (5.3), where C_{full} is the normalized CO_2 concentration for the full load test, C_{half} is the normalized CO_2 concentration for the half-full load test, and $\Delta\%$ is the percent change in normalized CO_2 concentration caused by the change in passenger density.

$$\Delta\% = \frac{C_{full} - C_{half}}{C_{full}} * 100\% \quad \textbf{(5.3)}$$

The percent change results are calculated for all three injection locations. The results from the 4B injection location are shown in Table 5.6 and Figure 5.26. The results from the 6D injection location are shown in Table 5.7 and Figure 5.27. The results from the 8F injection location are shown in Table 5.8 and Figure 5.28.

Table 5.6: Percent Change from Full to Half Load Test 4B Injection

	A	B	C	D	E	F	G
1		-83.3%	-82.2%		-84.9%	25.6%	
2		-80.6%	-83.7%		-96.4%	15.9%	
3		-44.9%	-83.9%		-91.1%	9.0%	
4		71.2%	10.4%		-37.4%	-1.9%	
5		66.6%	34.2%		-13.5%	3.6%	
6		30.9%	-13.1%		-11.6%	-4.2%	
7		21.6%	-13.7%		-7.8%	-9.5%	
8		13.6%	-51.2%		0.2%	8.3%	

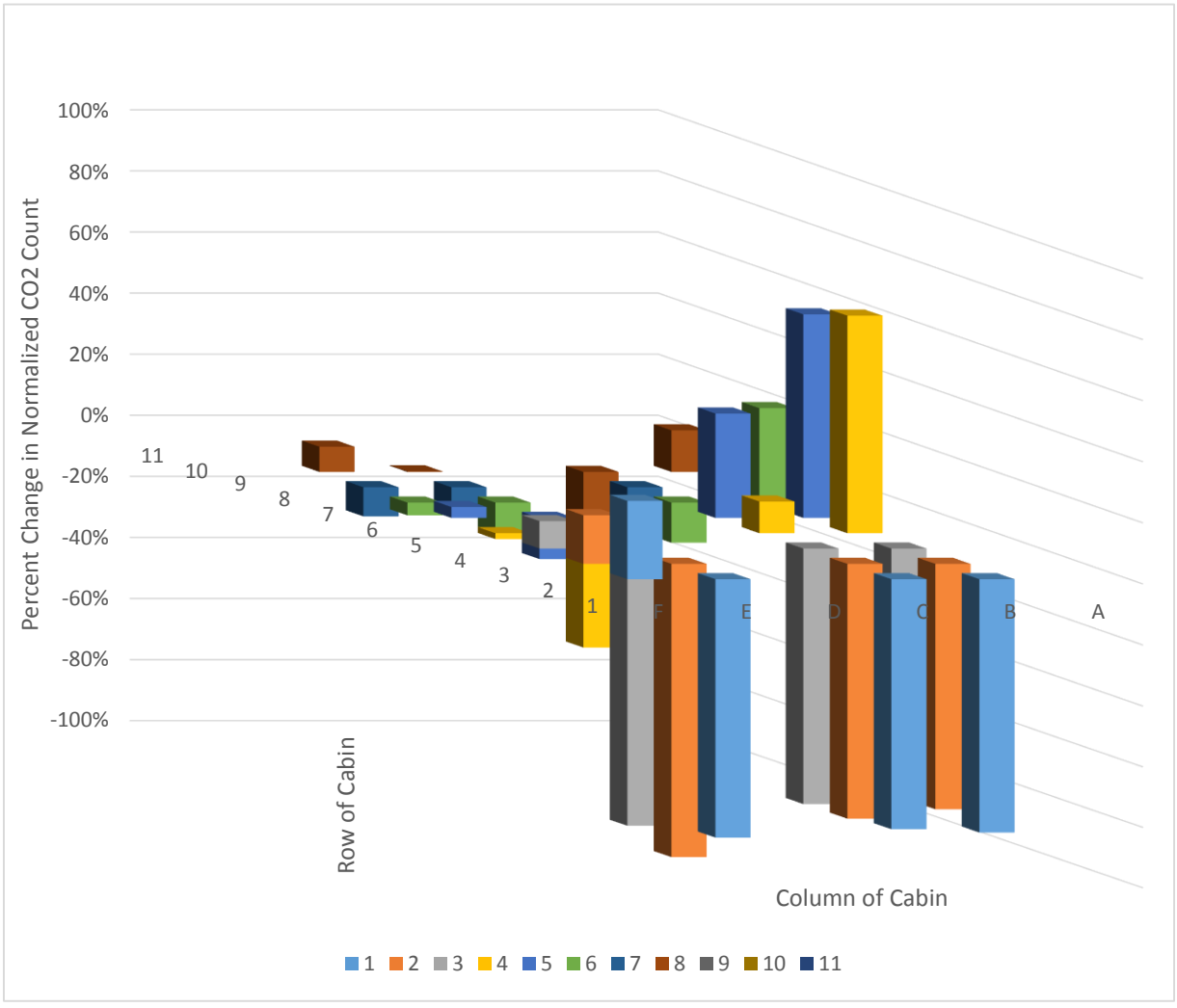

Figure 5.26: Percent Change from Full to Half Load Test 4B Injection

Table 5.7: Percent Change from Full to Half Load Test 6D Injection

	A	B	C	D	E	F	G
3		-42.5%	-8.8%		11.4%	42.3%	
4		-45.2%	-7.8%		54.5%	38.0%	
5		-81.8%	-93.2%		30.9%	22.7%	
6		-4.9%	31.9%		8.9%	-18.6%	
7		8.4%	20.2%		-28.1%	1.7%	
8		1.3%	19.7%		-26.1%	-31.7%	
9		16.8%	16.3%		-34.9%	4.9%	
10		15.7%	9.0%		-1.2%	10.2%	

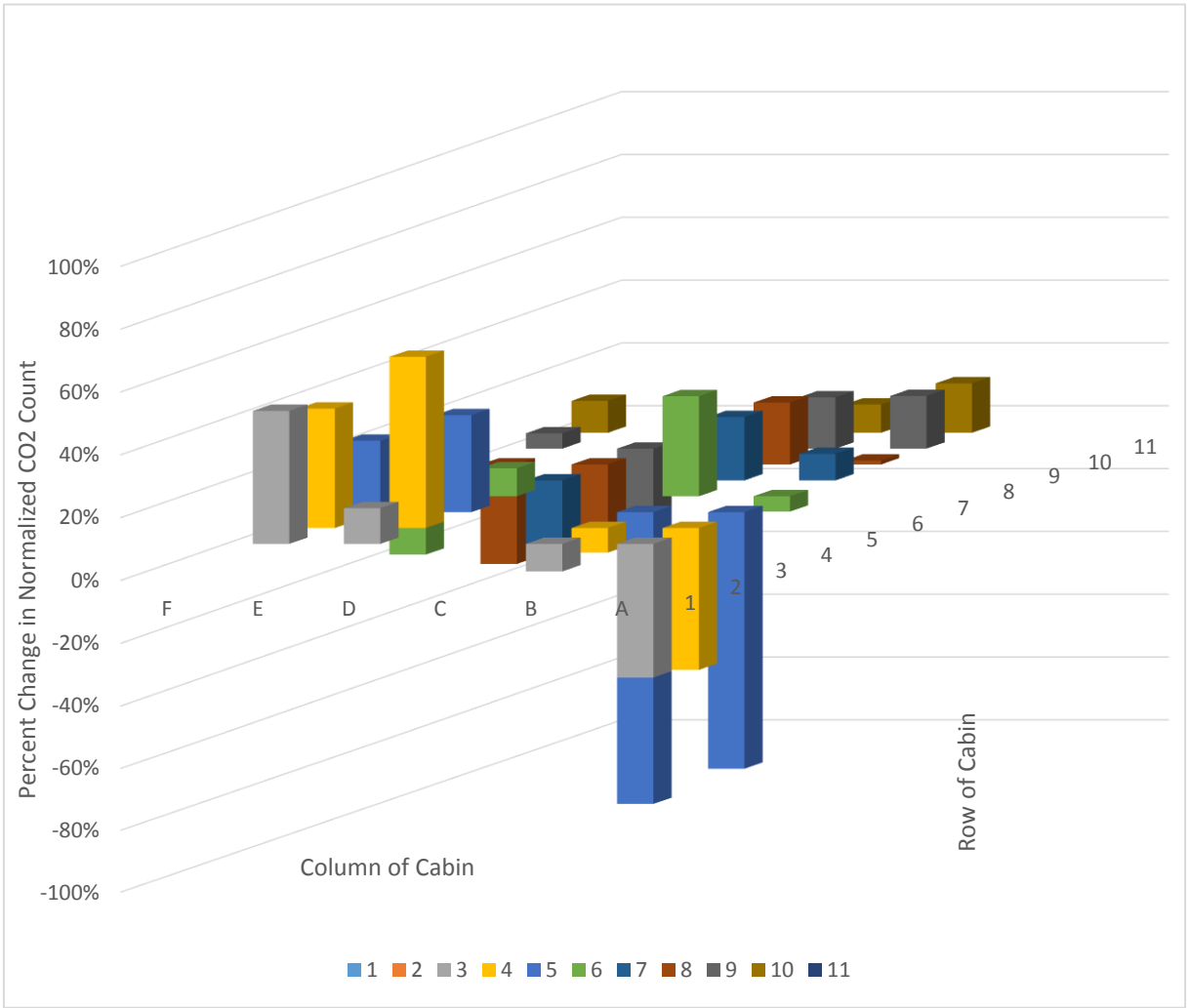

Figure 5.27: Percent Change from Full to Half Load Test 6D Injection

Table 5.8: Percent Change from Full to Half Load Test 8F Injection

	A	B	C	D	E	F	G
4		-3.1%	-13.1%		41.9%	-12.6%	
5		13.2%	-31.7%		59.4%	39.7%	
6		36.7%	24.1%		48.8%	41.2%	
7		37.1%	43.0%		65.4%	39.2%	
8		26.8%	34.5%		23.6%	12.8%	
9		23.4%	36.8%		-38.7%	-19.9%	
10		20.3%	18.4%		-23.5%	-9.7%	
11		19.2%	2.5%		11.5%	3.6%	

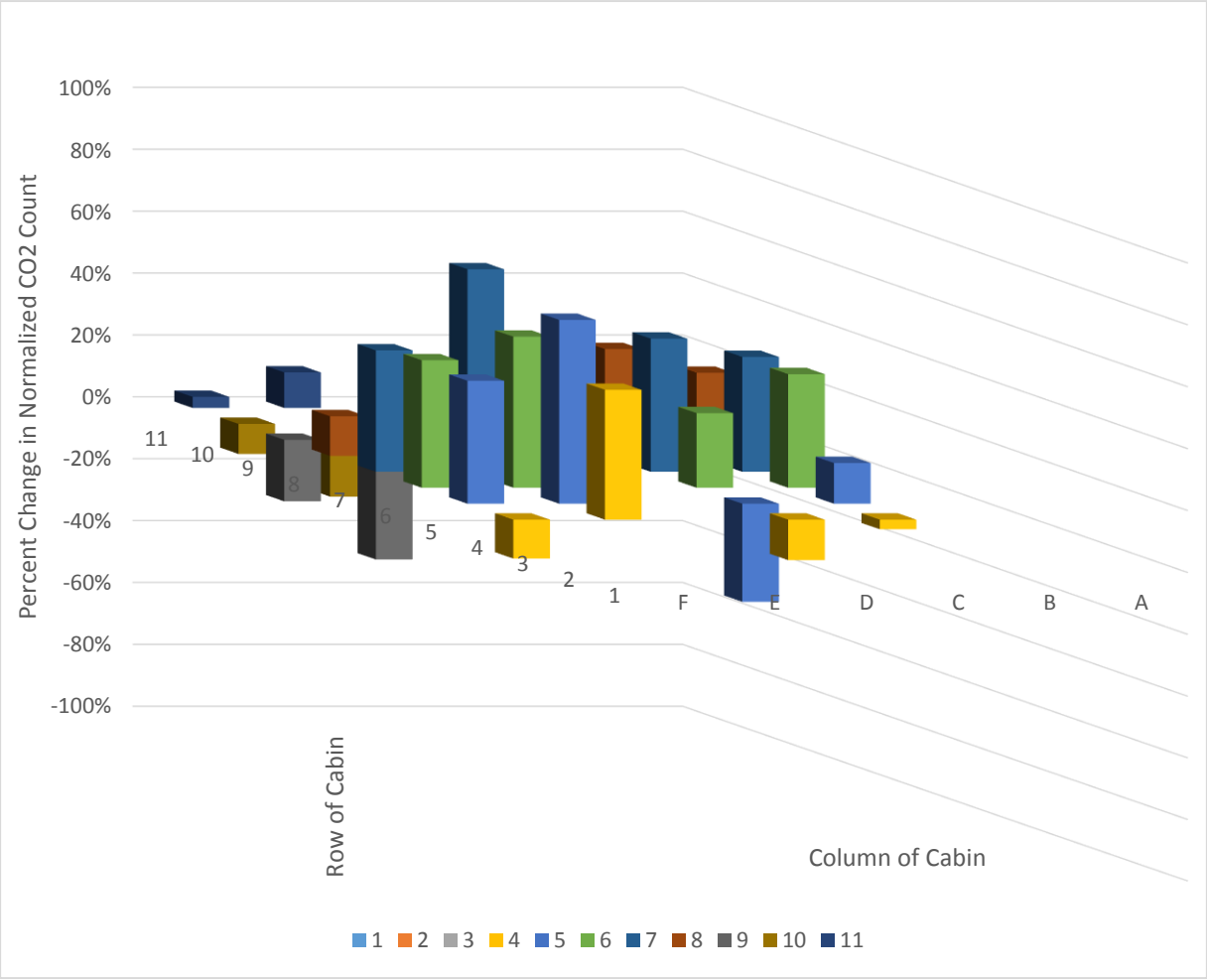

Figure 5.28: Percent Change from Full to Half Load Test 8F Injection

As can be seen from these figures, the distribution of passengers inside the cabin can have a significant impact on the airflow characteristics, but the exact effects vary greatly for the different injection locations tested. These results are discussed in greater detail in Chapter 6.

5.3 No Ventilation Air Results

The second method of testing completed finds the effects of turning off the ventilation air supply to the mock-up cabin. Unlike the cabin loading testing, only one tracer gas injection location is utilized for the no ventilation air testing. Seat 2D is selected as the injection location, and 12 seats throughout the cabin are chosen as sampling locations, which are shown in the cabin plan view in Figure 4.8. Each test is completed using the testing procedures outlined in Table 4.4. All 12 sampling locations are tested three times and results are averaged to give more reliable results. The averaged results for all 12 sampling locations are shown in Figure 5.29 through Figure 5.40.

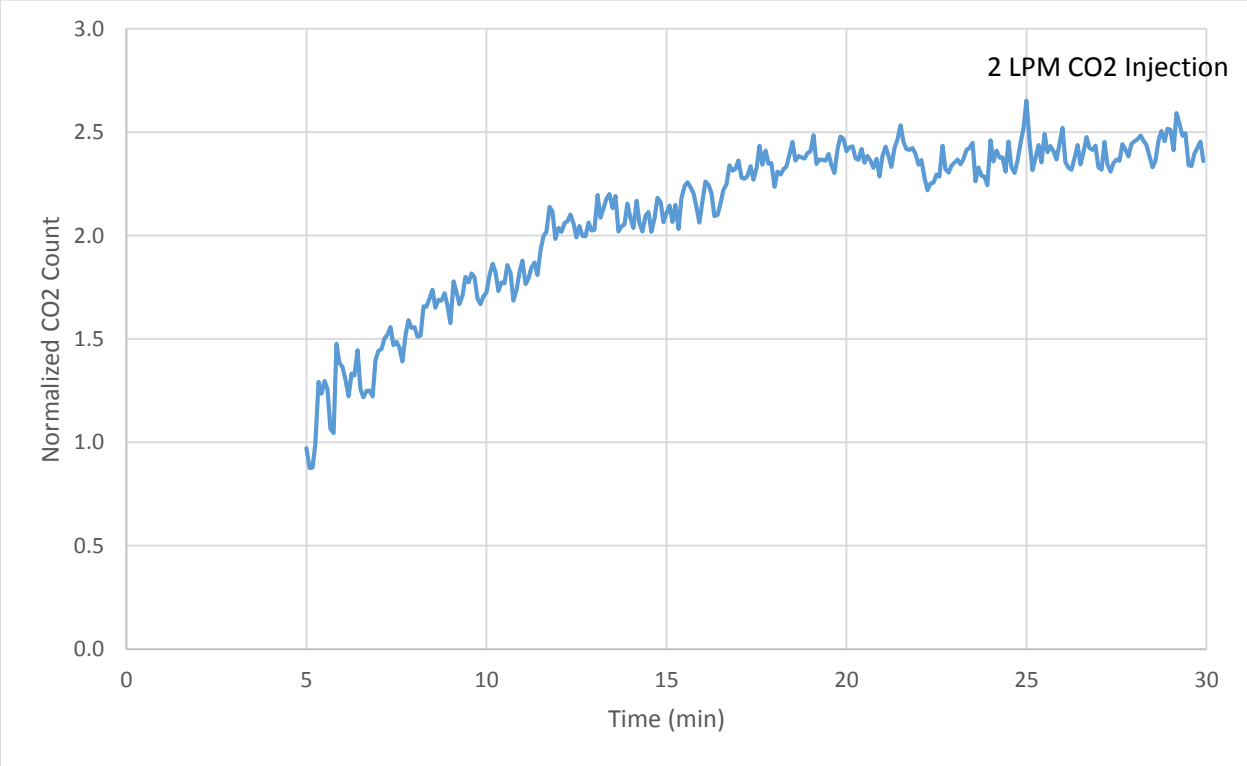

Figure 5.29: Seat 1D No Air Flow (3 Run Average)

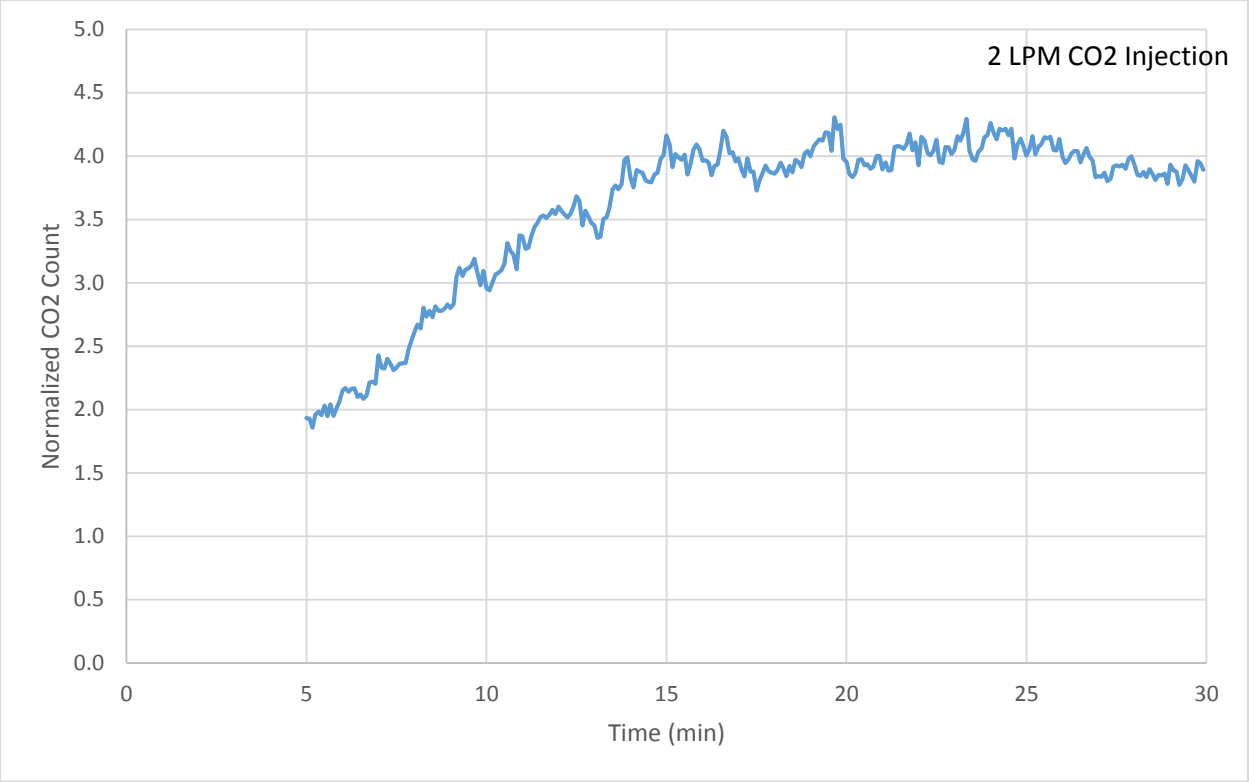

Figure 5.30: Seat 2A No Air Flow (3 Run Average)

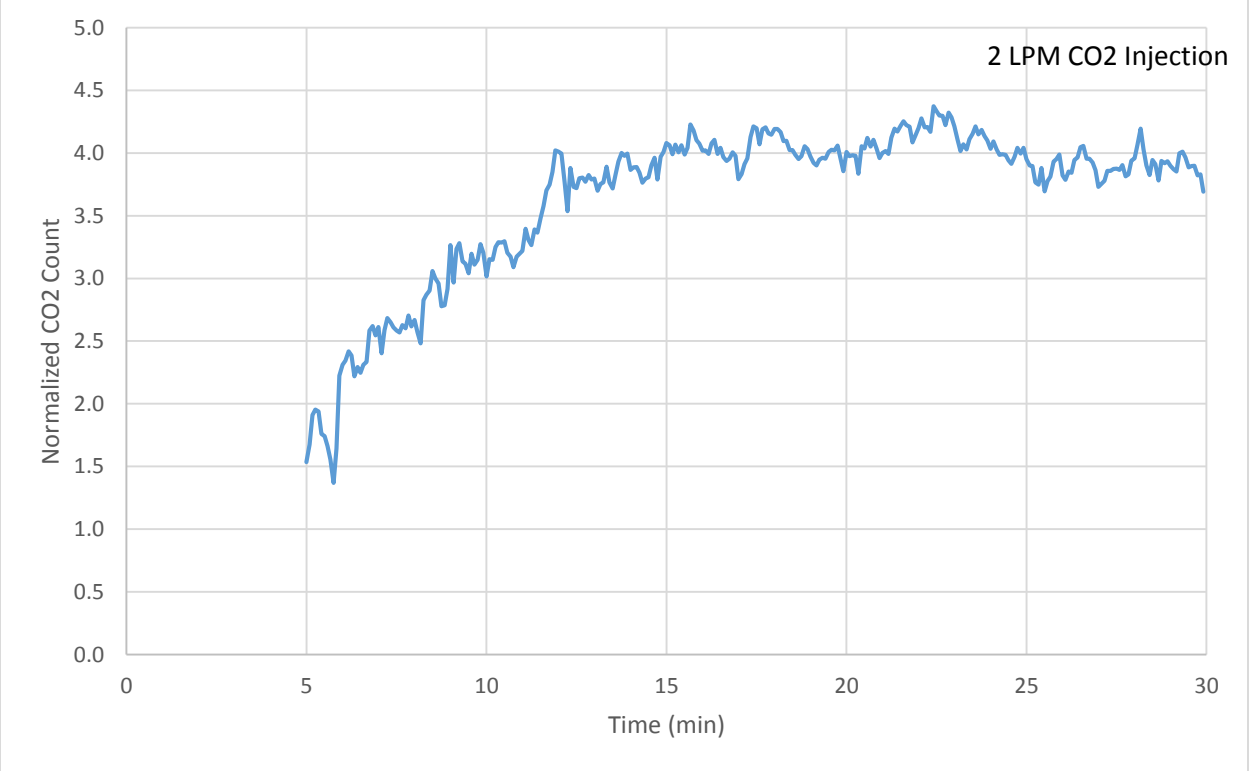

Figure 5.31: Seat 2B No Air Flow (3 Run Average)

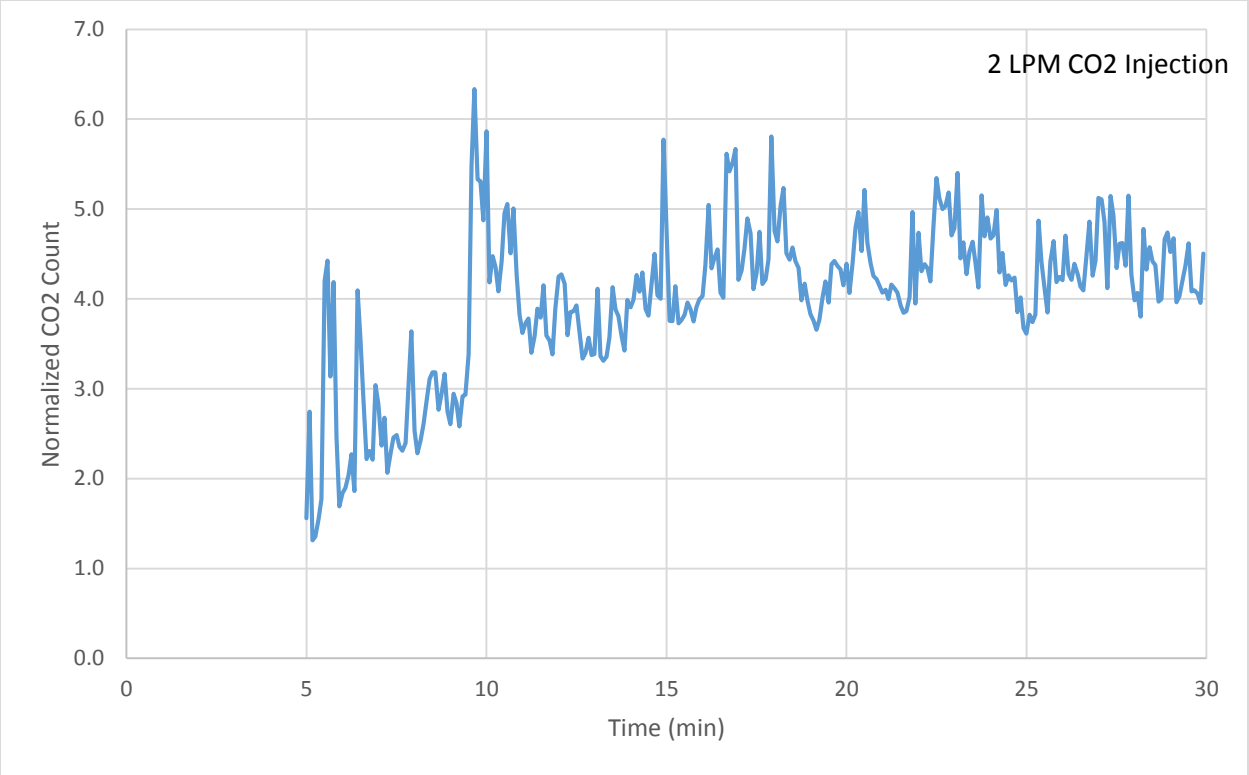

Figure 5.32: Seat 2C No Air Flow (3 Run Average)

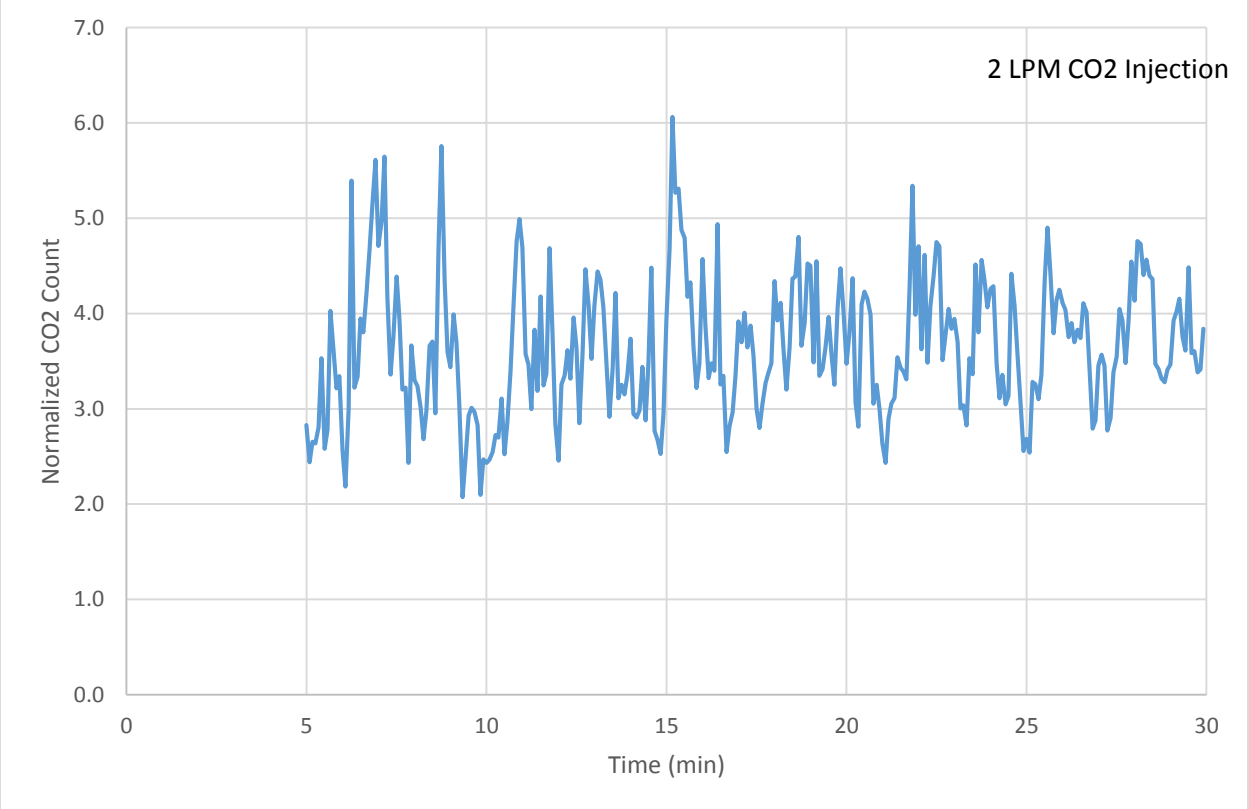

Figure 5.33: Seat 2E No Air Flow (3 Run Average)

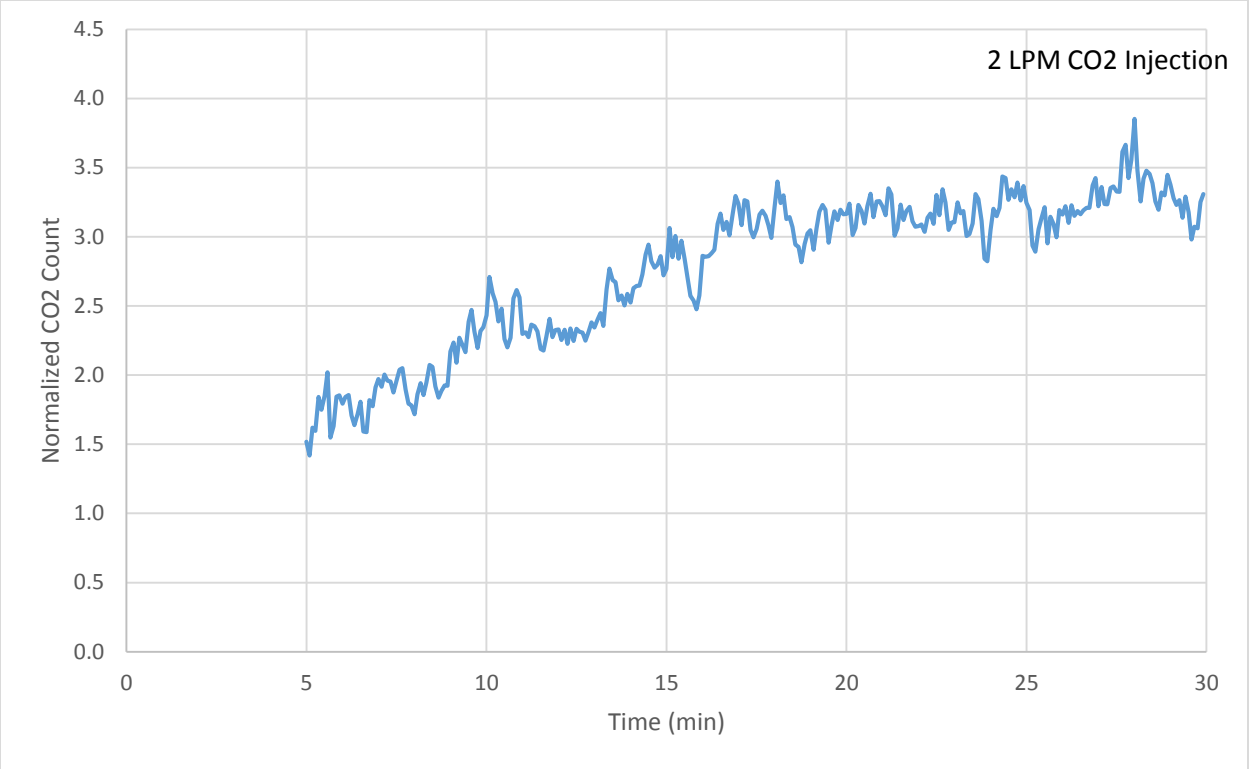

Figure 5.34: Seat 2F No Air Flow (3 Run Average)

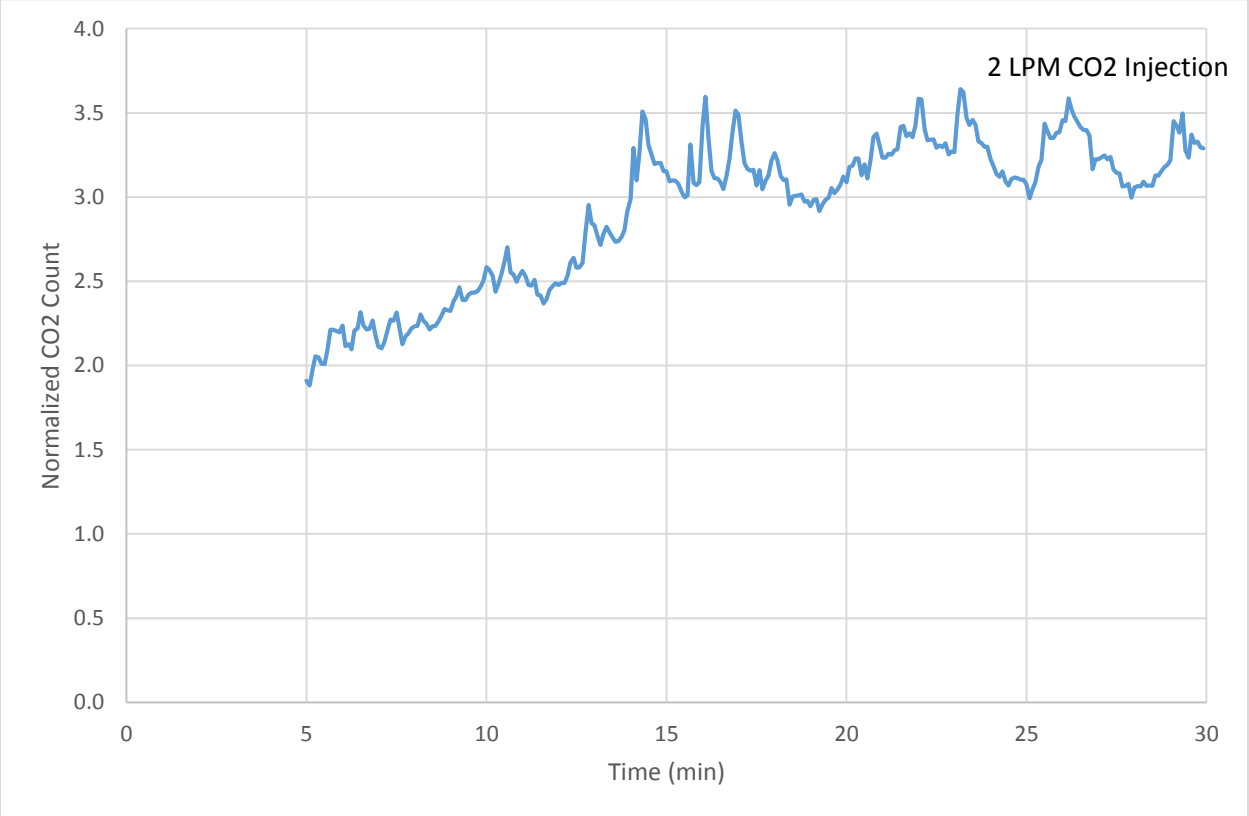

Figure 5.35: Seat 2G No Air Flow (3 Run Average)

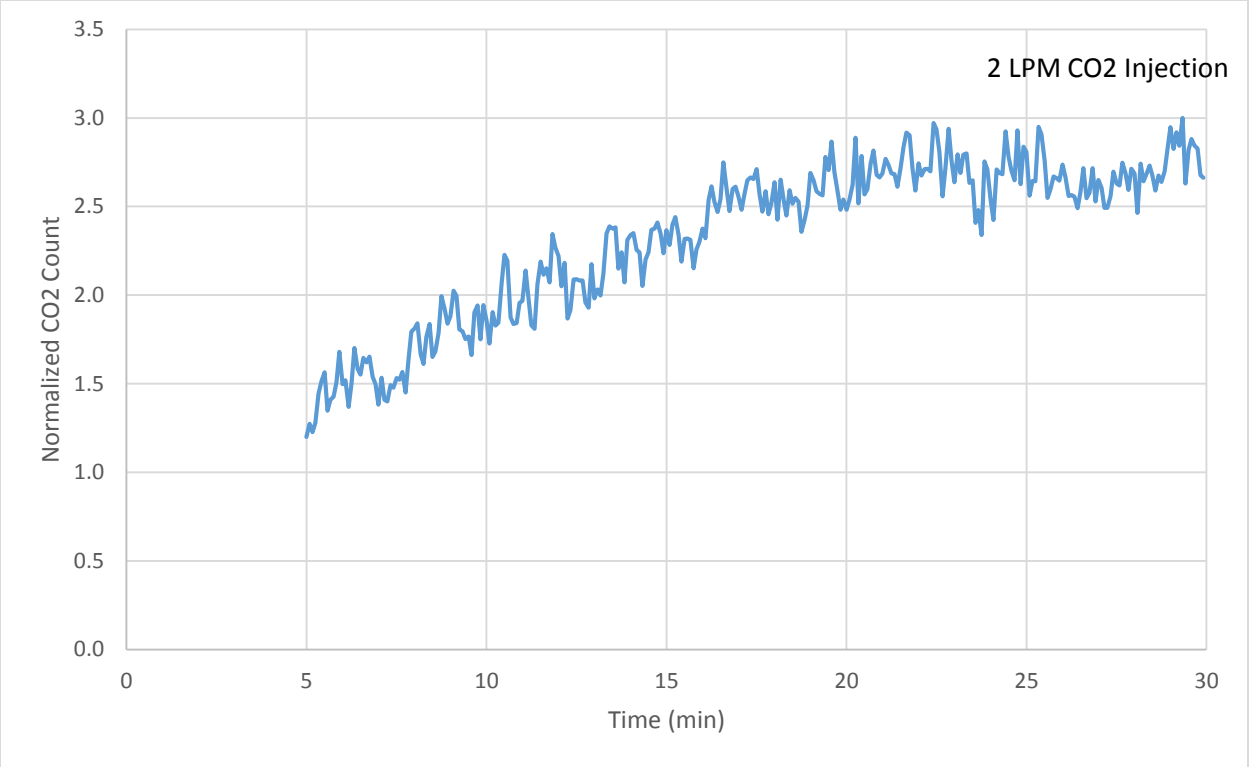

Figure 5.36: Seat 3D No Air Flow (3 Run Average)

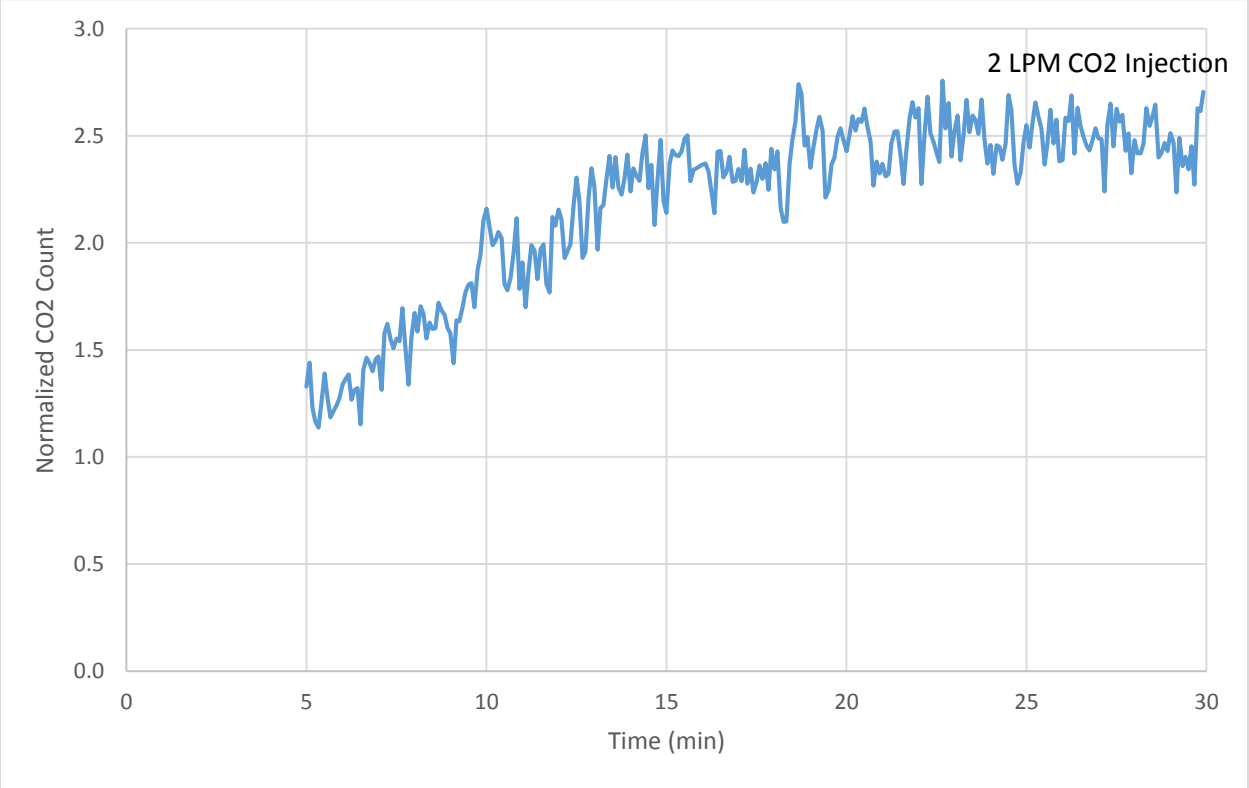

Figure 5.37: Seat 4D No Air Flow (3 Run Average)

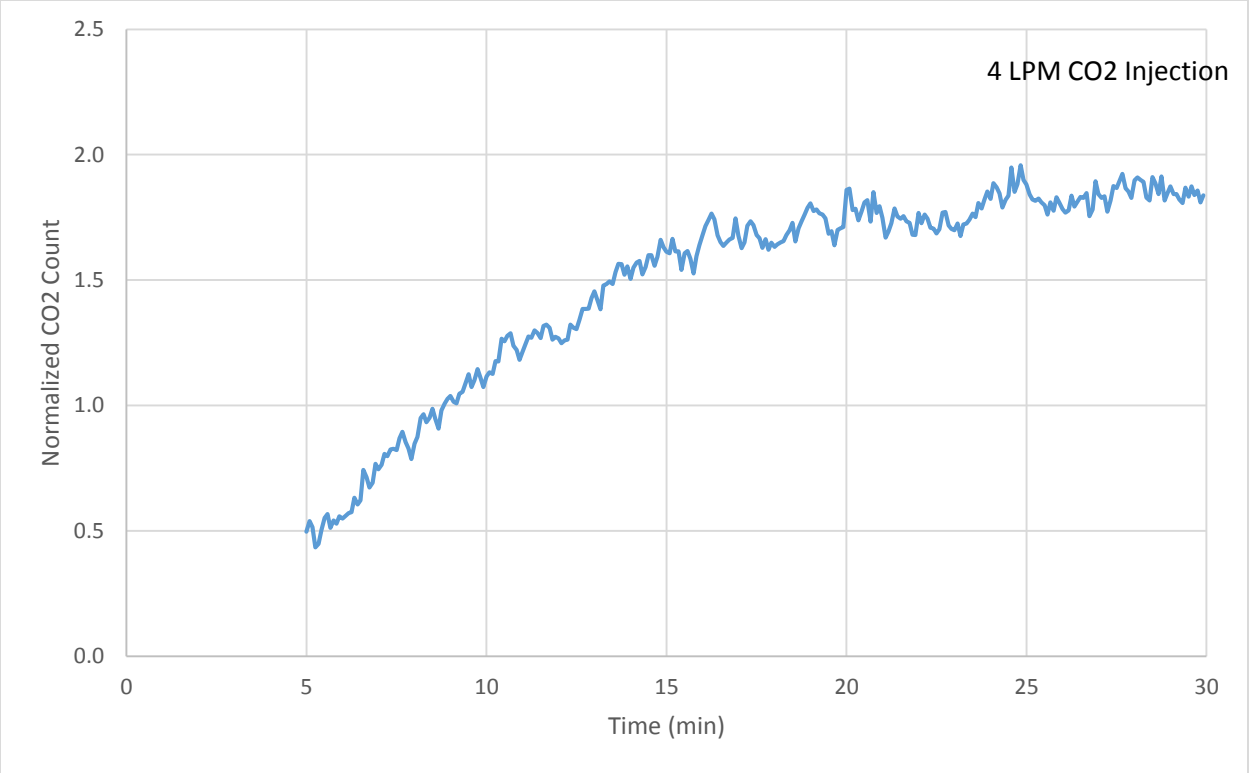

Figure 5.38: Seat 6D No Air Flow (3 Run Average)

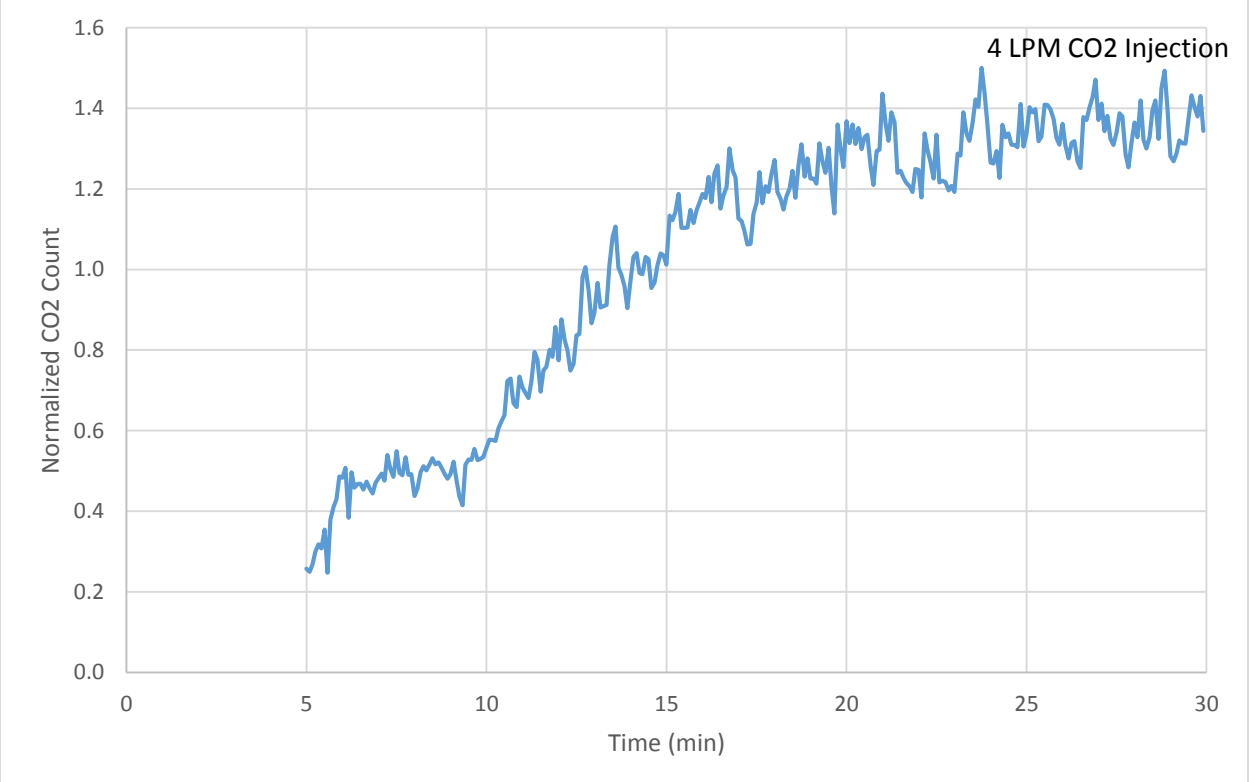

Figure 5.39: Seat 8D No Air Flow (3 Run Average)

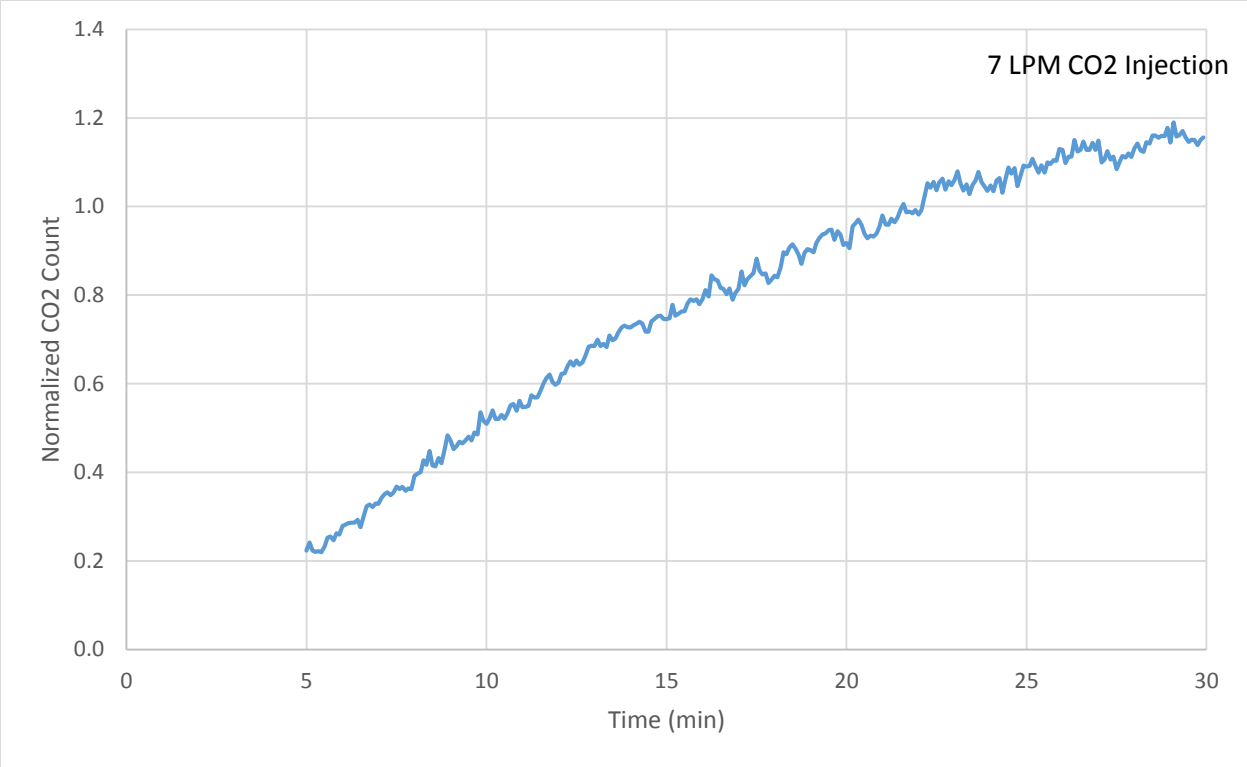

Figure 5.40: Seat 10D No Air Flow (3 Run Average)

After the three runs for each sampling location are completed, the normalized CO_2 concentrations are averaged over the 30 minute sampling interval for each seat location. These average values are then compiled to show the distribution throughout the mock-up cabin. The averaged results for all of the sampling locations are shown in Table 5.9 and Figure 5.41.

Table 5.9: No Air Flow Averaged Normalized CO_2 Concentrations

	A	B	C	D	E	F	G
1				2.39			
2	3.99	4.00	4.41		3.72	3.22	3.27
3				2.69			
4				2.49			
5							
6				1.81			
7							
8				1.33			
9							
10				1.07			

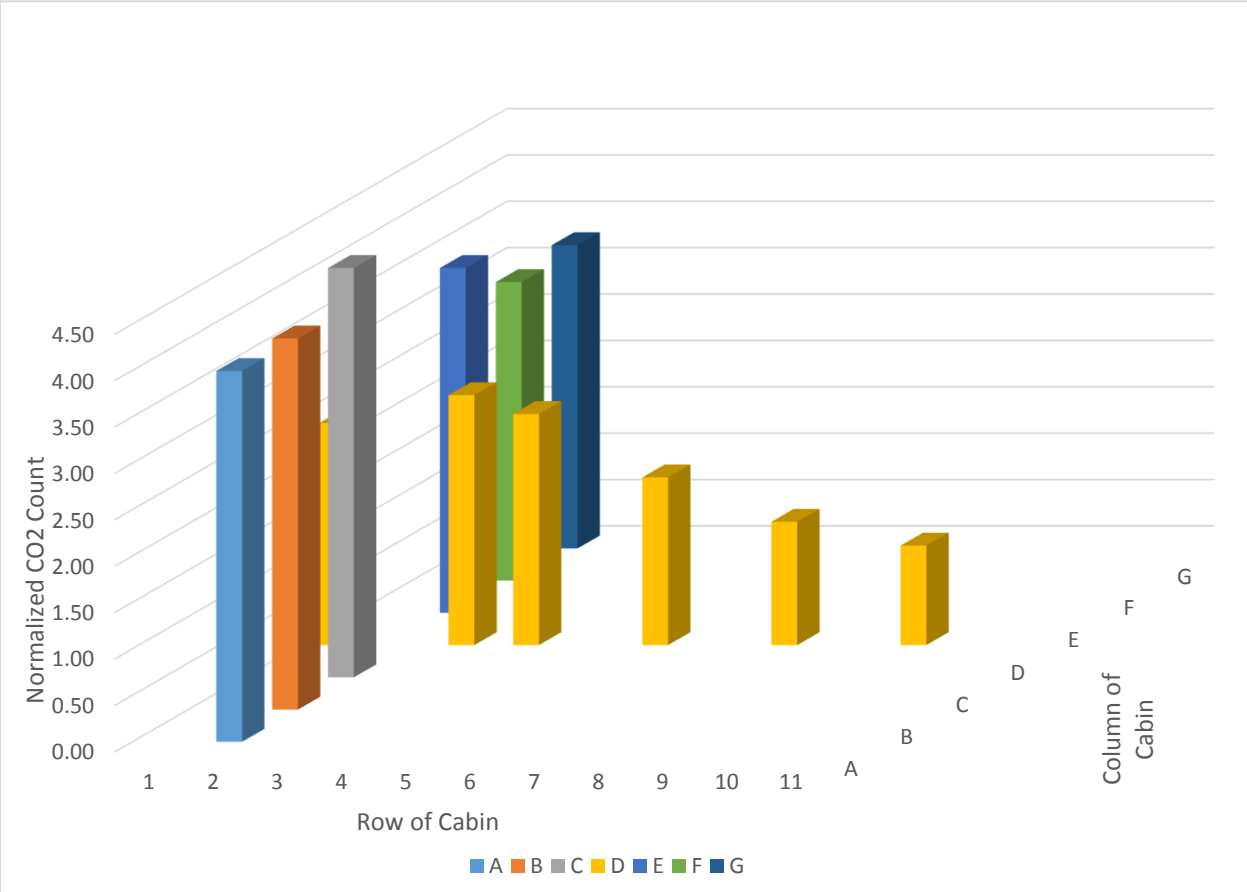

Figure 5.41: No Air Flow Averaged Normalized CO_2 Concentrations

As could be expected, the tracer gas distribution is less concentrated the greater the distance between the sampling and injection locations. The results of the tests without inlet air flow are discussed in greater detail in Chapter 6.

5.4 Uncertainty Analysis

A wide variety of instruments are used to complete the experiments in the mock-up cabin. Inherently, there are uncertainties that propagate error throughout each stage of testing. These apparatus uncertainties can be categorized into supply air and conditioning, tracer gas injection, and CO_2 sampling. The uncertainty created in each of the three systems is covered in the following sections and then compiled to calculate the maximum uncertainty of the entire passenger loading testing. An average uncertainty value for the passenger loading testing, and the uncertainty for the no supply air testing are shown in Appendix A.

5.4.1 Supply Air Uncertainty

The first subsystem of the experimental apparatus is the supply air system for the mock-up cabin. The temperature and pressure of the supply air is controlled by an Agilent DAQ collecting data from a pressure transducer, a flow meter, and temperature sensors. The uncertainty and operating range for each of these instruments is shown in Table 5.10, and the majority of the information in the table was gathered by (Trupka, 2011).

Table 5.10: Supply Air Equipment Uncertainty

Instrument	Uncertainty	Operable Range
Agilent 34970A DAQ	0.06 °C (RTD)	49Ω – 2.1kΩ
NI Field Point AI-110	0.07% of reading + 0.0007% of range	0 – 5 V
PCI FE-1500 Flow Meter	2%	100 – 10,000 fpm
Omega PX 653	0.25% FS	1 inch water column
	0.05% FS repeatability	0 – 5 V
Omega 3-wire RTD	± (0.30 + 0.005 * t) °C	-50 – 250 °C, Class B

The volumetric flow rate of ventilation air into the cabin is calculated using Bernoulli's equation from a PCI Flow Meter that measures the gage pressure inside the duct. The density of the

supply air is dependent on the temperature and pressure of the supply air, so the uncertainty of each of these properties are calculated and combined to find the overall uncertainty. Temperature is the first property to find the uncertainty for. As previously mentioned, the desired temperature of the supply air is 60 °F (288.8 K). The uncertainty of the supply air temperature is calculated by substituting the uncertainties from the instruments into Equation (5.4) through (5.7) below.

$$\frac{U_{RTD}}{T_{supp}} = \frac{0.38\,°C}{288.8\,K} = 0.132\% \tag{5.4}$$

$$\frac{U_{DAQ}}{T_{supp}} = \frac{0.06\,°C}{288.8\,K} = 0.0208\% \tag{5.5}$$

$$\frac{U_{temp}}{T_{supp}} = \sqrt{\left(\frac{U_{RTD}}{T_{supp}}\right)^2 + \left(\frac{U_{DAQ}}{T_{supp}}\right)^2} = \sqrt{0.132\%^2 + 0.0208\%^2} = 0.134\% \tag{5.6}$$

$$U_{temp} = 0.134\% \times 288.8\,K = 0.39\,°C = 0.70\,°F \tag{5.7}$$

After the temperature uncertainty calculations are completed, the next supply air property analyzed is the pressure. Since the supply air pressure measurement instruments used for this testing haven't been updated recently, the supply air pressure uncertainty calculation shown in Equation (5.8) through (5.10) was taken from the previous work by (Trupka, 2011).

$$U_{NI} = 0.08\% \tag{5.8}$$

$$U_{Omega} = 0.803\% \tag{5.9}$$

$$U_{press} = \sqrt{U_{NI}^2 + U_{PCI}^2 + U_{Omega}^2} = \sqrt{0.08\%^2 + 2\%^2 + 0.803\%^2} = 2.16\% \tag{5.10}$$

Once the temperature and pressure uncertainties are calculated, the overall supply air uncertainty is found using the root means squared method. According to the Bernoulli Equation, pressure is related to the square of the velocity. Since the uncertainty of the velocity of the supply air is the desired result, the temperature and pressure uncertainties are halved before being squared from

the principle of partial derivatives (Coleman & Steele, 1989). The total uncertainty of the supply air velocity is calculated in Equation (5.11) and (5.12) shown below.

$$U_{supp,air} = \sqrt{(\frac{1}{2}U_{temp})^2 + (\frac{1}{2}U_{press})^2} \quad \textbf{(5.11)}$$

$$U_{supp,air} = \sqrt{(\frac{1}{2} * 0.134\%)^2 + (\frac{1}{2} * 2.16\%)^2} = 1.08\% \quad \textbf{(5.12)}$$

5.4.2 Tracer Gas Injection Uncertainty

The second subsystem of the mock-up cabin experimental setup is the tracer gas injection system. The uncertainty introduced into the experiment by the tracer gas is separated into two categories. The first category is the purity of the gases used for calibration and injection. The CO_2 that is delivered to the laboratory in the 50 lb cylinders is "Industrial Grade" to allow for more economical testing. All other injection gases used throughout testing and calibration are "High Purity". The uncertainty levels for all five of the gases used for experimentation are shown in Table 5.11.

Table 5.11: Tracer Gas Mixture Uncertainty (Trupka 2011)

Gas	Uncertainty
CO_2	99.5% pure
He	99.997% pure
500 ppm CO_2 – Air Mixture	2%
1000 ppm CO_2 – Air Mixture	1%
2000 ppm CO_2 – Air Mixture	1%

The second category of uncertainty in the tracer gas injection system is the tracer gas mass flow controllers. The uncertainty and the maximum rated flow for both mass controllers are shown in Table 5.12. The PR 4000 power supply's 16 bit uncertainty is considered to be negligible compared to the other uncertainties in this experimental set-up.

Table 5.12: Tracer Gas Injection Equipment Uncertainty (Trupka 2011)

Equipment	Uncertainty	Rated Flow
CO_2 Controller	1.0% F.S. (accuracy)	100 SLM
	0.2% F.S. (repeatability)	
	0.1% F.S. (resolution)	
	15 to 40 °C (operation)	
He Controller	1.0% F.S. (accuracy)	10,000 SCCM
	0.2% F.S. (repeatability)	
	0.1% F.S. (resolution)	
	0 to 50 °C (operation)	
PR4000 (Controller/Indicator)	16-Bit	-

The values from the two previous tables are used to calculate the overall uncertainty of the tracer gas injection system. In order to calculate the uncertainty of the tracer gases, the injection rates of 4.21 and 7.00 LPM of He and CO_2, respectively are included in the calculations. The uncertainty of the calibration gas mixture is calculated using Equation (5.13). The uncertainty of the CO_2 injection is calculated in Equation (5.14) and (5.15). The He injection uncertainty is calculated in Equation (5.16) and (5.17). The repeatability values from Table 5.12 are used in both of the gas uncertainty calculations.

$$U_{calib} = \sqrt{U_{500}^2 + U_{1000}^2 + U_{2000}^2} = \sqrt{2\%^2 + 1\%^2 + 1\%^2} = 2.45\% \quad \textbf{(5.13)}$$

$$U_{rep,CO_2} = \frac{0.2\% * 100\ LPM}{7.00\ LPM} = 2.86\% \quad \textbf{(5.14)}$$

$$U_{CO_2} = \sqrt{U_{rep}^2 + U_{pure}^2} = \sqrt{2.86\%^2 + 0.5\%^2} = 2.90\% \quad \textbf{(5.15)}$$

$$U_{rep,He} = \frac{0.2\% * 10\ LPM}{4.21\ LPM} = 0.475\% \quad \textbf{(5.16)}$$

$$U_{He} = \sqrt{U_{rep}^2 + U_{pure}^2} = \sqrt{0.475\%^2 + 0.003\%^2} = 0.475\% \quad \textbf{(5.17)}$$

5.4.3 CO_2 Sampling Uncertainty

The final subsystem used for testing is the CO_2 sampling instrumentation. Three CO_2 analyzers are used for sampling throughout testing. The analyzers sampling the exhaust and cabin environments are both PP Systems WMA-4 models. The analyzer sampling the enclosure inlet air stream is an Edinburgh Gascard NG analyzer. Table 5.13 shows the uncertainty values for the CO_2 sampling equipment from the manufacturers' data.

Table 5.13: CO_2 Analyzer Measurement Uncertainty (Anderson 2012)

Model	Uncertainty	Range
Edinburgh Gascard NG	2% of range (accuracy)	0 – 3000 ppm
	0.3% @ zero, 1.5% @ span (repeatability)	
PP Systems WMA-4	20 ppm (accuracy)	0 – 2000 ppm
	<1% @ span (repeatability)	
Agilent 34970A DAQ	0.0035% of reading +0.0005% of range	10V

All three of the CO_2 analyzers used for testing are extremely linear in nature. Therefore, the repeatability of the analyzers is found by taking a linear interpolation of the repeatability values for each instrument. In addition to the repeatability, the linearity of each of the three analyzers is calculated by finding the R-squared value for each analyzer during every calibration session. The R-squared and linearity values for each analyzer are shown in Table 5.14.

Table 5.14: Calibration R-Squared Values & Linearity

Calibration Date	Inlet	Cabin	Exit
4/21/2014	0.9999809	0.9998410	0.9999997
6/2/2014	0.9999559	0.9999983	0.9999531
6/16/2014	0.9998961	0.9998545	0.9999254
6/30/2014	0.9999074	0.9999959	0.9998670
8/22/2014	0.9999686	0.9999200	0.9998718
9/5/2014	0.9999998	0.9996862	0.9999451
10/2/2014	0.9999983	0.9996616	0.9999643
Average	0.9999581	0.9998511	0.9999323
Linearity	0.0042%	0.0149%	0.0068%

A worst case scenario for the uncertainty value is assumed. The worst case scenario occurs at the minimum difference between the measured CO_2 concentrations of the inlet and cabin analyzers, which results in the largest overall uncertainty. The smallest average cabin CO_2 reading during the passenger loading testing occurred while injecting tracer gas in seat 4B and sampling in seat 8F. The average inlet and cabin concentrations for this worst case scenario, as well as the calculated accuracy values for these concentrations, are shown in Table 5.15.

Table 5.15: Worst Case CO_2 Analyzer Measurements & Repeatability

Location	CO_2 Concentration (ppm)	Output Voltage (V)	Repeatability
Inlet	395.7	0.64427	0.458%
Cabin	456.4	1.17300	0.228%
Exit	689.2	1.77261	0.345%

The values from Table 5.13 through 5.15 are utilized to calculate the uncertainty for each of the analyzers. The total uncertainty for each of the three instruments is shown in Equation (5.18) through (5.26).

$$U_{DAQ,inlet} = 0.0035 * 0.644 + 0.0005 * 10 = 0.00725\% \quad \textbf{(5.18)}$$

$$U_{inlet} = \sqrt{U_{calib}^2 + U_{linear}^2 + U_{rep}^2 + U_{DAQ,inlet}^2} \quad \textbf{(5.19)}$$

$$U_{inlet} = \sqrt{2.45\%^2 + 0.0042\%^2 + 0.458\%^2 + 0.0073\%^2} = 2.49\% \quad \textbf{(5.20}$$

$$U_{DAQ,cabin} = 0.0035 * 1.17 + 0.0005 * 10 = 0.00910\% \quad \textbf{(5.21)}$$

$$U_{cabin} = \sqrt{U_{calib}^2 + U_{linear}^2 + U_{rep}^2 + U_{DAQ,cabin}^2} \quad \textbf{(5.22)}$$

$$U_{cabin} = \sqrt{2.45\%^2 + 0.0149\%^2 + 0.228\%^2 + 0.0091\%^2} = 2.46\% \quad \textbf{(5.23)}$$

$$U_{DAQ,exit} = 0.0035 * 1.77 + 0.0005 * 10 = 0.0112\% \quad \textbf{(5.24)}$$

$$U_{exit} = \sqrt{U_{calib}^2 + U_{linear}^2 + U_{rep}^2 + U_{DAQ,exit}^2} \quad \textbf{(5.25)}$$

$$U_{exit} = \sqrt{2.45\%^2 + 0.0068\%^2 + 0.345\%^2 + 0.0112\%^2} = 2.47\% \quad \textbf{(5.26)}$$

5.4.4 Overall Testing Uncertainty

The uncertainty values calculated in the previous sections are combined into a single value for the maximum uncertainty of the entire testing duration. The root means squared method of partial derivatives was selected as the ideal method to calculate the overall maximum uncertainty. The overall uncertainty equation is shown in Equation (5.27). The individual terms from Equation (5.27) are then evaluated in Equation (5.28) through (5.31).

$$U_N^2 = \left(\frac{\partial N}{\partial C_{cabin}} U_{cabin}\right)^2 + \left(\frac{\partial N}{\partial C_{inlet}} U_{inlet}\right)^2 + \left(\frac{\partial N}{\partial \dot{V}_{CO_2}} U_{CO_2}\right)^2 + \left(\frac{\partial N}{\partial \dot{V}_{supp,air}} U_{supp,air}\right)^2 \quad \textbf{(5.27)}$$

$$\frac{\partial N}{\partial C_{cabin}} = \frac{\dot{V}_{supp,air}}{\dot{V}_{CO_2}} \quad \textbf{(5.28)}$$

$$\frac{\partial N}{\partial C_{inlet}} = -\frac{\dot{V}_{supp,air}}{\dot{V}_{CO_2}} \quad \textbf{(5.29)}$$

$$\frac{\partial N}{\partial \dot{V}_{CO_2}} = -\frac{\dot{V}_{supp,air}(C_{cabin} - C_{inlet})}{\dot{V}_{CO_2}^2} \quad \textbf{(5.30)}$$

$$\frac{\partial N}{\partial \dot{V}_{supp,air}} = \frac{C_{cabin} - C_{inlet}}{\dot{V}_{CO_2}} \quad \textbf{(5.31)}$$

The evaluated terms are then substituted back into Equation (5.27), and the entire equation is divided by N^2 to provide uncertainties as percentages of the normalized values. The equation in terms of percentages is shown in Equation (5.32). Remember that U_{CO2} and $U_{supp,air}$ are already calculated as percentages of the injection and supply air rates, respectively. Therefore, the two volumetric flow rates are absorbed into the uncertainty terms.

$$\left(\frac{U_N}{N}\right)^2 = \left(\frac{U_{cabin}}{C_{cabin} - C_{inlet}}\right)^2 + \left(\frac{U_{inlet}}{C_{cabin} - C_{inlet}}\right)^2 + \left(\frac{U_{CO_2}}{\dot{V}_{CO_2}}\right)^2 + \left(\frac{U_{supp,air}}{\dot{V}_{supp,air}}\right)^2 \quad \textbf{(5.32)}$$

The overall uncertainty calculation is completed for the worst case scenario described previously. The average inlet and cabin concentrations from Table 5.16 are substituted into the uncertainty equation as shown in Equation (5.33) through (5.35).

$$U_{norm} = \sqrt{\left(\frac{U_{cabin}}{C_{cabin} - C_{inlet}}\right)^2 + \left(\frac{U_{inlet}}{C_{cabin} - C_{inlet}}\right)^2 + U_{CO_2}^2 + U_{supp,air}^2} \quad \textbf{(5.33)}$$

$$U_{norm} = \sqrt{\left(\frac{11.2}{456 - 396} \times 100\%\right)^2 + \left(\frac{9.9}{456 - 396} \times 100\%\right)^2 + 2.90\%^2 + 1.08\%^2} \quad \textbf{(5.34)}$$

$$U_{norm,max} = 25\% \quad \textbf{(5.35)}$$

Keep in mind that this is a worst case scenario, and it is not an average representation for the majority of the passenger load testing completed. The overall uncertainty value calculated for the average cabin and inlet CO_2 concentrations from the passenger load testing is shown in Appendix A.

Chapter 6 - Summary & Conclusions

It is shown in Section 5.2 that the loading of passengers inside the aircraft cabin can have a significant impact on the dispersion of tracer gas throughout the cabin. On the other hand, the effects of passenger loading vary greatly for the different injection locations. The supply air testing results introduced in Section 5.3 show that injected tracer gas will still spread throughout the entire cabin without the supply air stream to assist in dispersion.

6.1 Passenger Loading Effects

Three tracer gas injection locations are used in order to determine the passenger loading effects in multiple sections of the cabin. In order to determine the effects in the front-left corner of the cabin, tracer gas is injected in seat 4B. Upon comparison of the full cabin load and half-full cabin load results, it can be seen that the injected CO_2 travels to the front of the cabin for the half-full test and to the rear of the cabin for the full test. The majority of the seats in front of the injection location experience more than an 80% increase in measured CO_2 for the half-full test compared to the full test.

Tracer gas is injected in seat 6D to determine the passenger loading effects in the center of the cabin. The passenger loading effects for the 6D injection location differ greatly from the 4B injection location results. When the cabin is only half-full, the tracer gas concentrations are higher in the front-left and rear-right sections of the cabin. For the fully loaded cabin, the tracer gas concentrations are higher in the front-right and rear-left sections of the cabin. The difference of measured CO_2 in the four quadrants of the cabin is noticeable and there are significant differences in several of the sampling locations.

The final injection location for the passenger loading testing is seat 8F, which is used to find the effects in the rear-right corner of the cabin. The passenger loading effects for the 8D injection location do not align with the 4B or 6D injection locations results. The vast majority of the sampling locations (24 of 32) measure a higher CO_2 concentration for the full load test than for the half-full load test. Since the sampling tree only samples CO_2 concentrations at the height of a seated passenger's breathing zone, this result implies that the CO_2 spreads to different heights inside the mock-up cabin for the half-full passenger load in the rear-right section of the cabin.

It is difficult to see any correlations in the passenger loading results for the three different tracer gas injection locations. The amount of passengers in the cabin has a noticeable effect on the distribution of tracer gas throughout the cabin, but the exact effect cannot be determined from the testing completed for this thesis. It should be noted that the 6D injection location provides the most realistic simulation of a contaminant release on a full-length aircraft due to the minimal effects from the end walls of the mock-up cabin. Possible avenues to gain a better understanding of the passenger loading effects are discussed in Chapter 7.

6.2 No Supply Air Tests Summary

The objective of the no supply air testing for this thesis is to determine the effectiveness of contaminants spreading throughout an airplane cabin after the ventilation air is switched off. As would be expected, the sampled normalized CO_2 concentrations decrease as the distance between the sampling and injection locations increase. It should be noted that the seats in the same row of the injection location measure much higher CO_2 concentrations than the seats in the same column of the injection location. This trend suggests that the lateral transport phenomena created by the supply air diffusers continues to exist after the flow is eliminated. Also, the two seats directly behind the injection location (3D & 4D) measure higher CO_2 concentrations than the seat directly forward of the injection location (1D). This suggests that the tracer gas tends to flow to rear of the cabin rather than to the front, but this phenomenon was only noticed at the 2D injection and should not be considered a general characteristic of the dispersion patterns in an aircraft with no ventilation. Looking at the big picture, even with no ventilation air being supplied to the cabin, tracer gas was detected eight rows behind the injection location, which suggests that contaminants can still effectively spread throughout the cabin.

Chapter 7 - Recommendations

Although the results presented in this thesis provide useful insights into the effects of passenger loading and eliminating the air supply on the airflow patterns inside the aircraft cabin, additional experimentation could expand upon these insights. The results for the passenger loading test are highly inconsistent across the three injection locations. Several improvements could be made to possibly produce more consistent results. One improvement would be to increase the number of sampling locations for each injection location in order to paint a more detailed picture of the tracer gas movement. Another option would be to increase the number of injection locations to investigate more areas of the cabin. Finally, it could be helpful to experiment with more passenger loading scenarios than half-full and completely full cabins.

The results for the no supply air testing are as expected, but the research could be furthered. Due to time constraints, only one injection location was tested. Repeating the testing with an injection location at the rear of the cabin could provide useful information about how the tracer gas travels forward in the cabin. Also, more sampling locations in different columns could be added to determine if the CO_2 trends towards either side of the cabin.

The majority of the instrumentation used for testing is well suited for the particular experiment. For practicality, the same mass flow controllers are used for both experiments. The CO_2 mass flow controller introduces a significant amount of error into the no supply air testing due to the reduced injection rates being at the bottom of the controller's operable range. Future testing could benefit from using a CO_2 mass flow controller designed for lower injection rates. The accuracy of the CO_2 analyzer placed at the inlet location was also the least accurate of the three analyzers used during testing. The overall uncertainty could be lowered by using a more accurate analyzer at the inlet location.

The mock-up cabin used for this testing is only 11 rows long, which is significantly less than the overall length of an actual Boeing 767 cabin. The dispersion of CO_2 at injection locations near the front and rear of the cabin is limited by the end walls of the mock-up cabin. Therefore, in theory, the most realistic CO_2 dispersion occurs in the center rows of the mock-up cabin (rows 5-

7). The simulation could be improved by constructing a longer enclosure that more accurately represents the entirety of a Boeing 767 cabin.

References

Air Transportation Center of Excellence (CoE) for Airliner Cabin Environment Research (ACER). (2007). Transport project.

Anderson, M. (2012). Effect of gaspers on airflow patterns and the transmission of airborne contaminants within an aircraft cabin environment. Kansas State University, Manhattan).

ASHRAE. (2005). ASHRAE Handbook of Fundamentals. *American Society of Heating Refrigerating and Air-Conditioning Engineers,*

ASHRAE. (2007). ASHRAE Handbook. *American Society of Heating Refrigerating and Air-Conditioning Engineers,*

Beneke, J. M. (2010). Small diameter particle dispersion in a commercial aircraft cabin. Kansas State University, Manhattan).

BTS. (2012). Www.bts.gov/press_releases/2012/bts014_12/pdf/bts014_12.pdf. *BTS Data,*

Cai, G. (2012). Modeling and optimization of air distribution systems for commercial aircraft cabins using CFD techniques. *50th AIAA Aerospace Sciences Meeting Including the New Horizons Forum and Aerospace Exposition,*

Coleman, H., & Steele, W. (1989). *Experimentation and Uncertainty Analysis for Engineers*. New York: John Wiley & Sons Inc.

FAA. (1996). FAR section 25.831, ventilation. *Federal Aviation Administration,*

FAA. (2008). Draft final technical report, contaminant transport in airliner cabin. *Kansas State University, Manhattan: FAA Cooperative Agreement 04-C-ACE-KSU, Institute for Environmental Research,*

Hunt, E., & Space, D. (1994). The airplane cabin environment, the boeing company. *International in-Flight Service Management Organization Conference,*

Isukapalli, S., Mazumdar, S., George, P., Wei, B., Jones, B., & Weisel, C. (2013). Computational fluid dynamics modeling of transport and deposition of pesticides in an aircraft cabin. *Atmospheric Environment, 68,* 198-207.

Jones, B. (2009). Advanced models for predicting contaminants and infectious disease virus transport in the airliner cabin environment. *Proceedings of the Transportation Research Board, Research on the Transmission of Disease in Airports and Aircraft,*

Lebbin, P. (2006). Experimental and numerical analysis of air, tracer gas, and particulate movement in a large eddy simulation chamber. Kansas State University, Manhattan).

Lin, C. H. (2006). Comparison of large eddy simulation predictions with particle image velocimetry data for the airflow in a generic cabin model. *HVAC & R Research, 12*(3 C), 935-951.

O'Donnell, A., & Donnini, G. (1991). Air quality, ventilation, temperature, and humidity in aircraft. *ASHRAE Journal*, 42-46.

Powell, R., Jones, B., & Hosni, M. (2014). Measurement of particle deposition rates in a commercial aircraft cabin. *HVAC & R Research, 20*(7), 770-779.

Shehadi, M. (2010). Experimental investigation of optimal particulate sensor location in an aircraft cabin. Kansas State University, Manhattan).

Trupka, A. (2011). Tracer gas mapping of beverage cart wake in a twin aisle aircraft cabin simulation chamber. Kansas State University, Manhattan).

United States Environmental Protection Agency. (2000). Carbon dioxide as a fire suppressant: Examining the risks.

Wang, A., Zhang, Y., Topmiller, J., Bennet, J., & Dunn, K. (2006). Tracer study of airborne disease transmission in an aircraft cabin mock-up. *ASHRAE Transactions, 112*(2), 697-705.

Zhang, Y., & Sun, Y. (2005). Experimental characterization of airflow in aircraft cabins. *ASHRAE Transactions, 111*, 45-59.

Zhang, T., & Chen, Q. (2007). Novel air distribution systems for commercial aircraft cabins. *Building and Environment, 42*(4), 1675-1684.

Appendix A - Aircraft Cabin Volume Normalization

The worst-case scenario for the passenger loading testing uncertainty is calculated in Section 5.4. This calculation is reiterated for an average scenario of the passenger loading testing. Additionally, the uncertainties for the multiple injection rates used in the no supply air testing are found.

A.1: Passenger Loading Average Uncertainty

The maximum uncertainty from the passenger loading testing is recalculated for a more realistic value. The calculation is repeated by replacing the worst case scenario of injection and sampling locations corresponding to seats 4B and 10F, respectively, with locations where there was a smaller distance between the injection and sampling locations. The average injection and sampling locations are 6D and 3B, respectively. The overall uncertainty of the system is reduced for this injection/sampling configuration due to the higher CO_2 concentration sampled by the cabin analyzer. The distance of five seats between the sampling and injection locations is a better representation of the majority of testing completed for the passenger loading testing. The supply air, tracer gas injection, and calibration gas uncertainties remain unchanged by updating the sampling and injection locations. The CO_2 sampling and overall uncertainties are recalculated for the new injection and sampling locations. The updated analyzer measurements are listed in Table A.1.

Table A.1: Average CO_2 Analyzer Measurements & Repeatability

Location	CO_2 Concentration (ppm)	Output Voltage (V)	Repeatability
Inlet	399.4	0.574737	0.460%
Cabin	650.2	1.63103	0.325%
Exit	580.3	1.50681	0.290%

The updated values are used to recalculate the CO_2 sampling uncertainty of the cabin and inlet analyzers, which can then be used to calculate the average overall experimental uncertainty. These calculations are performed in Equation (A.1) through (A.7).

$$U_{inlet} = \sqrt{U_{calib}^2 + U_{linear}^2 + U_{rep}^2 + U_{DAQ,inlet}^2} \quad \textbf{(A.1)}$$

$$U_{inlet} = \sqrt{2.45\%^2 + 0.0042\%^2 + 0.460\%^2 + 0.0070\%^2} = 2.49\% \quad \textbf{(A.2)}$$

$$U_{cabin} = \sqrt{U_{calib}^2 + U_{linear}^2 + U_{rep}^2 + U_{DAQ,cabin}^2} \quad \textbf{(A.3)}$$

$$U_{cabin} = \sqrt{2.45\%^2 + 0.0149\%^2 + 0.325\%^2 + 0.011\%^2} = 2.47\% \quad \textbf{(A.4)}$$

$$U_{norm} = \sqrt{\left(\frac{U_{cabin}}{C_{cabin} - C_{inlet}}\right)^2 + \left(\frac{U_{inlet}}{C_{cabin} - C_{inlet}}\right)^2 + U_{CO_2}^2 + U_{supp,air}^2} \quad \textbf{(A.5)}$$

$$U_{norm} = \sqrt{\left(\frac{16.1}{650 - 399} \times 100\%\right)^2 + \left(\frac{10.0}{650 - 399} \times 100\%\right)^2 + 2.90\%^2 + 1.08\%^2} \quad \textbf{(A.6)}$$

$$U_{norm,avg} = 8.2\% \quad \textbf{(A.7)}$$

This recalculated uncertainty value of 8.2% is a much more accurate representation for the majority of the passenger loading testing completed for this thesis. Due to the large number of tests completed, it is impractical to calculate an uncertainty value for every test.

A.2: No Supply Air Testing Uncertainty

As can be assumed from the description of the test, the no supply air testing does not involve the supply air system. Therefore, the uncertainty of the supply air system is irrelevant in the overall uncertainty. The calibration uncertainty calculated in Equation (5.12) remains unchanged at 2.45%. Three different CO_2 injection rates are used depending on the distance between the injection and sampling location (2.0, 4.0, and 7.0 LPM). The tracer injection uncertainty varies for each of the injection rates. The uncertainty of the CO_2 injection is calculated in Equation (A.8) and (A.9), where V is the volumetric flow rate and U is the uncertainty. The uncertainty values calculated for each of the three injection rates are shown in Table A.2.

$$U_{rep,CO_2} = \frac{0.2\% * 100\ LPM}{\dot{V}_{CO_2}} \quad \textbf{(A.8)}$$

$$U_{CO_2} = \sqrt{U_{rep}^2 + U_{pure}^2} \quad \textbf{(A.9)}$$

Table A.2: CO_2 Injection Uncertainty for Various Injection Rates

CO_2 Injection Rate (LPM)	CO_2 Repeatability	CO_2 Uncertainty
2.0	10.0%	10.01%
4.0	5.0%	5.02%
7.0	2.86%	2.90%

The next uncertainty found is for the CO_2 sampling system. This calculation is shown in Section 5.4.3 and Appendix A.1, so the calculations will be omitted for this iteration. The overall uncertainty for the no supply air testing is dominated by the CO_2 injection uncertainty for the majority of testing, so only a worst-case scenario uncertainty is calculated. The only injection location utilized for the no supply air testing is seat 2D, and the worst-case uncertainty occurs at sampling location 1D. The results of the uncertainty for the cabin analyzer for the worst-case sampling location are shown in Table A.3.

Table A.3: CO_2 Sampling Uncertainty for No Air Supply Testing

Measurement	CO_2 Concentration (ppm)	Output Voltage (V)	Repeatability	Uncertainty
Start	482.5	1.25290	0.241%	2.46%
Cabin	921.0	2.34164	0.461%	2.49%

The final step is to calculate the overall uncertainty of the no supply air experimentation. Since the supply air does not contribute to the uncertainty value, the uncertainty values of the inlet CO_2 analyzer and the supply air stream are omitted from Equation (5.26). The updated overall uncertainty is shown in Equation (A.10) and is derived in Equation (A.11) through (A.14).

$$U_N^2 = \left(\frac{\partial N}{\partial C_{cabin}} U_{cabin}\right)^2 + \left(\frac{\partial N}{\partial C_{start}} U_{start}\right)^2 + \left(\frac{\partial N}{\partial \dot{V}_{CO_2}} U_{CO_2}\right)^2 \quad \textbf{(A.10)}$$

$$\frac{\partial N}{\partial C_{cabin}} = \frac{V_{cabin}}{\dot{V}_{CO_2} \times T} \tag{A.11}$$

$$\frac{\partial N}{\partial C_{start}} = -\frac{V_{cabin}}{\dot{V}_{CO_2} \times T} \tag{A.12}$$

$$\frac{\partial N}{\partial V_{CO_2}} = -\frac{V_{cabin}(C_{cabin} - C_{start})}{\dot{V}_{CO_2}^2 \times T} \tag{A.13}$$

$$\left(\frac{U_N}{N}\right)^2 = \left(\frac{U_{cabin}}{C_{cabin} - C_{start}}\right)^2 + \left(\frac{U_{start}}{C_{cabin} - C_{start}}\right)^2 + \left(\frac{U_{CO_2}}{\dot{V}_{CO_2}}\right)^2 \tag{A.14}$$

Once the overall uncertainty equation is derived for the no supply air experimentation, the uncertainty values for the subsystems can be substituted into the overall equation. This process is shown in Equation (A.15) through (A.17).

$$U_{norm} = \sqrt{\left(\frac{U_{cabin}}{C_{cabin} - C_{start}}\right)^2 + \left(\frac{U_{start}}{C_{cabin} - C_{start}}\right)^2 + U_{CO_2}^2} \tag{A.15}$$

$$U_{norm} = \sqrt{\left(\frac{11.9}{921 - 483} \times 100\%\right)^2 + \left(\frac{22.9}{921 - 483} \times 100\%\right)^2 + 10.01\%^2} \tag{A.16}$$

$$U_{norm} = 12\% \tag{A.17}$$

Keep in mind that this value is the uncertainty for the 2.0 LPM CO_2 injection rate, and the uncertainty values for the 4.0 and 7.0 LPM injection rates are much lower due to the significant decrease in the CO_2 injection uncertainty term. Since the 2.0 LPM CO_2 injection rate was used for the majority of the sampling locations (9 of 12), 12% is considered to be an accurate representation of the average uncertainty as well.

Appendix B - Electronic Appendix Instructions

Due to the length constraints for this document, the data for each individual test run could not be included. The results for all testing, in their entirety, are included in a folder named "Electronic Appendix.zip" attached to this thesis. The entire folder should be extracted locally in order to preserve the links between the various spreadsheets. There are two subfolders inside the root folder named "No Supply Air" and "Passenger Loading", which each contain all of the data for that particular experiment.

B.1 No Supply Air Folder Directory

Under the "No Supply Air" folder is a single subfolder named "2D Inject", because this is the only injection location used for the no supply air testing. Inside the "2D Inject" folder are 12 subfolders for each sampling location used that are named for the sampling seat location. There is also a file named "Overall" that contains the average normalized CO_2 concentration for the final 10 minutes of each sampling location. Under each sampling location subfolder, are four files. Three of the files use a naming convention of (sampling seat row)(sampling seat column)_(run number). The other file uses a naming convention of (sampling seat row)(sampling seat column). The three files including the run number contain the data for each individual test run. The last file, that does not include a run number, contains the average of the three individual runs. This file naming is consistent throughout all 12 sampling locations subfolders.

B.2 Passenger Loading Folder Directory

The "Passenger Loading" folder contains three subfolders named "Comparison", "Full Passenger Load", and "Half-Full Passenger Load". The folder "Full Passenger Load" contains three subfolders that are named for the three injection locations used for the passenger load testing. Each of these folders contains eight subfolders that are named after the sampling tree location for that test. Each sampling tree location folder holds four files; three of which use the following naming convention: (injection row)(injection column)_(sampling tree first row)-(sampling tree last row)(sampling tree column)_(run number). These three files contain the data for each individual test run. The fourth file inside each sampling tree location folder contains the average

of the three individual runs. This naming convention is consistent for all sampling location subfolders under the “Full Passenger Load” and “Half-Full Passenger Load” folders. There is also a file named “Summary” in each injection location subfolder that contains the averaged normalized CO_2 concentration for all 8 sampling locations. These normalized values for both passenger loads are then compiled into the “Comparison” folder. The “Comparison” folder contains three files named after each injection location. These files compare the differences between the full load and half-full load cabin results.